GREEN NETWORKING: FROM CONVENTIONAL TO NEXT GENERATION HETEROGENEOUS CELLULAR NETWORKS

by

M. Aykut Yiğitel

B.S., Computer Engineering, Hacettepe University, 2005

M.S., Computer Engineering, Boğaziçi University, 2010

Submitted to the Institute for Graduate Studies in
Science and Engineering in partial fulfillment of
the requirements for the degree of
Doctor of Philosophy

Graduate Program in Computer Engineering

Boğaziçi University

2016

ACKNOWLEDGEMENTS

Firstly, I would like to thank my thesis supervisor Prof. Cem Ersoy. He is one of the greatest mentors I've ever seen both in my professional and academic career. I always admire his brilliant ideas and positive energy. His vision, patience, humor, wisdom and motto "Mezuniyet Yolları Taştan" made this thesis possible.

I would like to thank my thesis co-supervisor Assist. Prof. Özlem Durmaz İncel not only for her guidance throughout this thesis but also being a friend to me. She was always there to show me the right path whenever I need assistance.

I would like to express my deepest gratitude to my jury members Prof. Can Özturan and Prof. Tuna Tuğcu for their most valuable and constructive comments. I also would like to thank Prof. Necati Aras and Assoc. Prof. Ayşegül Gençata Yayımlı for their participation in my thesis committee.

I am really thankful to all my colleagues and friends in Netlab for their generous help and inspiration. I would like to deeply thank Hande, Bilgin, Can, Yunus, Sinan, Remzi and Orhan not only for their encouragement but also for their warm friendship.

Finally, I am really thankful to my family for their kindness and support throughout this thesis. Especially I would like to thank my spouse Ayla for shouldering the burden of a family with two wonderful kids. Without her, it would be impossible to finish what I've started.

This thesis is partially supported by the Scientific and Technological Research Council of Turkey (TÜBİTAK) under BİDEB 2211-D (National Industry-University PhD Scholarship), NETAŞ PhD Project Incentive Program, Türk Telekom Group Collaborative Research Program and by the Turkish State Planning Organization (DPT) under the TAM Project, number 2007K120610.

ABSTRACT

GREEN NETWORKING: FROM CONVENTIONAL TO NEXT GENERATION HETEROGENEOUS CELLULAR NETWORKS

Increasing energy costs drive the telecommunication service providers to become highly interested in energy efficient operations. The exponential growth in mobile data exchange which is further augmented by the rapid proliferation of smart phones increases the operational expenses of the cellular network operators significantly. Also, ecologists state that the primary triggering factor of the global warming is adding excessive amounts of greenhouse gases to the atmosphere and 72% of the totally emitted greenhouse gases is carbon dioxide (CO_2). Increasing environmental awareness combined with the high energy prices has driven the network operators to reduce their CO_2 footprint by adopting energy efficient green methods. In this thesis, our main focus is to save energy in three types of wireless cellular networks (i) Conventional Cellular Networks (ii) Packet-switched Cellular Networks and (iii) Next Generation Multi-tier Cellular Networks. We formulate novel mathematical optimization problems for each of the listed cellular networks to find the best possible topology which minimizes the overall power consumption of the network while satisfying a certain quality of service level. Our decision variables in the optimization models are switching base stations on/off and adaptively adjusting their transmission power levels as well as deploying additional pico base stations as a remedy according to the present traffic conditions. Although the optimization tools provide the optimum solutions for smaller instances of the problem, we propose novel heuristics to solve large-scale realistic instances due to their prohibitive complexity. Results of extensive simulations, which are designed as close to real life conditions as possible, show that the proposed green methods help to maintain an energy-aware network and save significant amount of energy by adjusting the network topology to the current traffic conditions adaptively.

ÖZET

GELENEKSEL AĞLARDAN YENİ NESİL ÇOKTÜREL HÜCRESEL AĞLARA YEŞİL İLETİŞİM

Artan enerji maliyetleri nedeniyle, telekomünikasyon servis sağlayıcılarının enerji etkin yöntemlere olan ilgisi her geçen gün artmaktadır. Telsiz veri iletişimi ve akıllı telefon kullanım oranlarının hızla artması, cep telefonu operatörlerinin işletme maliyetlerini de bir hayli arttırmıştır. Bunların yanı sıra, çevrebilimciler tarafından küresel ısınmanın başlıca nedeninin atmosfere fazla miktarda salınan sera gazı olduğu ve salınan sera gazının %72'sinin karbondioksit (CO_2) olduğu belirtilmektedir. Yüksek enerji maliyetleri ve artan çevresel farkındalık, cep telefonu operatörlerini enerji etkin yeşil yöntemler kullanarak CO_2 ayak izlerini ve enerji harcamalarını azaltmaya itmiştir. Bu tezde, (i) klasik hücresel ağlar (ii) paket anahtarlamalı çoktürel hücresel ağlar ve (iii) yeni nesil çok katmanlı hücresel ağlar olmak üzere üç farklı telsiz ağ tipi için enerji tasarruf yöntemleri önerilmektedir. Sıralanan her bir ağ tipi için toplam enerji tüketimini en aza indirmeyi amaçlayan, bunu yaparken de belirli bir servis kalitesini sağlayan matematiksel eniyileme modelleri geliştirilmiştir. Eniyileme modellerindeki karar değişkenleri ise, mevcut veri trafiği yoğunluğuna göre yeni baz istasyonları yerleştirmek, baz istasyonlarını açıp kapatmak ve yayım güçlerini değiştirmektir. Mevcut eniyileme araçları küçük ölçekli problemler için kesin sonuçlar üretse de, daha karmaşık büyük ölçekli problemlerin çözümü için yeni sezgisel algoritmalar tasarlanmıştır. Gerçek hayat koşullarına mümkün olduğu kadar yakın örneklerle yapılan başarım değerlendirmesi sonuçlarına göre, önerilen yeşil yöntemlerin ağ topolojisini mevcut veri trafiği koşullarına göre uyarlayarak enerji farkındalıklı ağlar yarattığı ve önemli miktarda güç tasarrufu sağladığı gösterilmiştir.

TABLE OF CONTENTS

LIST OF FIGURES

LIST OF TABLES

LIST OF SYMBOLS

$\mathcal{A}_x$	Area spectral efficiency after deployment of a pico base station to candidate location x
$\mathcal{A}_t$	Area spectral efficiency over the total coverage area at time t
$\mathcal{A}$	Area spectral efficiency
A_{bpt}	Transmission state variable for base station b power level p at time t
$\mathbf{B}$	Set of all base stations where $B = \{1, \ldots, N^B\}$
$\mathbf{B}^{\text{off}}$	Set of currently switched off base stations
$\mathbf{B}^{\text{on}}$	Set of currently switched on base stations ($\mathbf{B}^{\text{on}} = \mathbf{B} - \mathbf{B}^{\text{off}}$)
$\mathbf{B}^{\text{high}}$	Set of overloaded switched on base stations
$\mathbf{B}_b^{\text{neig}}$	Set of neighboring base stations of the base station b
$\mathbf{B}^M$	Set of micro base stations where $\mathbf{B}^M = \{1, \ldots, N^{B^M}\}$
$\mathbf{B}^P$	Set of pico base stations where $\mathbf{B}^P = \{1, \ldots, N^{B^P}\}$
C_b^{cur}	Current traffic load of base station b
C_{bpu}	Coverage variable for base station b for user u with power level p
$\hat{C}_{bp}$	Estimated traffic load of base station b if it is activated with power level p
CUE	Covered user per energy ratio of the current base station when it is switched on
$\mathcal{C}(g)$	Spectral efficiency at coverage grid g
$\mathcal{C}(g,t)$	Spectral efficiency at coverage grid g at time t
D_M	Data flow capacity of micro base station
D_P	Data flow capacity of pico base station
D_b	Data flow capacity of base station b
f_{gt}	Aggregate traffic occupancy of coverage grid g at time t
f_{bt}	Traffic load of base station b at time t
$f^{\min}$	Minimum aggregate traffic load throughout the day
$f^{\max}$	Maximum aggregate traffic load throughout the day
$f(t)$	Average aggregate traffic load function for time t

$f(g,t)$	Average aggregate traffic load function for grid g at time t
$f^{\text{flow}}(t)$	Traffic load per User Chunk with respect to time
f_b	Present traffic load of base station b
f_g^p	Peak aggregate traffic occupancy of grid g
$\mathbf{G}$	Set of grids where $\mathbf{G} = \{1, 2, 3 \ldots, N^G\}$
I^{in}	Intra-cell interference
I^{out}	Inter-cell interference
I_{gbt}^{in}	Intra-cell interference in grid g from base station b at time t
I_{gbt}^{out}	Inter-cell interference in grid g from base station b at time t
K_{bpt}	Activation variable for base station b with transmission power p at time t
$\mathcal{L}(b,p,g)$	Path loss from base station b transmitting with power level p to grid g
$\mathcal{L}(b,g)$	Path loss exponent from base station b to grid g
M_{ubt}	User selection variable for User Chunk u base station b at time t
m	Coverage grid size in square meter
N^B	Number of base stations
N^P	Number of power levels
N^U	Number of user chunks
N^G	Number of coverage grids
N^T	Number of time slots within the day
N^{X^P}	Number of candidate pico base stations deployment locations
$N^{X^{neig}}$	Number of neighboring candidate pico base stations deployment locations for overloaded base stations
N^{B^M}	Number of micro base stations
N^{B^P}	Number of pico base stations
N^{P^M}	Number of micro power levels
N_t^c	Number of covered user chunks at time t
N^{sw}	Number of base station on/off switches during 24h
O_{bt}	Activation variable for base station b at time t
OCA^{cur}	Overlapping coverage area of the current base station

$\mathrm{OCA}^{\max}$	Maximum allowed overlapping coverage area in order to switch a base station on during initialization phase
$\mathbf{PA}$	Set of active power levels where $\mathbf{PA} = \{2, \ldots, N^P\}$
$\mathbf{P}$	Set of power levels where $P = \{1, \ldots, N^P\}$
$\mathbf{P}^M$	Set of micro base station power levels
$\mathbf{P}^P$	Set of pico base station power levels
$p(g)$	Probability of a user being at a particular coverage grid g
P_b^{RF}	RF transceiver power consumption of base station b
P_b^{BB}	Baseband unit (digital signal processing) power consumption of base station b
$\mathrm{PW}^{\mathrm{core}}$	Core power consumed by the base station
$\mathrm{PW}^{\mathrm{tx}}(p)$	Function of transmission power consumed by the base station with respect to power level p
P^r	Received signal power
P^r_{gbt}	Received signal power in grid g from base station b at time t
$\mathcal{S}_{gb}$	Grid association variable for grid g and base station b
S_{ubt}	User association variable for user chunk u with base station b at time t
S_{gbt}	Grid association variable for grid g with base station b at time t
t^p	Time slot in which the traffic load peaks
$\mathbf{T}$	Set of discrete time intervals within the day where $T = \{1, 2, 3 \ldots, N^T\}$
$\mathbf{U}$	Set of user chunks where $U = \{1, 2, 3 \ldots, N^U\}$
w^h	Height of the sinusoidal traffic wave
w^o	Offset of the sinusoidal traffic wave
W^{cur}	Traffic load of the current base station
W_b^{cap}	Data flow capacity of base station b
W_b^{cur}	Current power consumption of base station b
W_b^c	Core power consumed by the base station b
$W(b, p, f)$	Total power consumption function of base station b transmitting with power p and with traffic load f
W_b^c	Core power consumption of base station b

W^{d}_{bpf}	Dynamic power consumption of base station b with transmit power level p and traffic load of f
W^{DC}_{b}	DC-DC power supply consumption of base station b
W^{MS}_{b}	mains supply (AC-DC unit) power consumption of base station b
W^{cool}_{b}	Active cooling power consumption of base station b
$W^{M}(p, f)$	Function of micro base station power consumption with transmission power p and traffic load f
$W^{P}(p, f)$	Function of pico base station power consumption with transmission power p and traffic load f
W^{tx}_{bp}	Transmission power consumed by the base station b while transmitting with power level p
$W(b, p)$	Total consumed power by base station b transmitting with power level p
$\mathbf{X}^{P}$	Set of candidate pico base stations deployment locations where $\mathbf{X}^{P} = \{1, \ldots, N^{X^{P}}\}$
$\mathbf{X}^{neig}_{b}$	Set of neighboring candidate pico base stations deployment locations for base station b where $\mathbf{X}^{neig}_{b} \subset \mathbf{X}^{P}$
α^{sw}	Penalty of making a base station switch (on/off)
α_{u}	Base station utilization penalty
α_{o}	Orthogonality loss factor
β	User satisfaction ratio during peak traffic conditions where $0 \leq \beta \leq 1$
$\beta^{\min}$	Minimum acceptable user satisfaction ratio where $0 \leq \beta^{\min} \leq 1$
β^{cur}	Current user coverage ratio of the network
β_{t}	Total coverage ratio at time t
$\Delta\ell_{bx}$	Handed over traffic load from over-utilized base station b to the newly deployed neighboring pico base station at candidate location x
$\Delta\xi_{b}$	Allowed Saturation Proximity Metric redundancy of base station b
η	Noise power

$\Gamma(g)$	Binary coverage function with respect to grid g
$\psi_b^{\max}$	Maximum Utilization Metric of the base station b
Ψ_{gb}	Received Signal to Interference and Noise Ratio by grid g from base station b
$\Psi^{\min}$	Minimum acceptable Signal to Interference and Noise Ratio at the receiver
Ψ_{gbt}	Received Signal to Interference and Noise Ratio by grid g from base station b at time t
ϕ_x	Difference between the maximum traffic load capacity of the newly deployed base station at location x and its current load after the deployment.
θ_{bx}	Neighbor Base Station Deployment metric
ξ_b	Current Saturation Proximity Metric of base station b
$\hat{\xi}_{bp}$	Estimated Saturation Proximity Metric of the base station b if it is activated with power level p
$\xi_{bp}^{\max}$	Maximum Saturation Proximity Metric of other active BSs when base station b is activated with power level p

LIST OF ACRONYMS/ABBREVIATIONS

AMPL	A Modeling Language for Mathematical Programming
ASE	Area Spectral Efficiency
BONMIN	Basic Open-source Nonlinear Mixed INteger programming
BS	Base Station
CAPEX	Capital Expense
CCN	Conventional Cellular Networks
CE	Cascade Effect
CO_2	Carbon Dioxide
CTO	Clear to Switch Off
CUE	Covered User per Energy
E-UTRA	Evolved Universal Terrestrial Radio Access
FDMA	Frequency Division Multiple Access
FIFO	First In First Out
GDBP	Green Dynamic BS Planning
GDOA	Greedy Dynamic Operation Algorithm
GPRS	General Packet Radio Service
GoS	Grade of Service
GTA	Green Traffic-Aware topology Management Algorithm
ICT	Information and Communication Technology
IMT-2000	International Mobile Telecommunications for the year 2000
LP	Linear Programming
LTE	Long-Term Evolution
LTE-A	Long-Term Evolution Advanced
MC	Monte Carlo
MIBD	Minimum Inter-BS Distance
MT	Mobile Terminal
NBD	Neighbor BS Deployment
NCTO	Negative Clear to Switch Off

NGMCN	Next-Generation Multi-Tier Cellular Networks
NIC	Network Interface Card
NLP	Nonlinear Programming
OPEX	Operational Expense
PL	Power Level
PSCN	Packet-Switched Cellular Networks
QoS	Quality of Service
RSSI	Received Signal Strength Indicator
RTO	Request to Switch Off
SF	Spreading Factor
SINR	Signal to Interference and Noise Ratio
SLAKE	Sleep-Wake
SPM	Saturation Proximity Metric
TAM	Traffic-Aware topology Management
TDMA	Time Division Multiple Access
TEDAS	Turkish Electricity Distribution Company
UC	User Chunk
UM	Utilization Metric
WiMAX	Worldwide Interoperability for Microwave Access
W-CDMA	Wideband Code Division Multiple Access

1. INTRODUCTION

Increasing energy costs force the telecommunication service providers to deliver energy efficient operations. The exponential growth in mobile data exchange rates [2] which is further augmented by the rapid proliferation of smart phones significantly increases the Operational Expenses (OPEX) of the cellular network operators. Also, ecologists state that the primary triggering factor of the global warming is adding excessive amounts of greenhouse gases to the atmosphere and 72% of the totally emitted greenhouse gases is carbon dioxide (CO_2) [3]. Information and communication technology (ICT) industry produces 2% of the overall CO_2 emission throughout the world by consuming 3% of the worldwide energy [4, 5]. When the exponential growth in data exchange [2] is considered, it is clear that the ICT sector will become one of the major CO_2 emission sources within the next few decades. Therefore, developing and applying energy-efficient green methods in the ICT industry and reducing its CO_2 footprint are now more essential than ever.

Since wireless cellular access networks constitute a significant portion of the ICT industry [6], it would not be wrong to think that measures to be taken in this field can significantly contribute to make the overall communication industry greener. Although wireless cellular access networks consist of two parts, which are radio and the core, vast majority of the energy is consumed by the radio segment [7, 8]. Therefore, it is considered that Base Stations (BSs) which are the integral part of the radio segment are the right place to start saving energy [9].

Parallel to the ubiquitous coverage demand and growing needs of the subscribers, cellular network operators increase their Capital Expenses (CAPEX) and invest more money to deploy large number of BSs to provide better service quality in terms of data rate, coverage, call blocking and dropping probabilities. Consequently, the BS density increases and yields to a significant amount of BS redundancy and electromagnetic pollution, especially in crowded urban areas. Figure 1.1 shows the BS location and coverage redundancy of a single operator from Sydney Central Business District, Aus-

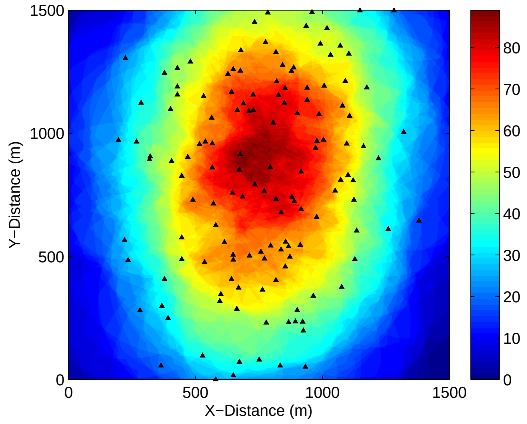

Figure 1.1. Base station location and coverage redundancy of a single operator based on the RSSI value from Sydney Central Business District, Australia.

tralia. This BS information on the map is extracted from a website [10] which makes use of the Australian Communications and Media Authority's RadCom registry. The area covered in the map is 1.5×1.5 km^2 and has a total of 139 BSs. As suggested in IEEE 802.16m Evaluation Methodology Document [11], the coverage map is created by using the COST-Hata [12] metropolitan area propagation model with 2000 Mhz frequency, 1.5 and 15 meters mobile station and BS antenna heights respectively. Each BS is transmitting with a power of 46 dBm, 17 dBi antenna gain and minimum acceptable Received Signal Strength Indicator (RSSI) at the receiver is assumed to be -90 dBm.

In order to fulfill the requirements of the users regardless of time and space, network operators usually place BSs to support the peak traffic conditions. Therefore, BSs are under-utilized during off-peak times such as late night hours or holidays. A real traffic profile collected from a central BS and four neighboring BSs during one week is given in Figure 1.2 [1]. As expected, the traffic load decreases dramatically during the late night hours. Yet, low traffic may also be observed all day long during weekends or holidays in particular places such as business or trade centers. Hence, adoption of green traffic-aware topology management schemes can save large amounts of energy by reducing the redundancy and decrease the OPEX of the service providers significantly. Moreover, reduction of the energy consumption also helps to slow down

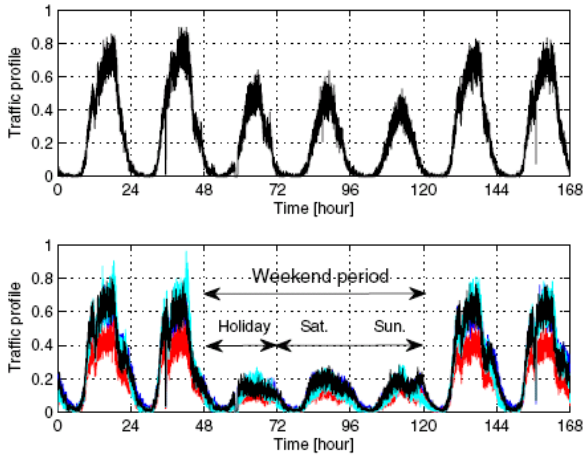

Figure 1.2. Normalized traffic profile of a central (top) and four neighboring (bottom) BSs during one week [1].

the global warming process by mitigating the CO_2 emission to the atmosphere.

This thesis addresses the above mentioned issues by proposing efficient green cellular network deployment and operation methods for three different cellular network types: (i) Conventional Cellular Networks (CCNs) (ii) Packet-Switched Cellular Networks (PSCNs) (iii) Next-Generation Multi-Tier Cellular Networks (NGMCNs). In the deployment phase, we analyze the traffic load pattern of the coverage area and focus on deploying minimum amount of pico BSs as a remedy. On top of that, we try to minimize the total power consumption of the network during operation phase by switching BSs on/off and adaptively adjusting their transmission powers according to the present traffic conditions. Through extensive real-life-scale simulation runs, it is shown that the proposed green networking methods help to maintain an energy-aware network and achieve significant amount of power savings.

1.1. Research Overview and Key Contributions

In this thesis, we concentrate on saving energy by (i) green BS design and deployment (ii) adaptive BS switching on/off (iii) adaptive BS transmission power adjustment according to the present traffic conditions in the coverage area. Particulary, we focus on conventional Time Division Multiple Access (TDMA) / Frequency Division

Multiple Access (FDMA) cellular networks, Wideband Code Division Multiple Access (W-CDMA) packet-switched cellular networks and Evolved Universal Terrestrial Radio Access (E-UTRA) based next generation cellular networks in order. However, the challenge is to decrease the energy expenditure while always guaranteeing an acceptable Quality of Service (QoS) level. To address this, we formulate novel linear and nonlinear programming models to find the best possible BS topology which minimizes the energy consumption while satisfying the certain service quality requirements of the subscribers. Although small instances of the derived problems can be solved by the optimization tools, large realistic size problems are quite difficult to be handled due to their prohibitive space and computational complexity. Therefore, we also propose novel heuristics to solve the large-scale instances of the formulated problem within reasonable time durations. In order to make accurate performance evaluation of our techniques, we use real-life network topologies and traffic data in our simulations, and compare our results with the previously proposed methods in the literature [13–15].

Main contributions of this thesis can be summarized as follows:

- *Integration of Dynamic Transmission Power Adjustment:* Unlike majority of the previous studies [15–18], where only BS on/off switching is utilized, we also take the dynamic power adjustment capability of the current BSs technology into account in order to create more energy-aware network topologies by defining a set of transmission power levels. Using different transmission power levels, we have the opportunity to dynamically change the coverage of the BSs according to the present traffic conditions.
- *Novel Optimization Models:* Detailed mathematical optimization models are formulated to minimize the total power consumption while satisfying a certain level of QoS. By using the derived models, we are able to obtain optimum results by using the optimization tools for the small instances of the problem.
- *Real-life Scenarios:* We justify our proposed methods by applying them to scenarios as close to real life conditions as possible. For this purpose Maslak and Taksim regions of Istanbul are used as a test case. Furthermore, we created a detailed

map of the Taksim area for better estimation of spatio-temporal user density. To the best of our knowledge, this kind of detailed user density estimation study of a particular area is one of its kind in the literature.

- *Novel Heuristics:* To overcome the prohibitive complexity of the formulated optimization problems, especially for the real-life scale large instances, fast and effective heuristics are proposed. They can be also considered as operating algorithms of the proposed methods to achieve the mentioned power savings in their respective performance evaluation sections.
- *Deployment of Pico BSs as a Remedy:* For the NGMCNs, we propose deploying additional pico BSs on top of the existing network infrastructure to meet the increasing data exchange demands of the subscribers. Therefore, our green networking strategy is not limited to dynamic adjustment only, but also encompasses the network design and BS deployment phases.

1.2. Thesis Outline

Chapter 2 presents a review of the state-of-the-art green networking techniques including a taxonomy of the previously proposed methods in the literature.

Chapter 3 describes the proposed green techniques for power saving in Hybrid TDMA/FDMA based conventional cellular networks. This chapter also elaborates the proper application areas of the derived green networking methods.

In Chapter 4, we discuss green W-CDMA based packet-switched cellular networks by taking the effect of interference into account. After we present the system model, assumptions and the problem formulation, we explain the proposed technique to minimize the power consumption. We also give a comparative performance evaluation of our method on a test case scenario based on Maslak district of Istanbul.

In Chapter 5, we present green BS deployment and operation strategies for E-UTRA based next-generation multi-tier cellular networks such as LTE-Advanced. Since NGMCNs are not fully deployed and operational for the time being, we also take the network design phase into account and try to keep the network green during the operation phase. In this chapter, we also create a detailed map of Taksim as the pilot application area and make a spatio-temporal user density estimation. We then propose an energy-aware pico BS deployment method as well as three different dynamic topology management techniques.

Chapter 6 draws the conclusions of the thesis with a summary of our contributions together with the possible research directions to explore.

2. STATE OF THE ART ON GREEN NETWORKING

In recent years, the advent of smart phones, tablets and laptops has enabled the widespread use of bandwidth-hungry applications, which in turn led an immense growth in mobile data usage. To accommodate increasing mobile data exchange requirements of the subscribers, network operators have started to deploy denser access networks per unit area, thus vastly increasing the energy consumption. Growing energy consumption with increasing energy costs coupled with its adverse impact on the environment have led to numerous research works on the topic called *green networking*. In this chapter, we provide an overview of the recent approaches for green networking along with an extensive taxonomy of the strategies proposed in the literature.

Energy efficient hardware and cooling system design techniques are proven methods to decrease the network power consumption considerably [19–24]. However, these methods are applied in the early hardware design and manufacturing phase at the physical layer. Since our research is focused on energy efficiency through network planning and management, energy efficient hardware design is outside the scope this thesis. The readers may refer to [19–24] for energy efficient hardware and cooling system design techniques.

2.1. Energy Efficient BS Deployment Strategies

There are numerous works in the literature addressing the problem of energy efficient BS deployment in wireless cellular networks. Among them, Zheng *et al.* [25] propose a cellular network planning framework considering the use of renewable energy sources and energy balancing. They formulate an optimization problem with an objective function of minimizing three components: (i) total installation cost (ii) total connection cost and (iii) total cost of consumed power from the electric grid. According to the results of their novel heuristics proposed to solve the formulated optimization problem, they achieve considerable CAPEX and OPEX savings in comparison with the traditional deployment strategies.

In [26], authors focus on the problem of energy efficient base station positioning and frequency assignment based on a realistic traffic estimation for the city of Zurich given in [27]. They follow a heuristic approach and propose multi-objective genetic algorithms with very low computational complexity to solve the problem. Given the CAPEX for BS installation, they show that their approach satisfies the traffic demand in the coverage area with minimum amount of BSs and decreases the inter-cell interference significantly. Similarly, discrete optimization models and algorithms are proposed to determine where to locate the new BSs in [28]. Authors propose different versions of two greedy procedures and a tabu search algorithm, which take the installation costs, signal quality and traffic coverage into account.

Boiardi *et al.* [29] propose an optimization framework that selects the BSs to be installed and jointly switches them on/off with respect to changing traffic load conditions. According to their findings, for the power management to be truly effective, networks have to be designed by taking the operational management into account. Hence, they focus on finding the best trade-off between keeping low initial investments and reducing energy consumption. They introduce a trade-off parameter between CAPEX and OPEX, and their optimization framework allows network operators to obtain network topologies with different characteristics by varying that parameter.

On the other hand, finding the optimal BS density in the coverage area rather than the specific BS locations to accommodate the user requirements is attracting significant amount of attention in the literature. Recently, Peng *et al.* [30] formulate a network energy consumption minimization framework which jointly optimizes the BS density and BS transmission power. Their numerical simulation results show that the heterogeneous network deployment has an advantage in energy efficiency performance compared to the homogeneous network deployment. In Section 5.5.2, we provide a comparative performance evaluation of the BS deployment strategy proposed in this study with our green pico BS deployment method.

Another study related to optimal BS density is given in [31]. Authors adopt stochastic geometry theory to analyze the optimal BS density for both homogeneous and heterogeneous cellular networks to minimize network energy cost. Based on realistic parameters of the EARTH [32, 33] project, compared to the traditional macro-only homogeneous cellular network, deploying micro BSs can reduce about 40% of the total energy cost, and further reduce up to 35% with BS sleeping capability. A similar stochastic geometry based model is also proposed in [34] for energy efficiency in single-tier homogenous and K-tier heterogeneous cellular networks.

2.2. Energy Efficient Dynamic Resource Management

Due to fluctuating traffic conditions during the day, static resource management is not considered as optimal in terms of energy efficient network operation. However, dynamic resource management methods are effective only when cellular networks are experiencing low traffic load. If the traffic demand is intense all the time, there will not be any available margin for power saving.

One of the most utilized resource for dynamic management in cellular networks is the BS transmission power. In the literature, there are example studies which consider the dynamic cell size adjustment in order to reduce the energy consumption. Among them, Niu *et al.* [14] introduce the cell zooming concept for energy saving to adaptively adjust the size of the cells according to the current traffic load. In their work, a cell zooming server which is a virtual entity in the network controls the procedure of cell zooming. The cell zooming server collects the information such as the traffic load, channel conditions and user requirements; then analyzes whether there are opportunities for cell zooming or not. Based on the cell zooming concept, they propose centralized and distributed versions of user association algorithms to save energy by putting redundant BSs into sleep mode. In Section 4.5.2, we also provide a comparative performance evaluation of the centralized algorithm proposed in this study with our methods.

Oh *et al.* [15] proposed an algorithm called SWES along with three other versions of it for BS on/off switching. They introduce the notion of network-impact which considers the effect of BS transitions on the neighboring BSs in terms of traffic load and try to find solutions which have the minimum effect on the network. It is shown that, according to the test case results conducted with a real-life topology and traffic load data, their algorithms can achieve energy savings up to 50-80%. In Section 5.5.2, we use SWES algorithm as a competitor and provide comparative performance evaluation with our green networking methods.

Another work considering variable cell sizes for energy saving is presented in [16]. In this work, Bhaumik *et al.* consider two types of BSs which are subsidiary BSs with low transmit power and umbrella BSs with high transmit power. They propose a self operating network by adaptively switching subsidiary and umbrella BSs on and off according to the current traffic demands. Similarly, Kokkinogenis *et al.* [17] assume a cellular network consisting of micro and macro BSs where micro BSs have the ability of being switched on/off while macro BSs can iteratively adjust their transmission power until the required QoS is achieved. They propose static centralized, dynamic distributed and hybrid topology management schemes to reduce the overall energy consumption of the network while satisfying certain QoS requirements.

Chiaraviglio *et al.* [18] propose a novel approach to save energy in UMTS networks by reducing the number of active access devices when they are under-utilized. Authors derive two models for both circuit switched and packet switched services separately for quantification of possible energy savings.

Recently, a green cell breathing and offloading mechanism for heterogeneous networks is proposed in [35]. Authors control the BS switching-off aggressiveness by using a traffic threshold approach in the context of heterogeneous macro and femto cell deployments. They explore the impact of combining cell breathing with a second layer of small cells, i.e. femtocells, on BS offloading and switch-off. The effect of access policies from 3GPP Closed Subscriber Groups on the network performance is also analyzed.

In another recent study, Son *et al.* [36] investigate the energy-efficient design of heterogeneous cellular networks, especially with a focus on deployment and operation strategies. They formulate a general optimization problem with an objective of minimizing the total energy consumption cost while satisfying the requirement of area spectral efficiency. This problem is then decomposed into two problems: (i) deployment problem at peak time and (ii) operation problem at off-peak time. They propose a greedy algorithm as an offline centralized solution and two online distributed algorithms using the Lagrangian relaxation technique.

In [37], traffic-aware sleeping control and power matching technique of a single BS in cellular networks are studied. The aim of this study is to find the sleeping control and power matching configurations that achieve the Pareto optimal tradeoff between total power consumption and average delay. According to proposed sleeping control schemes; the BS goes to sleep whenever there is no active user, and wakes up when N users are assembled or after a period of multiple or single vacation time. Authors also analyze the relationship between total power consumption and average delay with varying service rate theoretically and argue that sacrificing delay cannot always be traded for energy saving. Similarly, Niu *et al.* [38] characterize the fundamental tradeoffs between total energy consumption and overall delay in a BS with sleep mode operations by queueing models. Authors derive closed-form formulas to demonstrate the tradeoffs between the energy consumption and the mean delay for different wake-up policies.

In the literature, there are example studies which consider distributed dynamic resource management such as [39] and [40]. Authors propose a distributed cooperative framework to improve the energy efficiency of green cellular networks in [39]. Based on the traffic load, neighboring BSs cooperate to optimize the BS sleeping strategies while guaranteeing QoS requirements of the subscribers. An energy saving problem is formulated as a constrained graphic game and the existence of a generalized Nash equilibrium is proved. Accordingly, a decentralized iterative algorithm to find the best equilibrium point is designed where only local information exchange among the neighboring BSs is needed. Similarly, a distributed BS switch on/off algorithm is proposed for LTE-Advanced networks which exploits the knowledge of the distance between the MTs and their associated BS in [40].

In [41], authors focus on energy efficiency in densely deployed femtocell networks where a large number of open-access femto BSs are deployed in a public hotspot area such as airport or shopping mall. The effect of the femto BS-sleeping ratio on the energy efficiency is quantitatively studied by using a stochastic geometry-based model. Then the optimal femto BS-sleeping ratio is obtained by considering both the network traffic load and the location of the designated femtocell deployment area in order to maximize the total energy saving.

Rengarajan *et al.* [42] present a novel approach for estimating both the energy savings that can be achieved in cellular access networks by using sleep modes, as well as the energy-optimal BS densities as a function of user density. Their approach allows the derivation of realistic estimates of the energy-optimal density of BSs corresponding to a given user density, under fixed performance constraints.

Another network sleep mode scheme for reducing energy consumption of radio access networks is proposed in [43]. An optimal Markov Decision Processes based controller that associates to each traffic an activation/deactivation policy is derived. This controller reduces the ping-pong effect resulting in unnecessary BS on/off oscillations and focuses on finding the optimal policy dynamically based on the present user activity in the cell.

In [44], the problem of finding the fraction of BSs that can be switched off while maintaining QoS for given load conditions is explored. As a QoS metric, authors measure the average waiting time of subscribers. Their approach consists of two steps. In the first step, they determine the optimal on/off pattern of base stations and MT-BS association policy for a fixed fraction of base stations to be switched off. In the second step, they focus on finding the maximum fraction of base stations that can be switched off for given traffic load conditions.

2.3. Energy Efficiency Through BS Cooperation

Mobile service providers recently introduced the concept of network sharing with the objective of reducing both their CAPEX and OPEX. The main idea is cooperating and sharing infrastructures of the service providers with each other in order to adapt the active capacity to the current traffic conditions, and thus save energy. This sharing may further include their approaches for implementing sleep modes [45].

In [46], a traffic-intensity-aware multicell cooperation scheme is introduced which adapts the cellular network topology according to user traffic demands in order to reduce the number of active BSs. Then a novel energy-aware multicell cooperation method is proposed to reduce on-grid power consumption by offloading traffic from on-grid base stations to off-grid base stations powered by renewable energy. Moreover, coordinated multipoint transmission is investigated to improve the energy efficiency of cellular networks.

A resource on/off switching framework that adapts to the changing network traffic load and maximizes the amount of energy saving under service quality constraints in a cooperative networking environment is presented in [47]. The proposed framework relies on cooperation among different networks to save energy on two scales: (i) On a large scale, networks with overlapped coverage alternately switch their BSs on and off according to the long-term fluctuations in traffic load (ii) On a small scale, each active BS switches its channels on and off according to the short-term fluctuations in traffic load.

Ghazzai *et al.* [48] investigate the collaboration between multiple mobile operators to optimize the energy efficiency of cellular networks. They use LTE-A case for their framework study and try to reduce CO_2 emission of the network via collaborative techniques and using BS sleeping strategy. A low complexity algorithm is proposed that establishes the cooperation decision criteria based on roaming prices and profit gains of competitive mobile operators. Similarly, Bousia *et al.* [49] study energy efficiency issues in multi-operator mobile networks. Their aim is to save energy by switching off the redundant BSs without compromising the offered QoS. They propose a novel game theoretic strategy using cost-based functions to decide the most suitable BSs to remain active.

Inspired by the ecological protocooperation principle, Hossain *et al.* [13] propose a BS cooperation scheme to achieve higher energy efficiency in cellular access networks. BSs cooperatively and dynamically switch between on/off states and adjust their transmission power levels depending on the current traffic conditions. They introduce a distributed sleep-wake up algorithm called SLAKE which consists of a sleeping and a traffic distribution procedure. Since their algorithm also utilizes BS transmission power adjustment besides BS on/off switching similar to our focus, we compare the performance of our methods with SLAKE in Section 4.5.2.

In [50], authors propose an energy-efficient BS switching strategy, and use cooperative communication techniques among the BSs to effectively extend network coverage. They take both the path-loss and fading effects into consideration, and derive closed-form expressions for the call blocking and the channel outage probability. They also try to guarantee the QoS of the subscribers by identifying the MTs situated at the worst-case locations.

Unlike other studies related to cooperative green networking, Zou *et al.* [51] investigate MT cooperation with each other in transmitting their data packets to BS by exploiting the multiple network access interfaces to improve the energy efficiency in cellular uplink transmission. They develop a closed-form expression of energy efficiency (Bits/Joule) given target outage probability and data rate requirements. Their numerical results show that their proposed inter-network cooperation significantly improves the energy efficiency when the cooperating users move towards to each other.

2.4. Renewable Energy Resources

Green energy resources such as sustainable biofuels, solar and wind energy are promising options to reduce the CO_2 footprint of the cellular networks. Ericsson [52] has developed a wind-powered BS for cellular networks and Nokia Siemens Networks [53] has also introduced a green BS which totally relies on a combination of solar and wind power without any grid electricity.

In [54], authors study cellular access networks which solely rely on renewable energy resources. They focus on BS power generator (photovoltaic panels) and energy storage dimensioning according to daily power consumption of the BSs and daily / seasonal radiative power of the sun in three different locations: (i) Torino (ii) Palermo (iii) Aswan. They also investigate the effectiveness of solar power system with wind turbines, along with BS sleep modes.

However, due to unreliable dynamics of green energy harvesting and the limited capacity of the current energy storage technology, green energy may not guarantee sufficient power supplies for BSs. Thus, researchers have been investing significant amount of effort to overcome these challenges by introducing hybrid powered BSs where BSs use the green energy if they have enough energy stored in their batteries; otherwise, the BSs switch to on-grid power to operate. Among them, Han *et al.* [55] propose an optimization problem to maximize the utilization of the green energy harvested by renewable resources, and hence reduce the on-grid energy consumption of the BSs. They decompose the problem into two sub-problems (i) the multi-stage energy allocation problem (ii) the multi-BSs energy balancing problem. Then, they propose three algorithms to solve these sub-problems.

Recently, Wang *et al.* [56] proposed a new model to capture the dynamic energy flow behavior of solar powered BS by using stochastic queue model. They also consider fluctuation of energy generation, nonlinearity of energy storage and indeterminacy of traffic load. Subsequently, they define three performance metrics which are (i) service outage probability (ii) solar energy utilization efficiency and (iii) mean depth of discharge. Under constraints on the defined metrics, they formulate a CAPEX minimization problem and propose an adaptive genetic algorithm to solve it.

New design methodologies for hybrid energy supply green cellular networks with the help of Lyapunov optimization techniques are proposed in [57]. Authors adopt grid energy consumption and achievable QoS as their performance metric and try to optimize these metrics via BS assignment and power control. Their main contribution is a low-complexity online algorithm to minimize the long-term average network service cost.

2.5. Energy Efficiency in Mobile Terminals

Majority of the existing studies in the literature investigate energy efficiency of dynamic planning approaches only from the network operator perspective. Dynamic planning, if not carefully designed, can lead to higher energy consumption for the mobile users in the uplink due to larger transmission distances, which in turn degrades the uplink service quality caused by the fast depletion of mobile terminal's battery.

In order to balance the trade-off in energy efficiency among network operators and mobile users, Ismail *et al.* [58] investigate dynamic planning not only from the network operator perspective, but also from the mobile user perspective. They propose a dynamic planning scheme which takes both network operators (downlink) and mobile users (uplink) energy consumption into account based on a two timescale (slow and fast) decision strategy. In the slow scale, BS on/off switching and antenna tilting decisions are taken while BS and MT transmission power control decision are taken in the fast scale.

De Turck *et al.* [59] investigate the power saving mechanisms in mobile devices by taking both downlink and uplink traffic into account. They analyze the effect of a generic sleep mode mechanism in terms of mean packet delay and power consumption tradeoff for both LTE and WiMAX networks under Markovian traffic model. According to their findings from a real life application scenario, even a modest amount of uplink traffic has a tremendous influence on the system performance.

In [60], authors propose a novel traffic coalescing scheme to reduce the platform wake events motivated by bursty and random behavior of real-world traffic workloads. Their adaptive traffic coalescing method monitors the incoming traffic at the Network Interface Card (NIC), and adaptively coalesces the packets for a limited duration in the NIC buffer. They try to reduce mobile terminal wake events and enable them to enter and stay in the low-power state longer for energy efficiency. According to real life implementations on various mobile platforms, the proposed adaptive traffic coalescing scheme achieves around 20% power saving without impacting performance and user experience.

For further information, reader may refer to extensive survey studies in the literature. Among them, Ismail *et al.* [61] focus energy efficient techniques in BSs and MTs from the operator and user perspectives. A survey on energy efficiency of wireless multimedia streaming in mobile hand-held devices presented in [62] where a survey on optimal control of sleep periods for MTs can be found in [63].

2.6. Taxonomy

In this section, we provide a classification of green dynamic BS operation schemes previously proposed in the literature. Our first classification criteria is the scope of the network in which green dynamic BS operation techniques are designed to be applied. We basically divide the network scope into three parts: (i) Flat (ii) Multi-tier (iii) Heterogeneous. Flat networks consist of single type of BS where multi-tier networks consist of more than one type of BS (e.g. macro, micro, pico). On the other hand, heterogeneous networks consist of different type of BSs with different type of communication technologies (e.g. GPRS, IMT-2000, LTE, WiMAX). Our second classification criteria is the metrics in which performance of the green BS operation schemes are evaluated. Since main objective of all green networking methods is to save energy, we excluded energy efficiency in this taxonomy. Majority of the works previously proposed in the literature utilize aggregate throughput and average delay as their primary metrics. Coverage is another important metric since it is enforced by the governmental laws to cover a certain percentage of the population or geographical area. Hybrid met-

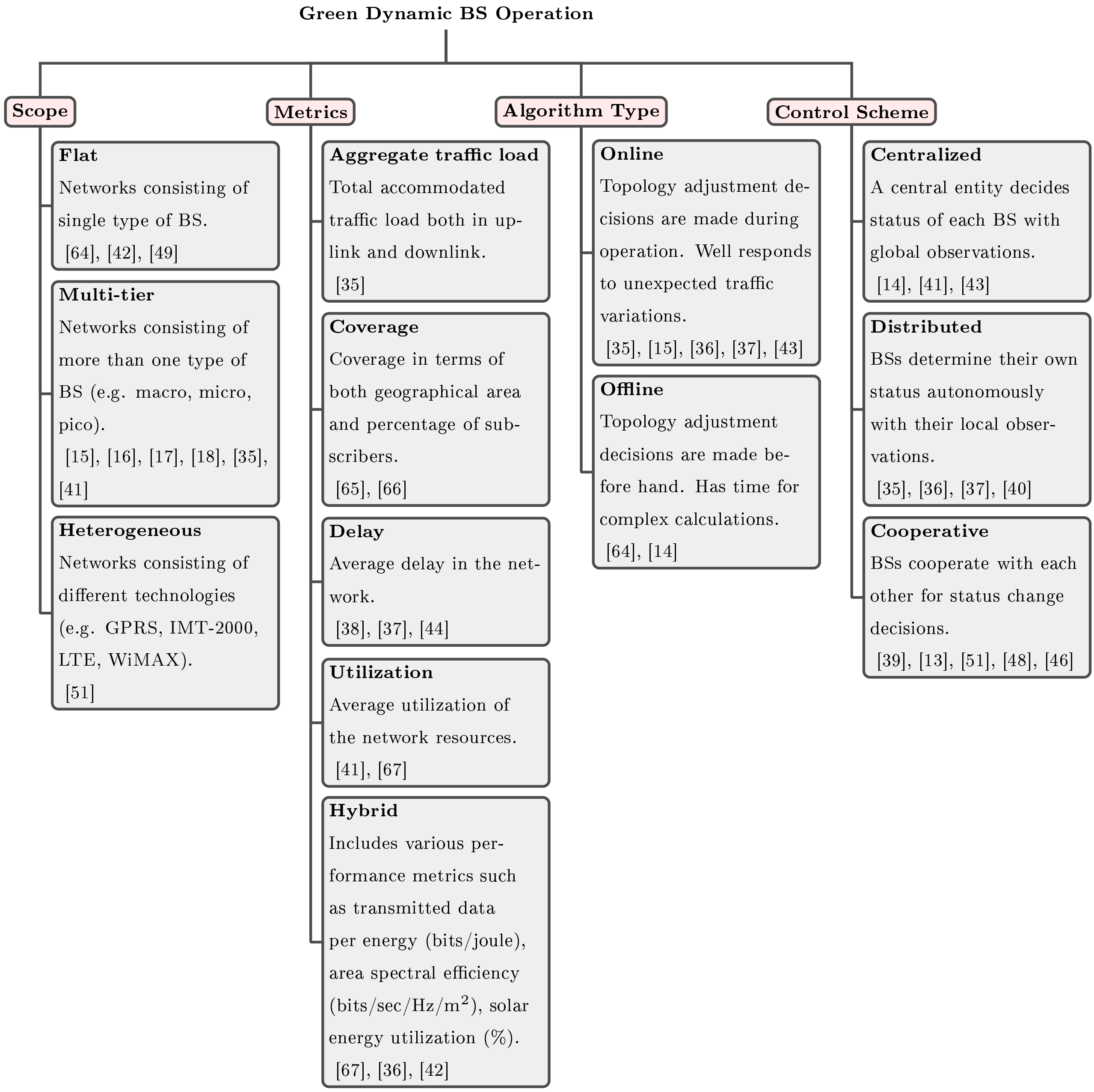

Figure 2.1. Classification of green dynamic BS operation strategies.

rics include a variety of performance indicators such as transmitted data per energy (bits/Joule), area spectral efficiency (bits/sec/Hz/m^2) and solar energy utilization. Our third classification criteria is algorithm type. We observe two main trends in green dynamic BS operation algorithms: Online and Offline. Online algorithms make topology adjustment decisions during operation and well respond to unexpected traffic variations. In Offline algorithms, topology adjustment decisions are made beforehand and they have more time for complex calculations. Fourth and the last classification criteria is the type of control scheme and we divide it into three parts: (i) Centralized (ii) Distributed (iii) Cooperative. In centralized scheme, a central entity decides the status of each BS with global observations throughout the network. On the other hand, BSs determine their own status autonomously with their local observations in distributed scheme. Lastly, neighboring BSs cooperate with each other for status change decisions in the cooperative scheme.

3. GREEN CONVENTIONAL CELLULAR NETWORKS

3.1. Introduction

In this chapter, we focus on saving energy by adaptively switching the BSs of wireless cellular access networks on and off according to the current traffic conditions. Moreover, we also adopt dynamic transmission power adjustment with the help of high-efficiency power amplifiers. However, the challenge is to decrease the energy expenditure while always guaranteeing a certain Grade of Service (GoS) over the whole area. Therefore, we formulate a novel nonlinear programming (NLP) model for the Green Dynamic BS Planning (GDBP) problem to find the best possible BS topology which minimizes the energy consumption while satisfying the communication demands of the users. We then propose a heuristic to solve that problem and compare our results with the results of a non-commercial optimization software and numerous Monte Carlo (MC) experiments. It is shown that our green dynamic BS planning scheme saves significant amount of energy. Although there are some studies in the literature related to the dynamic BS switching, our method differs in the following aspects:

- Unlike most of the previous studies, we utilize the dynamic power adjustment capability of the current BSs technology by adjusting the output of the power amplifier. Using different transmission PLs, we have the opportunity to dynamically change the coverage of the BSs according to the present traffic conditions.
- Majority of the studies in the literature assume that BSs make switch on or off decisions locally by comparing their current traffic loads with a predefined threshold. In our work, we try to satisfy certain GoS requirements collectively by making system-wide decisions throughout the whole network.
- The BS on/off transitions are taken into account in order to minimize the additional overhead introduced by frequent topology changes such as BS initialization, user association, and handover.
- We justify our proposed methods by applying them to real-life-scale scenarios rather than small-scale test cases.

- A detailed integer NLP model is formulated for the GDBP problem and solved by a non-commercial optimization tool. By using the derived programming model, optimum results can be obtained from the optimization tools for the small instances of the problem. In order to show the significance of the results, a very large number of MC experiments are also conducted.
- A fast and effective heuristic called FastWISE is proposed for solving large instances of the GDBP problem.

The rest of this chapter is organized as follows: In Section 3.2, we elaborate the proper application areas of the GDBP, assumptions, and problem formulation. The proposed GDBP algorithm is explained in Section 3.3. An example application scenario, details of the system parameters, and comparative performance analysis of the proposed methods are presented in Section 3.4. Finally, Section 3.5 draws the conclusions.

3.2. System model

Before going into detail, possible application areas of the GDBP along with their advantages and disadvantages are investigated from the green networking perspective.

3.2.1. Where should GDBP be applied?

As we mentioned before, the primary objective of GDBP is to save energy while satisfying a certain level of service quality. Hence, there must be excess energy consumption in order to benefit from GDBP properly. If the energy is already being used effectively, applying an energy-saving method will be nothing more than unnecessary increase of complexity.

Crowded urban areas with high BS densities are the most suitable places for GDBP rather than suburban or rural areas. However, each urban area has its own traffic pattern which directly determines the efficiency of the GDBP. Therefore, we categorize urban areas into four distinct regions and comment on those regions whether

GDBP should be applied or not.

- *Town centers (business).* Business, trade, or industrial areas as well as commercial centers can be considered in this class. The user density, hence the offered traffic load, is quite high in these places during the daytime. However, the user density and the traffic load drop sharply during the night-time since most of the business and commercial areas are closed. Moreover, low traffic profiles continue all day long during weekends and holidays. Therefore, a significant change in the traffic profile occurs throughout the day and week, which makes business town centers the most suitable place for GDBP to be applied.
- *Town centers (entertainment).* This kind of places include shopping and exhibition centers, tourist attraction points, museums, and concert halls. Although the traffic profile of entertainment and business town centers follow a similar pattern, they differ during weekends and holidays. Entertainment town centers are also highly preferred during weekends and holidays, even more than weekdays. However, the temporal change throughout the day does not happen to be as much as in the business town centers. Therefore, entertainment town centers are our secondary target for energy savings.
- *Residential areas.* These regions are mostly occupied by houses, schools, hospitals, and small commercial shops such as grocery stores. User density increases here in the evening for sure. However, it would not be true to say that there is no traffic at all during the day time. Individuals such as pensioners, housekeepers, or children spend most of their time within the territory of their houses. Although the traffic load changes in residential areas within the day, it is not as explicit as in town centers.
- *Seasonal tourism centers.* In seasonal tourism centers, there happens to be two colossal changes in user density throughout the year. Sunny seasides are filled up with tourists during summer, whereas snowy ski centers are very crowded during winter. However, most of the wireless network operators simply deploy mobile BSs to those areas in order to meet the high season requirements. Since using mobile BSs is a kind of dynamic planning itself, it can be considered as a broader

and more systematic approach to GDBP including additional capabilities of BS installment and replacement.

In summary, the application site should have at least two important features in order to fully benefit from GDBP: (i) unbalanced temporal distribution of the traffic load and (ii) high BS density.

3.2.2. Assumptions

A BS can be on or off depending on the current traffic conditions in our work. When it is switched on, the total power consumption of the BS is the combination of two components [68]: (i) core power and (ii) transmission power. The BS core power consumption (such as air conditioning, signal processing) is assumed to be fixed regardless of the traffic load. However, the transmission power is adaptively adjusted to the current traffic conditions. A set of transmission PLs need to be defined according to the application requirements and the capabilities of the BS equipment in use. Each BS can select a certain PL for transmission and cannot change it during that particular time slot. Since it is not practical to model a huge number of subscribers individually, we assume users are placed as chunks, like group of workers in a floor of a building or customers waiting in a bank office.

3.2.3. Problem formulation

In order to solve the problem by classical optimization tools, we need to first put the GDBP problem into a mathematical form. In this section, we formulate our problem by using two different objective functions. The first one minimizes the total energy consumption, while the second one additionally minimizes the BS on/off transitions in order to reduce the amount of topology changes. Hence, the overhead caused by frequent topology changes, such as BS initialization, user association, and handover, can be minimized.

3.2.3.1. Plain GDBP. Our formulation consists of three parts. The first part contains the constant parameters given by our sample application scenario. The second part is the model variables which will be determined by the solver, and the last part is the problem itself.

Parameters:

N^B : Number of BSs

N^P : Number of PLs

N^U : Number of user chunks (UCs)

N^T : Number of time intervals

B : Set of BSs where $B = \{1, 2, 3 \ldots, N^B\}$

P : Set of PLs where $P = \{1, 2, 3 \ldots, N^P\}$

U : Set of UCs where $U = \{1, 2, 3 \ldots, N^U\}$

T : Set of discrete time intervals within the day where $T = \{1, 2, 3 \ldots, N^T\}$

$\mathrm{PW}^{\mathrm{core}}$: Core power consumed by the BS

$\mathrm{PW}^{\mathrm{tx}}(p)$: Function of transmission power consumed by the BS with respect to PL

α^{sw} : Penalty of making a BS switch (on/off)

W_b^{cap} : Data flow capacity of BS b

$f^{\mathrm{flow}}(t)$: Function of traffic load per UC with respect to time

β^{min} : Minimum acceptable user coverage ratio

C_{bpu} : $\begin{cases} 1, & \text{BS } b \text{ can cover user } u \text{ with power } p \\ 0, & \text{otherwise} \end{cases}$

Model variables:

$$O_{bt} = \begin{cases} 1, & \text{BS } b \text{ is up at time } t \\ 0, & \text{otherwise} \end{cases}$$

$$A_{bpt} = \begin{cases} 1, & \text{BS } b \text{ transmits with power } p \text{ at time } t \\ 0, & \text{otherwise} \end{cases}$$

$$M_{ubt} = \begin{cases} 1, & \text{UC } u \text{ selects BS } b \text{ at time } t \\ 0, & \text{otherwise} \end{cases}$$

Dummy variables:

$$\begin{aligned} S_{ubt} &= \begin{cases} 1, & \text{UC } u \text{ is served by BS } b \text{ at time } t \\ 0, & \text{otherwise} \end{cases} \\ &= \sum_{p \in P} O_{bt} C_{bpu} M_{ubt} A_{bpt} \ \forall u \in U, \forall b \in B, \forall t \in T \\ N_t^c &= \text{Number of covered UCs at time } t \\ &= \sum_{u \in U} \sum_{b \in B} S_{ubt} \quad \forall t \in T \\ N^{\text{sw}} &= \text{Number of BS switches (on/off) during 24h} \\ &= \sum_{b \in B} \sum_{t \in T} \left(O_{bt} \oplus O_{b((t+1) \bmod N^T)} \right) \end{aligned}$$

The objective function is given as

$$\min \sum_{b \in B} \sum_{p \in P} \sum_{t \in T} O_{bt} \left(\mathrm{PW}^{\text{core}} + A_{bpt} \mathrm{PW}^{\text{tx}}(p) \right) \tag{3.1}$$

subject to

$$\sum_{p \in P} A_{bpt} = 1 \quad \forall b \in B, \forall t \in T \tag{3.2}$$

$$\sum_{b \in B} M_{ubt} = 1 \quad \forall u \in U, \forall t \in T \tag{3.3}$$

$$\sum_{u \in U} S_{ubt} f^{\text{flow}}(t) \leq W_b^{\text{cap}} \quad \forall b \in B, \forall t \in T \tag{3.4}$$

$$\frac{N_t^c}{N^U} \geq \beta^{\min} \quad \forall t \in T \tag{3.5}$$

As mentioned earlier, the ultimate goal of our first objective function in Equation 3.1 is to minimize the energy power consumption of the network. The constraint in Equation 3.2 makes sure that a BS operates at a single transmission power level at any time, and Equation 3.3 is responsible for a user being served by a single BS at a particular instant. Equations 3.4 and 3.5 ensure that the resulting energy-efficient topology does not violate the capacity constraint of the BSs and provides the required coverage ratio over the area, respectively. By not violating the capacity constraints of the BS, it is also assured that subscribers receive an acceptable service quality.

3.2.3.2. GDBP with BS transition overhead. In this section, we are taking the BS transitions into account in order to minimize the additional overhead introduced by frequent topology changes such as BS initialization, user association, and handover [69]. Among them, handling the handovers is the most crucial one since it directly affects the service quality of the subscribers. Besides well-known problems inherited from conventional handover procedures, another challenging issue is to handover a group of subscribers at the same time when a serving BS is switched off. There has been some research effort on group handover techniques [70, 71], and most of them target the passengers traveling on public transportation vehicles such as buses and trains. Majority of the group handover schemes require predicting the handover and make necessary preparations before starting the handover procedure itself. In our case, the central control entity, which decides and implements the network topology changes, may do the necessary control signaling and inform the neighboring BSs about the possible group handover before shutting a BSs down. Also, a possible BS transition and handover procedure is discussed in [15].

In order to minimize the side effects of topology changes, we use a second objective function given in Equation 3.6 which minimizes the BS on/off switches in addition to the overall power consumption. The BS switch penalty, α^{sw}, controls the power consumption vs. BS transition overhead trade-off. Thus, network operators have the chance to fine tune the objective function according to their priorities. The effect of this parameter is further investigated in Section 3.4.3.

$$\min \sum_{b\in B}\sum_{p\in P}\sum_{t\in T} O_{bt}\left(\mathrm{PW}^{\mathrm{core}} + A_{bpt}\mathrm{PW}^{\mathrm{tx}}(p)\right) + \alpha^{\mathrm{sw}}N^{\mathrm{sw}} \tag{3.6}$$

Although we put the GDBP problem into a mathematical form, it is still a challenging task to solve it with the optimization tools since we use large real-life-scale test scenarios for performance evaluation. Furthermore, nonlinearity of the problem also increases its complexity and yields to longer run times. Therefore, we propose a fast heuristic to solve large-scale instances of the problem within acceptable time durations.

3.3. Green dynamic BS planning algorithm

In this section, we derive a heuristic called FastWISE which consists of three phases for the GDBP problem. Additional variables used in FastWISE:

$\mathrm{OCA}^{\mathrm{cur}}$	:	Overlapping coverage area of the current BS
$\mathrm{OCA}^{\mathrm{max}}$	:	Maximum allowed overlapping coverage area in order to switch a BS on during initialization phase
$\mathbf{B}^{\mathrm{off}}$	:	Set of currently switched off BSs
W^{cur}	:	Traffic load of the current BS
$\mathbf{B}^{\mathrm{high}}$	:	Set of switched on BSs having $W^{\mathrm{cur}} \geq W^{\mathrm{cap}}$ (users served by those BSs most likely to suffer high blocking probabilities)
CUE	:	Covered[1] user per energy ratio of the current BS when it is switched on
β^{cur}	:	Current user coverage ratio of the network

[1]Incremental users covered by that particular BS when it is switched on

————*Initialization phase*————

for all B **do**

    calculate proper[2] PL

    calculate $\mathrm{OCA}^{\mathrm{cur}}$

    if $\mathrm{OCA}^{\mathrm{cur}} \leq \mathrm{OCA}^{\mathrm{max}}$ **then**

        switch current BS on

    end if

end for

—————*Iteration phase*—————

repeat

    for all $\mathbf{B}^{\mathrm{off}}$ **do**

        calculate CUE for each power level

    end for

    switch on BS having maximum CUE

until $\beta^{\mathrm{cur}} \geq \beta^{\mathrm{min}}$

—————-*Validation phase*—————-

for all $\mathbf{B}^{\mathrm{high}}$ **do**

    repeat

        switch on the closest BS

    until $W^{\mathrm{cur}} \leq W^{\mathrm{cap}}$

end for

Figure 3.1. FastWISE algorithm.

The complete procedure of FastWISE is given in Figure 3.1. It starts with the *initialization phase*. In this phase, FastWISE visits all BSs and activates the ones which have smaller overlapping coverage than a predefined threshold with the maximum possible transmission power level. By doing this, FastWISE tries to use BSs with higher transmission power levels without violating the capacity constraints in order to give energy-saving opportunities to neighboring BSs. Therefore, a preliminary coverage is provided at the end of this phase. FastWISE continues with the *iteration phase*. The aim of this phase is to make incremental improvements at each step on top of the preliminary coverage produced by the initialization phase until a target coverage ratio throughout the network is achieved. Initially, a Covered User per Energy (CUE) ratio

[2]Proper PL is the highest possible PL that a BS can operate without violating the capacity constraint.

is calculated for each inactive BS for each power level. This ratio implies the number of additional covered users per unit energy if that particular BS is switched on. As long as the desired coverage ratio is not achieved, the BS having the highest CUE ratio is simply switched on. Unlike the initialization, the iteration phase tries to maximize the energy utilization without making any capacity constraint checks. However, this may yield to overloaded BSs which in turn cause higher call blocking probabilities. Therefore, the third step is required to validate that the traffic capacity constraints are met for all serving BSs, which is the *validation phase*. In this last part of the heuristic, all serving BSs are visited and a list of neighboring BSs is created for all overloaded ones. In order to share the load of the overloaded BSs, starting from the closest one, neighboring BSs in the list are simply activated until the offered traffic load drops below its capacity. At the end of this phase, FastWISE ensures that all serving BSs are operating well below their capacities.

3.4. Application scenario and performance evaluation

3.4.1. Application scenario and parameters

In order to model the unbalanced temporal distribution of the load created by mobile users, we assume a sinusoidal pattern throughout the day resembling the real-life traffic load given in Figure 1.2 and many other measurement studies presented in [1, 72, 73]. However, the traffic profile does not strictly have to follow the shape of a sine wave. For the GDBP, reasonable amount of temporal traffic fluctuations through out the day will create a margin for energy saving. Although we have a certain traffic profile assumption, it is still possible to engineer the shape of that profile up to some extent. For example, the night-time traffic load may not be as low as we expect or the peak-time traffic may not even get close to 100% utilization in some particular places. Therefore, we introduce a lower and a higher bound for the traffic load rather than assuming a regular sinusoidal wave ranging between 0% and 100% utilization. In fact, when we introduce those lower/higher bounds, we practically define the height and offset of the sinusoidal wave itself. Hence, they together define how the traffic load changes throughout the day. The final and vital parameter to construct the traffic

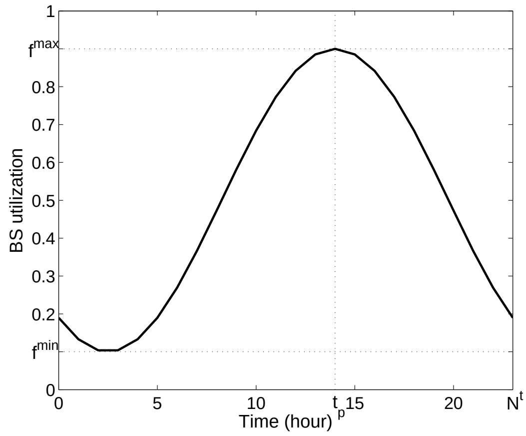

Figure 3.2. An example sinusoidal traffic load for 24h with $f^{\min} = 0.1$, $f^{\max} = 0.9$, and $\mathrm{t}^{p} = 14$h.

profile is the time slice in which the traffic load reaches its peak. With this parameter, we can shift the sinusoidal wave in time domain until it fits the traffic profile of a region of interest. The traffic function is defined as

$$w^h = \frac{f^{\max} - f^{\min}}{2} \tag{3.7}$$

$$w^o = \frac{f^{\max} + f^{\min}}{2} \tag{3.8}$$

$$f(t) = w^h \cos(2\pi \frac{t - t^p}{N_T}) + w^o \tag{3.9}$$

where $f^{\min}$ and $f^{\max}$ are the minimum and the maximum traffic loads throughout the day, w^h and w^o are the height and offset of the sinusoidal traffic wave, and t^p is the time slice in which the traffic load has its peak. An example traffic profile created by Equation 3.7 can be seen in Figure 3.2.

We adopt three distinct transmission PLs for BSs, which we believe is not irrational when the current state of the BS manufacturing technology is considered. If a BS is up, then it is transmitting with one of PL_n where $n \in \{1, 2, 3\}$. When we change the transmit power of a BS, we subsequently change its coverage range. Since all of our test area exhibits the same terrain feature (urban), a single propagation model is used throughout the whole area. However, in case of need, test area may be partitioned

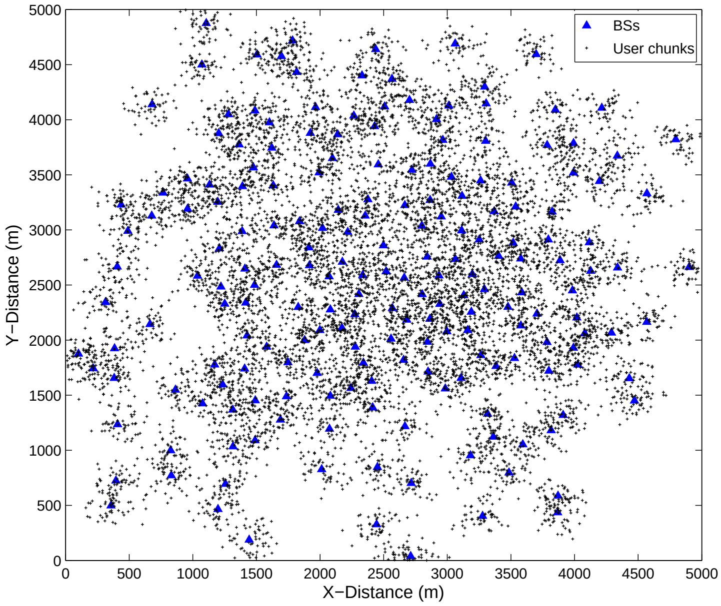

Figure 3.3. A Sample deployment configuration with 10000 UCs (1 mil. users) and 200 BSs in a 5 x 5 km^2 area.

into different terrain features and other propagation models can be incorporated for those specific portions of the coverage area. We assume perfect free-space path loss for calculating the omnidirectional coverage ranges. When we fixed the signal frequency, free-space path loss becomes proportional to the square of the distance between the transmitter and receiver. However, all propagation models can be used with our problem formulation according to the wireless channel conditions in the coverage area.

Although our model can accommodate BSs with different traffic flow capacities, we assume all BSs are identical and have the same capacity. Both user chunks and BS locations follow Gaussian distributions where BSs are centered in the middle of the area and user chunks are centered around the BSs. However, two BSs cannot be closer than the Minimum Inter-BS Distance (MIBD) to each other.

In order to make proper assessment of the proposed methods, it is required to create a test environment as close to real life conditions as possible. Therefore, we envision a densely populated (1 million subscribers) business center as advised in Section 3.2.1 which is covering an area of 5×5 km^2. We assume the traffic load follows the same pattern given in Figure 1.2 and there are 200 BSs deployed to accommodate the peak-time traffic. A sample deployment configuration used for performance evaluation is given in Figure 3.3. As GoS metrics, the network should provide the maximum of 10^{-2} blocking probability [74] and cover at least 99% of the area at all times. Important parameters used in the sample application scenario are summarized in Table 3.3. For the sake of variance control, 10 different test cases are generated and average of the results are presented.

Table 3.3. Scenario parameters.

Parameter	**Value**
Coverage Area	$5 \times 5km^2$
# BSs (N^B)	200
# UCs (N^U)	10000
Chunk size	100 users
BS Location Std.Dev.	1000m
User Location Std.Dev.	100m
MIBD	150m
BS Core Power	150 Watt
# PLs (N^P)	3
BS Transmission PLs	30 - 90 - 270 Watt
BS Coverage Distances	300 - 520 - 900 m
BS Capacity (W^{cap})	66 Erlang
Max. Prob. of Blocking	10^{-2}
Average Call Duration	30 sec
Average Call Arrival Rate	10 calls/day/user
# Time Slots Within a Day (N^T)	24
Min. Acceptable Coverage Ratio (β^{min})	99%
Penalty of a BS Switch (α^{sw})	0 - 75 - 300 - 1500

3.4.2. Experiment Methodology

Performance of FastWISE is evaluated by using real-life-scale test cases and compared with the results of a NLP tool [75]. Also, MC experiments are used by generating a large set of random solutions to investigate the statistical quality of the FastWISE results. However, the initial results of fully random MC experiments were mostly unfeasible and too poor to be compared with other results. In order to obtain more challenging results, we change the random solution generation method by assigning different probability of drawing to each case and call it MC*. By this way, we create a hundred thousand biased samples which contain much more feasible results than the fully random MC method. The idea behind MC* is to generate more suitable topology instances by taking the current traffic load into account. For example, MC* switches more BS on if the traffic load is high and less BS if the traffic load is low. Similarly, MC* favors higher power levels for the activated BSs during low traffic conditions to create a margin for neighboring BSs to save energy. Thus, MC* creates more feasible solutions than the plain MC and gives us the chance to make better assessment of the proposed techniques.

We model the problem with A Modeling Language for Mathematical Programming (AMPL) [76] and used a non-commercial nonlinear optimization tool called Basic Open-source Nonlinear Mixed INteger programming (BONMIN) [75]. However, although we use a very powerful computer, it was not possible to solve the problem as a whole due to high space and computational complexity. Therefore, we decompose the problem into smaller parts. For Plain GDBP, we solve each time slot separately and add them up to find the objective function given in Equation 3.1. We approach the second problem similarly but this time we feed the results of the previous slot as an input to the next one in order to compute the objective function given in Equation 3.6.

3.4.3. Performance Evaluation

Before proceeding to the comparative performance evaluation, we find it useful to start with examining the run times. Average run times of FastWISE and NLP which are collected from a powerful computer with 4 hexa-core Xeon x5650 2.67 GHz processors and 24 GB of memory are given in Table 3.5. For FastWISE, the iteration is observed to be the most time consuming phase as expected since small improvements are done until a target coverage ratio is achieved. However, the overall execution time of the FastWISE can be considered as acceptable. On the other hand, NLP takes longer time to find feasible solutions than FastWISE, and it increases parallel to the offered traffic load. In Table 3.5, 24 time slots are reduced to 12 since some of them have the same amount of traffic load due to the sinusoidal traffic profile. It takes close to an average of four days for the NLP tool to find a solution for one instance.

Table 3.5. Comparison of average run times.

FastWISE		**NLP**	
Phase	Run Time	Time Slot	Run Time
Initialization	4m 3s	1, 6, 24	296m
		2, 5	268m
		3, 4	253m
		7, 23	312m
Iteration	65m 46s	8, 22	423m
		9, 21	456m
		10, 20	501m
		11, 19	517m
Validation	12s	12, 18	538m
		13, 17	542m
		14, 16	535m
		15	548m
Total	70m 01s	Total	5189m

The comparative power consumptions throughout a day are given in Figure 3.4. If none of the green techniques applied to the network, the power consumption does not change throughout the day regardless of the varying traffic load. Although some amount of power can be preserved with MC*, it is clear that both FastWISE and NLP perform better in terms of the power consumption. NLP outperforms FastWISE in

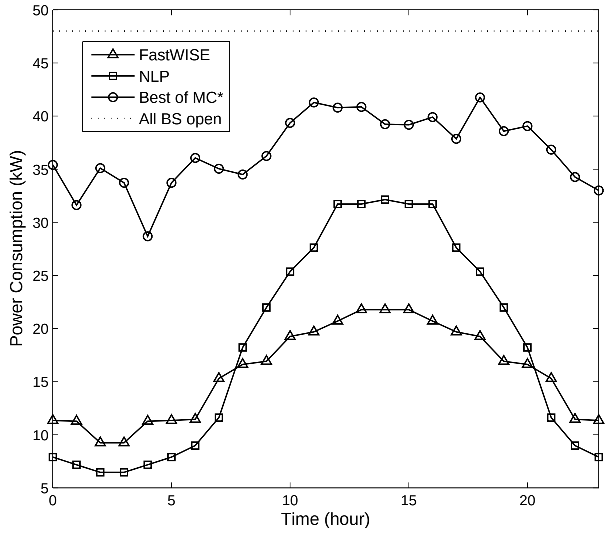

Figure 3.4. Comparative power consumption throughout a day.

light traffic conditions while the opposite is valid under heavily loaded conditions. Due to large scale of the test scenario and high computational complexity of the proposed NLP, we set a maximum iteration limit on the optimization software in order to bound the run times. It returns the best possible solution found within the given number of branch-and-bound iterations.

In Table 3.6; daily, monthly, and annual energy cost savings are given. The electricity prices for peak (2pm-8pm), shoulder (7am-2pm and 8pm-10pm) and off-peak (all other times) times are 44.11, 18.7 and 10.34 cents/kWh respectively in compliance with the EnergyAustralia [77], one of Australia's largest electricity retailers. When the given figures in Table 3.6 are scaled for the whole country, it is clear that GDBP can

Table 3.6. Comparative energy cost saving.

	Daily($)	Monthly($)	Annual($)
FastWISE	168	5,043	60,521
NLP	143	4,317	51,809
MC*	55	1,654	19,857

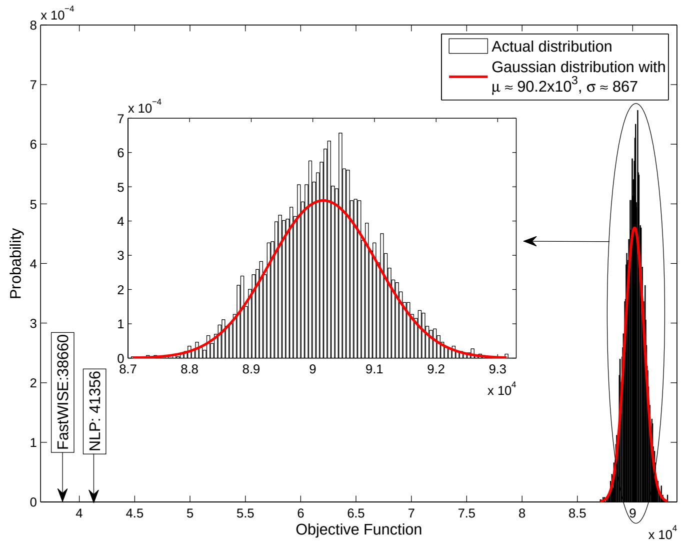

Figure 3.5. Distribution of feasible MC experiments and its comparison with FastWISE and NLP.

dramatically decrease the energy expenditures of the service providers, possibly a few millions of dollars per year, which constitutes the largest portion of the OPEX.

In Figure 3.5, the probability distribution of feasible MC experiments is given with a fitted Gaussian Distribution. When averaged results of FastWISE and NLP are given in the same figure compared with the results of the MC experiments, it is quite certain that they are statistically significantly better. In other words, it is nearly impossible to generate results with MC experiments as power efficient as the ones with FastWISE and NLP.

Figures 3.6 and 3.7 evaluate the GDBP with BS transition overhead introduced in Section 3.2.3.2. Figure 3.6 depicts the effect of α^{sw} on the objective function given in Equation 3.6. When we set $\alpha^{\text{sw}} = 0$, the objective function reduces to Plain GDBP given in Equation 3.1. For its maximum value, we set $\alpha^{\text{sw}} = 1500$. In this case, BS transition penalty in the objective function dominates the transmission power consumption and the network tends to keep its current topology rather than adapting to the changing traffic conditions. As the BS switch penalty increases, the objective function value also increases. When we set the switch penalty to higher values, the

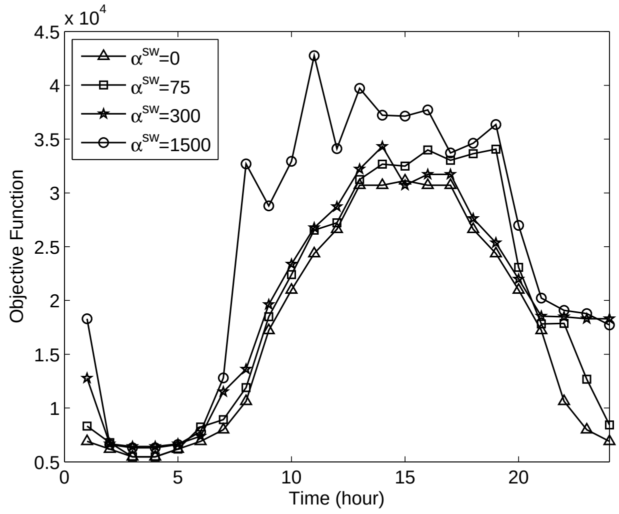

Figure 3.6. Effect of α^{sw} on the objective function given in Equation 3.6.

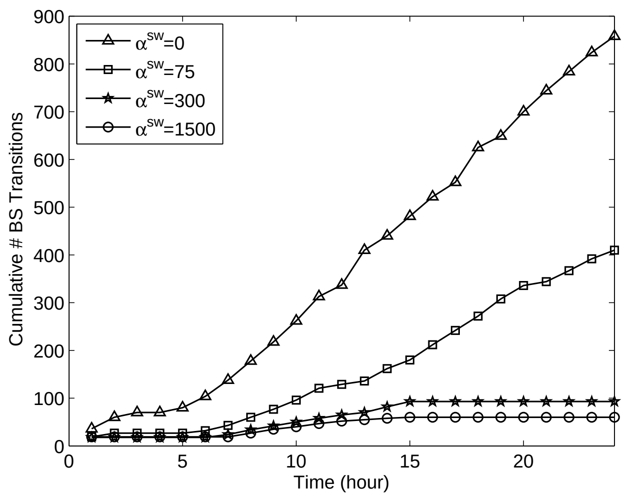

Figure 3.7. Effect of α^{sw} on the cumulative number of BS on/off transitions.

optimization tool does not switch off the redundant BSs as long as the resulting energy saving is smaller than the introduced transition overhead. Therefore, the topology is adjusted by switching large number of BSs on or off for higher transition penalties. As a result, the objection function graph takes a more zigzag like shape for higher penalties while it is smoother for lower values of α^{sw}.

When a switching penalty is introduced in the objective function, the number of BS transitions dramatically decreases as seen in Figure 3.7. This figure depicts the

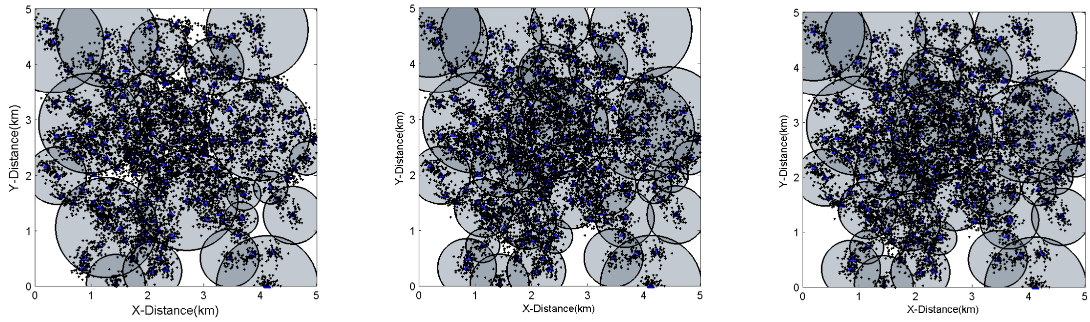

(a) After initialization phase ($\beta^{\text{cur}} = 83.06\%$, $p^{\text{blck}} = 1.7\text{x}10^{-3}$)

(b) After iteration phase ($\beta^{\text{cur}} = 99.02\%$, $p^{\text{blck}} \approx 0$)

(c) After validation phase ($\beta^{\text{cur}} = 99.02\%$, $p^{\text{blck}} \approx 0$)

Figure 3.8. Resulting coverage of FastWISE under light traffic load.

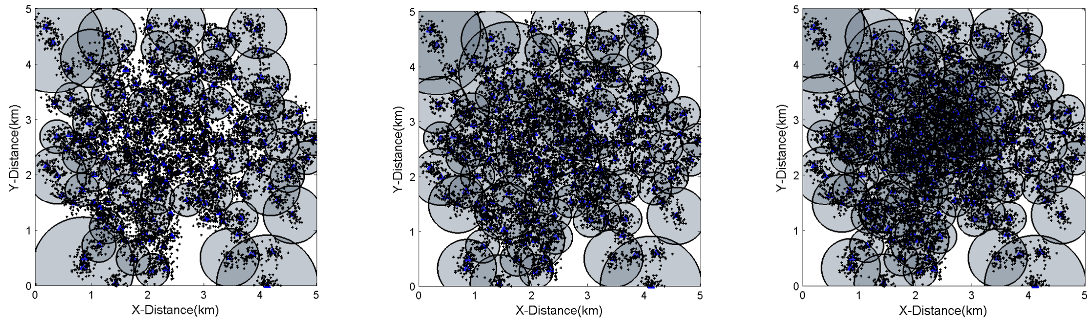

(a) After initialization phase ($\beta^{\text{cur}} = 49.12\%$, $p^{\text{blck}} = 16\text{x}10^{-3}$)

(b) After iteration phase ($\beta^{\text{cur}} = 99.1\%$, $p^{\text{blck}} = 892\text{x}10^{-3}$)

(c) After validation phase ($\beta^{\text{cur}} = 99.12\%$, $p^{\text{blck}} = 9\text{x}10^{-3}$)

Figure 3.9. Resulting coverage of FastWISE under heavy traffic load.

cumulative sum of BS transitions for different α^{sw} values. The total number of BS transitions throughout the day is reduced by 52%, 89% and 93% for $\alpha^{\text{sw}} = 75$, 300 and 1500 respectively. Hence, the additional overhead introduced by frequent topology changes are significantly reduced. However, as the BS switch penalty gets higher, the flexibility of the GDBP decreases which yields to less energy efficient solutions. Therefore, the network operators should delicately choose this parameter according to their requirements.

Figures 3.8 and 3.9 depict the coverage of FastWISE after each phase during light and heavy traffic conditions. In the initialization phase, FastWISE tries to fill the gaps without violating the capacity constraints as seen in Figures 3.8(a) and 3.9(a). Then in the iteration phase, it switches on the BSs with appropriate power levels in order to satisfy the coverage constraints as seen in Figures 3.8(b) and 3.9(b). Finally in the validation phase, FastWISE checks the offered loads for each BS and validates that they are not overloaded. If a BS is overloaded, FastWISE switches the neighboring cells on to alleviate its load until that particular BS can accommodate the offered traffic without violating the GoS constraints. The resulting coverage after the validation phase given in Figures 3.8(c) and 3.9(c).

3.5. Conclusion

In this chapter, we focus on saving energy by both switching BSs on/off and adaptively adjusting their transmission power according to the current traffic conditions. To achieve that goal, we formulated a novel nonlinear programming model for the GDBP problem to find the best possible BS topology which minimizes the energy consumption of the network while satisfying a certain level of GoS. Although optimization tools can produce optimum results for the small instances of the problem, they cannot cope with large instances as their complexity becomes prohibitive. Therefore, we derived a greedy heuristic called FastWISE to solve the large realistic size instances of the formulated problem and compared our results with the results of a non-commercial optimization tool and numerous MC experiments. It is shown that our green dynamic BS planning scheme adaptively adjusts to the current traffic load and saves significant amount of energy without violating the GoS constraints such as the probability of blocking and the coverage ratio.

4. GREEN PACKET-SWITCHED CELLULAR NETWORKS

4.1. Introduction

In this chapter, we focus on saving energy by adaptively switching the BSs of packet-switched cellular networks on and off and by adjusting the BS transmission power levels according to the present traffic conditions. Particulary, we focus on W-CDMA based packet-switched cellular networks and adopt dynamic transmission power adjustment with the help of high efficiency power amplifiers. However, the challenge is to decrease the energy expenditure while always guaranteeing a certain QoS level over the whole coverage area. We define this problem as Traffic-Aware Topology Management (TAM) problem. To address this, we formulate a novel Linear Programming (LP) model for the described TAM problem to find the best possible BS topology which minimizes the energy consumption while satisfying the certain service quality requirements of the subscribers. Although small instances of the TAM problem can be solved by the optimization tools, large realistic size problems are quite difficult to be handled due to high space and computational complexity. Therefore, we propose a novel heuristic to solve the large-scale instances of the formulated problem and compare our results with the results of two previously proposed methods [13] [14], a greedy heuristic and a commercial optimization tool. It is shown that the proposed TAM scheme helps to maintain an energy-aware network and saves significant amount of energy by adaptively adjusting the network topology according to the present traffic conditions. Although there are some studies in the literature related to the traffic-aware topology management, our method differs in the following aspects:

- Unlike most of the previous studies, where only BS on/off switching is utilized [15] [16] [17] [18], we also take into account the dynamic power adjustment capability of the current BSs technology in order to create energy-aware network topologies by defining a set of transmission PLs.
- Compared to solutions that show how much energy efficiency can be achieved or that propose heuristic algorithms [18] [65] [78], we first formulate a detailed

integer LP model for the TAM problem to minimize energy consumption while satisfying a certain level of QoS. Using this model, the problem is solved by a commercial optimization tool which provides the optimum solutions to the smaller instances of the problem.

- While some of the existing studies show how much energy efficiency can be achieved, they do not propose operating algorithms to achieve such savings [15]. Additionally, although the LP tool provides the optimum solutions, it requires long computational times and it is not possible to handle large instances due to the computational complexity. Therefore, a fast and effective heuristic called Green TAM Algorithm (GTA) is proposed and its performance is compared with the results obtained with the optimization tool and two competitor methods from the literature (i) SLAKE [13] (ii) Niu *et al.*'s Algorithm [14] in terms of running times, energy savings and energy-cost savings.
- Majority of the studies in the literature assume that the BSs make on/off decisions locally by comparing their current traffic loads with a predefined threshold [13] [15] [16]. In our work, we try to satisfy certain QoS requirements collectively by making system-wide decisions throughout the whole network. Although such a solution requires a centralized controller, it provides better energy savings by considering the system-wide details. The distributed solution for the TAM problem is studied in Chapter 5.

The rest of this chapter is organized as follows: Section 4.2 elaborates the system model, assumptions and problem formulation while the proposed solution technique is explained in Section 4.3. The proposed greedy heuristic is explained in Section 4.4. Application scenarios, details of the system parameters and comparative performance evaluation of the proposed methods are presented in Section 4.5. Finally, Section 4.6 concludes this chapter.

4.2. TAM Problem Formulation

We assume that a BS can be remotely switched on and off from a central entity according to the present traffic conditions. When a BS is up, it has the ability to change its transmission power [79] by using power amplifiers. Therefore, a set of transmission power levels is required to be defined according to the application requirements and the capabilities of the BS equipment in use. When a BS is up, it transmits with a certain power level and the status of a BS cannot be changed until the next time slot.

Since it is not practical to model a huge number of subscribers and their mobility patterns individually, the coverage region is divided into small grids. Each grid has its own characteristics in terms of user density, user mobility and traffic profile. In our system model, we take the aggregate traffic load created by the users located in these grids into account.

4.2.1. General Problem Formulation

Parameters:

N^B	: Number of BSs
N^P	: Number of PLs
N^G	: Number of grids
N^T	: Number of time slots within the day
$\mathbf{B}$	: Set of BSs where $\mathbf{B} = \{1, \ldots, N^B\}$
$\mathbf{P}$	: Set of PLs where $\mathbf{P} = \{1, \ldots, N^P\}$
$\mathbf{PA}$	: Set of active[1] PLs where $\mathbf{PA} = \{2, \ldots, N^P\}$
$\mathbf{G}$	: Set of grids where $\mathbf{G} = \{1, 2, 3 \ldots, N^G\}$
$\mathbf{T}$	: Set of discrete time slots within the day where $\mathbf{T} = \{1, 2, 3 \ldots, N^T\}$
$W(b, p)$	: Total consumed power by BS b transmitting with PL p
D_b	: Data flow capacity of BS b
$f(g, t)$	: Average aggregate traffic load generated by grid g at time t

[1] The first PL simply means that the BS is switched off and $\mathbf{PA} \subseteq \mathbf{P}$

$\beta^{\min}$: Minimum acceptable user satisfaction ratio where $0 \leq \beta^{\min} \leq 1$

$\Psi^{\min}$: Minimum acceptable SINR at the receiver

Ψ_{gbt} : Received SINR by grid g from BS b at time t

$\mathcal{L}(b,p,g)$: Path loss from BS b transmitting with PL p to grid g

Model variables:

$$A_{bpt} = \begin{cases} 1, & \text{BS } b \text{ transmits with power } p \text{ at time } t \\ 0, & \text{otherwise} \end{cases}$$

$$S_{gbt} = \begin{cases} 1, & \text{Grid } g \text{ is associated with BS } b \text{ at time } t \\ 0, & \text{otherwise} \end{cases}$$

The objective function is given as

$$\min \sum_{b\in\mathbf{B}} \sum_{p\in\mathbf{P}} \sum_{t\in\mathbf{T}} A_{bpt} W(b,p) \tag{4.1}$$

subject to

$$\sum_{g\in\mathbf{G}} S_{gbt} f(g,t) \leq \sum_{p\in\mathbf{PA}} A_{bpt} D_b \quad \forall (b \in \mathbf{B}, t \in \mathbf{T}) \tag{4.2}$$

$$\Psi_{gbt} \geq S_{gbt} \Psi^{\min} \quad \forall (g \in \mathbf{G}, b \in \mathbf{B}, t \in \mathbf{T}) \tag{4.3}$$

$$\sum_{g\in\mathbf{G}} \sum_{b\in\mathbf{B}} S_{gbt} \geq \beta^{\min} N^G \quad \forall t \in \mathbf{T} \tag{4.4}$$

$$\sum_{p\in\mathbf{P}} A_{bpt} = 1 \quad \forall (b \in \mathbf{B}, t \in \mathbf{T}) \tag{4.5}$$

$$\sum_{b\in\mathbf{B}} S_{gbt} \leq 1 \quad \forall (g \in \mathbf{G}, t \in \mathbf{T}) \tag{4.6}$$

Goal of our objective function in Equation 4.1 is to minimize the total energy consumption throughout the network. Equation 4.2 ensures that all active BSs do not exceed their data flow capacity. Equation 4.3 provides that each grid associated with a BS is being served by at least a certain Signal to Interference and Noise Ratio (SINR) value. By not violating the BS capacity and SINR constraints given in Equations 4.2 and 4.3; TAM scheme ensures the subscriber satisfaction at all times by maintaining acceptable level of quality in terms of both delay and data rate. Equation 4.4 is responsible for obtaining the required user satisfaction ratio over all users, i.e., it is guaranteed that a certain percentage of the users are covered and served properly. The constraint in Equation 4.5 makes sure that a BS operates at a single transmission PL in a particular time slot and Equation 4.6 is responsible for that a grid is being served by a single BS at a particular instant.

By integrating the capability of different capacity and power consumption models for each BS type, our TAM problem formulation gains the ability to support heterogeneous networks. Although frequent topology changes introduce additional overhead such as BS initialization, user association and handover, we believe that the overhead introduced by the BS transitions may be tolerated with proper handling mechanisms such as proactive handoff signaling and smart user association since we are working with one hour-time resolution. However, the overhead stemming from BS transitions needs to be taken into account and addressed carefully in case of shorter time slots.

4.2.2. Details of the Problem Formulation

4.2.2.1. BS Power Consumption. The total power consumption of the BS is the combination of two components: (i) Core power (ii) Transmission power. The BS core power consumption (such as air conditioning, signal processing) is assumed to be fixed regardless of the traffic load. On the other hand, the transmission power can be dynamically adjusted with the help of high efficiency power amplifiers. The total power consumption of the BS is given by [37] [80]

$$W(b,p) = \begin{cases} 0, & p = 1 \\ W_b^c + W_{bp}^{tx}, & \text{otherwise} \end{cases} \tag{4.7}$$

where W_b^c is the core power consumed by the BS b and the W_{bp}^{tx} is the transmission power consumed by the BS b while transmitting with PL p.

4.2.2.2. Interference. There are two sources of interference in W-CDMA cellular networks: intra-cell and inter-cell. The intra-cell interference is the total interference caused by the signals emitted from the serving BS and the inter-cell interference is caused by the signals transmitted from all other BSs. In perfect transmission conditions, there should be no intra-cell interference since all of the signals are orthogonal. However, the intra-cell interference cannot be totally avoided due to multipath propagation and SINR is given by

$$\Psi = SF \frac{P^r}{\alpha_o I^{\text{in}} + I^{\text{out}} + \eta} \tag{4.8}$$

where SF is the spreading factor, P^r is the received signal power, I^{in} is the intra-cell interference, I^{out} is the inter-cell interference, α_o is the orthogonality loss factor and η is the noise power.

In the TAM problem, P_{gbt}^r, I_{gbt}^{in}, and I_{gbt}^{out} are the received signal power, intra-cell interference and inter-cell interference experienced in grid g from BS b at time t in order and they are given by

$$P^r_{gbt} = \sum_{p \in \mathbf{PA}} A_{bpt} \mathcal{L}(b,p,g) W(b,p) \tag{4.9}$$

$$I^{\text{in}}_{ubt} = \alpha_o \sum_{p \in \mathbf{PA}} A_{bpt} \mathcal{L}(b,p,g) W(b,p) \tag{4.10}$$

$$I^{\text{out}}_{ubt} = \sum_{i \in \mathbf{B} | i \neq b} \sum_{p \in \mathbf{PA}} A_{ipt} \mathcal{L}(i,p,g) W(i,p) \tag{4.11}$$

When Equations 4.9, 4.10 and 4.11 are plugged in to Equation 4.8, we get Equation 4.12 and it is possible to calculate the SINR of a particular grid g served by BS b at time t. Accordingly, the achievable data rate of each user located at their corresponding grids can be inferred from their SINR value by using Shannon's formula. Since the interference dominates the SINR value, we will neglect the effect of the noise factor in the performance evaluation section for the sake of simplicity. Also, the path loss matrix $\mathcal{L}(b,p,g)$, for each BS b, PL p and grid g triple is generated beforehand by using the COST-Hata metropolitan area propagation model [12] and fed to the optimization software as an input to speed up the calculation of the SINR.

$$\Psi_{gbt} = SF \frac{\sum_{p \in \mathbf{PA}} A_{bpt} \mathcal{L}(b,p,g) W(b,p)}{(\alpha_o - 1) \sum_{p \in \mathbf{PA}} A_{bpt} \mathcal{L}(b,p,g) W(b,p) + \sum_{i \in \mathbf{B}} \sum_{p \in \mathbf{PA}} A_{ipt} \mathcal{L}(i,p,g) W(i,p) + \eta} \tag{4.12}$$

Although some assumptions are made about the BS capacity, BS power consumption, propagation and interference; our problem formulation can easily incorporate other models according to the specific requirements of the application area and BS equipments.

4.3. Green Traffic-Aware Topology Management Algorithm

In this section, we derive a deterministic heuristic called GTA to solve the large realistic instances of the formulated TAM problem. Before going into details of the GTA, some additional variables are explained.

Additional variables used in GTA:

$\mathbf{B}^{\text{off}}$: Set of currently switched off BSs

$\mathbf{B}^{\text{on}}$: Set of currently switched on BSs ($\mathbf{B}^{\text{on}} = \mathbf{B} - \mathbf{B}^{\text{off}}$)

$\mathbf{B}^{\text{high}}$: Set of BSs having $C_b^{\text{cur}} > D_b$; $b \in \mathbf{B}^{\text{on}}$ (Users served by those BSs most likely to suffer worse service quality than expected)

$\mathbf{B}_b^{\text{neig}}$: Set of neighboring BSs of the BS b; $b \in \mathbf{B}$ (At most two maximum[2] coverage distance away)

$\psi_b^{\max}$: Maximum UM of the BS b; $b \in \mathbf{B}$

ξ_b : Current SPM of BS b; $b \in \mathbf{B}^{\text{on}}$

$\hat{\xi}_{bp}$: Estimated SPM of the BS b if it is activated with PL p; $b \in \mathbf{B}^{\text{off}}, p \in \mathbf{PA}$

$\xi_{bp}^{\max}$: $max(\xi_i), i \in \mathbf{B}^{\text{on}}$ when BS b is activated with PL p; $b \in \mathbf{B}^{\text{off}}, p \in \mathbf{PA}$

$\Delta\xi_b$: Allowed SPM redundancy of BS b; $b \in \mathbf{B}^{\text{off}}$

C_b^{cur} : Current traffic load of BS b; $b \in \mathbf{B}^{\text{on}}$

W_b^{cur}: Current power consumption of BS b; $b \in \mathbf{B}^{\text{on}}$

$\hat{C}_{bp}$: Estimated traffic load of BS b if it is activated with PL p; $b \in \mathbf{B}^{\text{off}}, p \in \mathbf{PA}$

β^{cur} : Current user coverage ratio of the network

We define a new BS Utilization Metric (UM) where the optimum value is obtained when a BS is consuming minimum amount of power while operating with its maximum permitted traffic load without violating the QoS constrains. In this way, we

[2]The longest possible coverage distance between any grid-BS pair in an interference-free environment

are trying to maximize the utilization of the BS while minimizing the consumed power per bit. However, 100% BS capacity utilization may cause some problems in terms of providing the required service quality to the subscribers since there will not be any residual resources available in case of an unexpected traffic demand. Therefore, setting the maximum traffic load capacity of a BS as the 90% or 95% of its total capacity and sparing some slack resources would be useful. The maximum possible UM of a particular BS b is denoted by $\psi_b^{\max}$ and given by Equation 4.13. Additionally, we introduced a new term called Saturation Proximity Metric (SPM) which is used to measure “how close a BS is to its maximum UM" and given by Equation 4.14. As this metric gets closer to zero, it means that the BS is operating closer to its maximum UM and vice versa. High SPM values mean that the BSs are operating whether overloaded or under-utilized. $\hat{\xi}_{bp}$ is the estimated SPM of BS b if it is activated with PL p and given by Equation 4.15. This metric is calculated to decide whether a BS is eligible to be switched on or not.

$$\psi_b^{\max} = \frac{1}{W(b, p=2)} \tag{4.13}$$

$$\xi_b^{cur} = \left| \psi_b^{\max} - \frac{C_b^{\text{cur}}}{D_b W_b^{\text{cur}}} \right| \tag{4.14}$$

$$\hat{\xi}_{bp} = \left| \psi_b^{\max} - \frac{\hat{C}_{bp}}{D_b W(b, p)} \right| \tag{4.15}$$

Before explaining the algorithm itself, we will elaborate on the trade-offs and design criteria. The design criteria behind the GTA algorithm is to maximize the utilization of the active BSs in order to create a margin for the other BSs to switch off, hence save energy. To achieve that goal, we defined the previously explained parameters of UM and SPM. These parameters are merely indicators of BS utilization to observe the current status of the network and take corrective actions for saving energy. However, there is a trade-off between saving energy and subscriber satisfaction. To overcome this challenge, GTA provides required coverage while trying to keep the energy expenditure as low as possible and ensures that all BSs are operating below their maximum traffic load capacities, thus being certain that all served users are satisfied in terms of their QoS requirements.

The GTA algorithm consists of two phases which are the coverage assurance and the quality assurance phases. In the coverage assurance phase, the ultimate goal is to provide the required coverage while trying to keep the energy expenditure as low as possible. At the beginning of the coverage assurance phase, estimated SPM values are calculated for every switched off BS and PL couple and sorted ascending. Beginning from the BSs having the lowest estimated SPM value, each switched off BS is assumed to be activated. Then, the impact of that activation on the network is observed by calculating and storing the actual SPM values of all active BSs. After activating each switched off BSs and observing their impact on the network, the one having minimum estimated SPM value satisfying that the difference between the maximum SPM of switched on BSs and the estimated SPM of the current BS is smaller than a predefined threshold is switched on. Hence, we prevent the currently activated BS from reducing the SPM values of the other switched on BSs and keep the overall network energy efficient.

In summary, each switched off BS is assumed to be activated one by one, and the state of the network after this step is observed. By this way, we look one step ahead of the current state of the network for making the right decision. We activate the BS having the smallest SPM value which means that particular BS is operating close to its minimum possible power consumption rate and maximum possible traffic load. However, SPM value of a currently active BS may be reduced while switching on an additional BS since users are associated with the BS providing the best SINR value. To avoid that situation, we introduced a threshold called allowed SPM redundancy. When a BS is assumed to be activated, SPM of the other active BSs are recalculated. If switching on a BS reduces the SPM of currently active BSs less than the defined SPM redundancy threshold, that BS is allowed to be activated. However, if activating that particular BS creates more than an anticipated level of coverage redundancy, i.e., decreases the SPM of an already activated BS more than the threshold value, that BS is not activated and the next BS having the minimum estimated SPM is taken into consideration.

————–*coverage assurance phase*————–

1: Switch off all BSs
2: **repeat**
3: **for all** $i \in \mathbf{B}^{\text{off}}$ and $j \in \mathbf{PA}$ **do**
4: calculate $\hat{\xi}_{ij}$
5: **end for**
6: sort_ascending($\hat{\xi}_{ij}$)
7: **for all** $i \in \mathbf{B}^{\text{off}}$ and $j \in \mathbf{PA}$ **do**
8: assume BS i is switched on with PL j
9: **for all** $k \in \mathbf{B}^{\text{on}}$ **do**
10: calculate ξ_k^{cur}
11: **end for**
12: **end for**
13: activate BS $i \in \mathbf{B}^{\text{off}}$ with PL $j \in \mathbf{PA}$ having minimum possible $\hat{\xi}_{ij}$ satisfying $\xi_{ij}^{\max} - \hat{\xi}_{ij} < \Delta\xi_i$
14: **until** $\beta^{\text{cur}} \geq \beta^{\min}$

————–*quality assurance phase*————–

15: **repeat**
16: **for all** $i \in \mathbf{B}^{\text{high}}$ **do**
17: **for all** $j \in (\mathbf{B}_i^{\text{neig}} \bigcap \mathbf{B}^{\text{off}})$ and $k \in \mathbf{PA}$ **do**
18: calculate $\hat{\xi}_{jk}$
19: **end for**
20: activate BS $j \in \mathbf{B}_i^{\text{neig}}$ with PL $k \in \mathbf{PA}$ having the smallest $\hat{\xi}_{jk}$
21: **end for**
22: **until** $\mathbf{B}^{\text{high}} = \emptyset$

Figure 4.1. Green TAM algorithm.

The second phase is the quality assurance phase. The aim of this phase is to ensure that all BSs are operating below their maximum traffic load capacities, thus making sure that all served users are satisfied in terms of their QoS requirements. If offered traffic load of a particular BS is higher than its capacity, all switched off neighboring BSs are visited and their estimated SPMs are calculated. The neighboring BS having the smallest estimated SPM is activated until the traffic load of that particular BS decreases below its maximum traffic load capacity.

The complexity function of the GTA is polynomial and the highest order is found in line 10 of the algorithm. Computational complexity of the GTA is $O(N^7)$ and the affecting parameters are the number of time slots, the number of BSs, the number of power levels, the coverage area and the grid area.

4.4. Greedy TAM Heuristic

In this section, we introduce a greedy heuristic to solve the formulated TAM problem. The results of this heuristic are also used during the comparative performance evaluation in Section 4.5.2. It starts with activating all BSs with their maximum transmission PL. Then the heuristic visits each BS one by one and tries to deactivate the under-utilized ones. If deactivation is not possible, then seeks for an opportunity to decrease their transmission PL without violating the QoS constraints.

```
Activate all BSs with max PL
for all i ∈ B and j ∈ P do
    Set PL of BS i to minimum possible[3] j without violating the QoS constraints
end for
```

Figure 4.2. Greedy TAM Heuristic.

4.5. Application Scenario and Performance Evaluation

4.5.1. Application Scenario and Parameters

In order to make proper assessment of the proposed methods, it is required to create a test environment as close to real life conditions as possible. However, it is mostly not possible to solve large problem instances with the formal optimization tools like CPLEX [81] or GUROBI [82]; due to very high space and computational complexity. Therefore, we envisioned a small and a large test scenario for the performance evaluation. By solving the small instances of the TAM problem with the optimization tool and the proposed GTA, we show the effectiveness of our heuristic and then apply our heuristic to large problem instances confidently.

[3] Note that $j \in \mathbf{P}$ which includes switching a BS off with $j = 0$

We adopt three distinct transmission PAs for BSs in compliance with the current state of the BS manufacturing technology. If a BS is up, it transmits with one of the power levels p_i where $i \in \{2, 3, 4\}$ and if the BS is switched off its power level is set to one. Since all of our test area exhibits the same terrain feature (urban), a single propagation model suitable for metropolitan areas (COST-Hata [12]) is used throughout the whole area. However, in case of need, the test area may be partitioned into sub-areas containing different terrain features and other propagation models can be incorporated for these specific portions of the coverage area.

Although our model can accommodate BSs with different traffic load capacities, we assume all BSs are identical and have the same capacity for the performance evaluation purposes. For the small test instance, the whole coverage area is composed of a business center and the maximum aggregate traffic load of each 50×50 m^2 grid is assumed to be 4 Mbps. For the large test instance, there are three different regions which are a business center, a residential area and a forest/park. Each 100×100 m^2 grid creates an aggregate of 10, 4 and 0.01 Mbps maximum traffic respectively. BSs are deployed according to the specific traffic requirements of each grid in the coverage area. However, two BSs cannot be closer than the MIBD to each other.

We take the Maslak district of Istanbul as an example for our test scenarios which is covering an area of $5 \times 5\, km^2$ as depicted in Figure 4.3. We assume that the aggregate traffic load of each grid type follows their specific patterns given in Figure 4.4 and there are 200 BSs deployed to accommodate the peak-time traffic. As QoS metrics, proposed adaptive topology should satisfy the minimum aggregate data rate requirements of each grid in the coverage area and cover at least 99% of the area at all times. Important parameters used in the sample application scenario are summarized in Table 4.3. For the sake of variance control, 10 different test cases are generated for each of the small and large scenarios and the average of the results are presented.

4.5.1.1. Traffic Pattern. Similar to Section 3.4, we assume a sinusoidal pattern throughout the day resembling the real-life traffic profile given in Figure 1.2 and the many other

Table 4.3. Scenario parameters.

Parameter	**Value**	
	Small	**Large**
Coverage Area	$1 \times 1\, km^2$	$5 \times 5\, km^2$
# BSs (N^B)	30	200
Grid Area	$50 \times 50\, m^2$	$100 \times 100\, m^2$
# Grid Types	1	3
MIBD	100m	
BS Core Power	60 Watt	
# PLs	3	
BS Transmission PLs	12 - 36 - 108 Watt	
BS Traffic Capacity (D)	100 Mbps	
# Time Slots in a Day	24	
Min. Coverage Ratio ($\beta^{\min}$)	99%	
Min. SINR ($\Psi^{\min}$)	6 dB	
Spreading Factor	32	
Orthogonality Loss Factor (α_o)	0.5	
Allowed SPM Redundancy ($\Delta\xi$)	20%	

measurement studies presented in [1, 72, 73]. The traffic function is defined as:

$$w_g^h = \frac{f_g^{\max} - f_g^{\min}}{2} \tag{4.16}$$

$$w_g^o = \frac{f_g^{\max} + f_g^{\min}}{2} \tag{4.17}$$

$$f(g,t) = w_g^h cos(2\pi \frac{t - t_g^p}{N^T}) + w_g^o \tag{4.18}$$

where $f_g^{\min}$ and $f_g^{\max}$ are the minimum and the maximum aggregate traffic loads of grid g throughout the day, w_g^h and w_g^o are the height and offset of the sinusoidal traffic wave

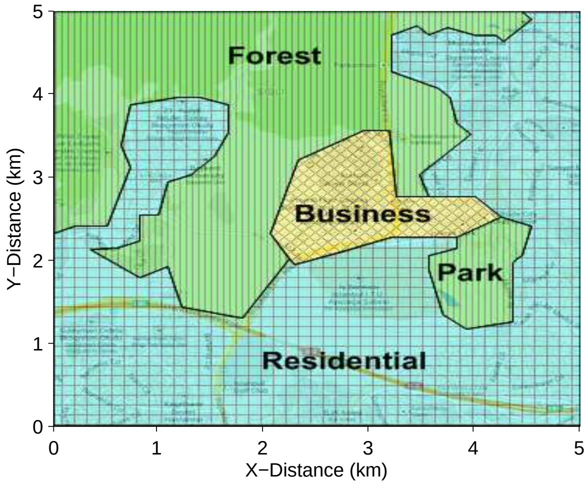

Figure 4.3. Three different regions of Maslak, Istanbul.

of grid g and t_g^p is the time slot in which the aggregate traffic load of grid g has its peak. Although the TAM problem formulation has the flexibility to assign different traffic profiles for each grid, we define three distinct traffic profiles for the business center, the residential area and the forest/park as seen in Figure 4.3 by utilizing Equation 4.16. Figure 4.3 depicts a rough partitioning of the Maslak district and its neighborhood. Created traffic profiles can be seen in Figure 4.4 where t_b^p, t_r^p and t_f^p are the peak time slots; $f_b^{\min}$, $f_r^{\min}$ and $f_f^{\min}$ are the minimum aggregate traffic loads and finally; $f_b^{\max}$, $f_r^{\max}$ and $f_f^{\max}$ are the maximum aggregate traffic loads of the girds for business center, residential area and forest/park respectively.

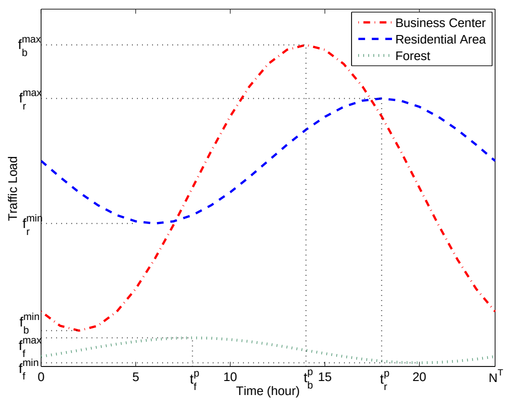

Figure 4.4. Three example normalized traffic profiles created by using Equation 4.16 for $N^T = 24$.

4.5.2. Performance Evaluation

Performance of GTA is evaluated by using both small-scale and large real-life-scale test cases and compared with the results of an LP tool [81], a greedy heuristic and two competitor green BS planning algorithms previously proposed in the literature [13,14]. Among the competitor algorithms, SLAKE [13] is a distributed sleep-wake up algorithm inspired by the ecological protocooperation principle. It consists of a sleeping and a traffic distribution procedure. On the other hand, Niu et al. Algorithm [14] utilizes the cell zooming concept for energy saving to adaptively adjust the size of the cells according to the current traffic load. It is assumed that a cell zooming server which is a virtual entity in the network controls the procedure of cell zooming.

We modeled the TAM problem with AMPL [76] and used a commercial linear optimization tool IBM ILOG CPLEX [81] to solve it. In order to reduce the space and computational complexity of the problem, we decompose the problem into smaller parts independent from each other. We solve the problem for each time slot separately and add them up to find the objective function given in Equation 4.1.

Before proceeding to the details of the comparative performance evaluation, we find it useful to start with examining the average run times of the applied methods. Average run times of GTA, greedy heuristic, LP tool and SLAKE which are collected from a computer with 4 hexa-core Xeon x5650 2.67 GHz processors and 24 GB of

Table 4.5. Comparison of average run times.

	Small Scenario	Large Scenario
GTA	33s	3h 14m 13s
Niu et al. Algorithm	20s	2h 16m 44s
Greedy Heuristic	2s	13m 23s
LP Tool	5m 46s	-
SLAKE	9s	39m 31s

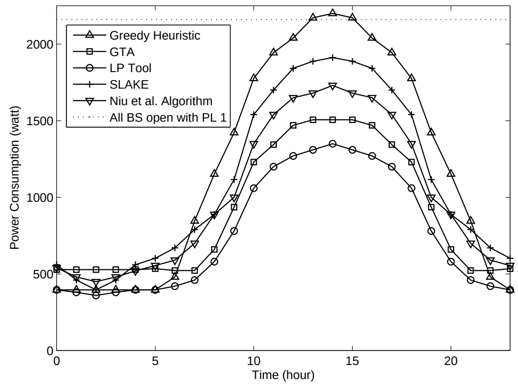

Figure 4.5. Comparative power consumption throughout a day for the small test scenario.

memory are given in Table 4.5. For the small test scenario, the greedy heuristic is the fastest method as expected. On the other hand, the LP tool consumes much more time compared to the other methods since it tries to find the exact optimum solution. For the large test scenario, GTA requires more than three hours to find an energy efficient topology for one day. Although each time slot has different run times due to the different amount of offered traffic loads, it takes approximately 8 minutes to find a feasible solution for a time slot.

The comparative power consumptions throughout a day are given in Figure 4.5 for the small test scenario. If none of the green techniques are applied to the network, the power consumption does not change throughout the day regardless of the varying traffic load. On the other hand, LP tool provides the optimum solutions and finds the most power efficient topologies possible. Although some amount of power can be preserved with the greedy heuristic, it is clear that GTA, SLAKE and Niu *et al.*'s Algorithm perform better in terms of power efficiency. When we compare GTA and SLAKE, GTA achieves an average of 19% more power savings and creates a more energy-aware network compared to SLAKE. Similarly, GTA achieves 11% more power savings than Niu *et al.*'s Algorithm. As opposed to competitor methods, our proposed GTA utilizes the dynamic tx power adjustment capability of BSs and incorporates better decision metrics such as BS UM and SPM to minimize the total network power consumption.

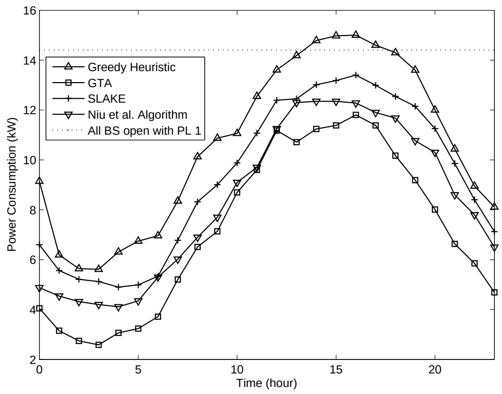

Figure 4.6. Comparative power consumption throughout a day for the large test scenario.

Figure 4.6 depicts the comparative power consumptions for the large test scenario. It is possible to observe that the power expenditure trends of all methods are proportional to the total aggregate traffic load of the network. However, GTA saves the largest amount of power and achieves 50%, 32%, 22% and 14% more power reduction with respect to the static BS operation, greedy heuristic, SLAKE and Niu *et al.*'s Algorithm in order.

In Table 4.6; daily, monthly and annual energy cost savings are given. The electricity prices for peak (5pm-10pm), morning (6am-5pm) and off-peak (10pm-6am) times are 39.38, 22.01 and 9,48 kurus/kWh (0,18, 0,1 and 0,04 $/kWh) respectively including the 22% tax for the industrial consumers in compliance with the TEDAS (Turkish Electricity Distribution Company) [83], Turkey's governmental electricity retailer company. City-wide and country-wide savings are calculated by comparing parameters of the test case with the total urban surface area and total urban population of Istanbul and Turkey respectively. Istanbul with more than 14 million inhabitants, is one of the biggest cities in the world and constitutes approximately 20% of the Turkey's population. Therefore, the respective increase between the test case and the city-wide cost savings may seem to be very high while the increase between the city and country-wide cost savings are quite low for this specific example. On the other hand, for another service provider operating in a country with smaller but many cities, significant savings can be still obtained.

Table 4.6. Comparative energy cost saving.

	Daily($)	Monthly($)	Annual($)			
			Test Case	City-wide	Country-wide	Country-wide with CE
GTA	60	1,827	21,925	4,670,025	17,279,092	49,072,621
Niu et al. Algorithm	58	1,744	20,929	4,457,877	16,494,144	46,843,368
SLAKE	55	1,674	20,096	4,280,448	15,837,657	44,978,945
Greedy Heuristic	52	1,575	18,901	4,025,913	14,895,878	42,304,293

When the numbers in Table 4.6 are examined, it is possible to say that the proposed traffic-aware topology management scheme can dramatically decrease the energy expenditures of the service providers. For this example, GTA can achieve more than 4 million $ cost savings for Istanbul and 17 million $ for Turkey. Moreover, a new term called “Cascade Effect" (CE) is introduced in [84] and demonstrated that a 1 Watt savings at the processor level produced a 2.84 Watt savings at the facility level through the CE. When this effect is taken into account, the actual amount of energy savings and CO_2 emission reduction becomes much more than the predicted raw amounts as shown in the last column of Table 4.6.

In Table 4.7; the total energy savings throughout a day compared to the cases that all BSs operate with PL 1, PL 2 and PL 3 are given. As expected, more energy can be saved as the normal operation transmission power of the BSs increases. GTA

Table 4.7. Total energy savings throughout a day compared to all BSs operate with PL 1, PL 2 and PL 3.

	PL 1 (kWh)	PL 2 (kWh)	PL 3 (kWh)
GTA	173.65	288.85	634.45
Niu et al. Algorithm	146.41	261.60	607.20
SLAKE	124.06	239.26	584.86
Greedy Heuristic	91.47	206.67	552.27

achieves 18%, 39% and 89% more energy consumption for the PL 1 case; 10%, 21% and 40% for PL 2 case; 5%, 9% and 15% for the PL 3 case with respect to Niu *et al.*'s Algorithm, SLAKE and greedy heuristic in order.

4.6. Conclusion

In this chapter, we focus on saving energy in heterogeneous packed-switched cellular networks by both switching BSs on/off and adaptively adjusting their transmission powers according to the current traffic conditions. We formulated a novel linear programming model for the TAM problem and try to find the best possible network topology which minimizes the total energy consumption without degrading a certain level of QoS. We also derived a deterministic heuristic called GTA to solve the large realistic instances of the formulated TAM problem. In order to make an accurate performance evaluation of the proposed methods, we derived small and large test scenarios and compared our results with the results of a commercial optimization tool, a greedy heuristic and two competitor green BS planning algorithms previously proposed in the literature. It is shown that our traffic-aware topology management scheme adapts the current traffic conditions and saves significant amount of energy without violating the QoS constraints of the subscribers.

5. GREEN NEXT GENERATION MULTI-TIER CELLULAR NETWORKS

5.1. Introduction

In this chapter, our goal is to derive efficient green network design, deployment and operation techniques for NGMCNs. Since NGMCNs are not fully deployed and operational for the time being, we design the network as green from the beginning and keep green during the network operation phase. This chapter of the thesis consists of three work packages. The first work package is the mapping process of a pilot application area and creating a spatio-temporal user density estimation. The second work package is the deployment of additional pico BSs on top of the existing network infrastructure to accommodate the peak traffic conditions. We keep the current network infrastructure because it is more cost-efficient from the service provider's point of view. Finally, the third work package is the green dynamic BS operation of the network consisting of heterogeneous elements for power saving.

In the first work package, we create a detailed 3-Dimensional map of the pilot application area to be used in the second and third work packages. In the second work package, given the peak traffic loads and a set of currently deployed micro BSs in the coverage area, we formulate a mathematical optimization model to address the green pico BS deployment problem. We also propose a novel heuristic and a greedy algorithm to install the minimum number of pico BSs to support the peak traffic conditions without compromising the QoS requirements of the subscribers. Lastly, in the third work package, we formulate a novel LP model for the green dynamic BS operation problem to find the optimum topology which minimizes the power consumption while satisfying certain service quality standards such as coverage and achievable data rate. Along with the problem formulation, we also propose an offline-centralized, an online-distributed and two centralized greedy algorithms to solve it. For comparative performance evaluation, we compare the results of our proposed green BS deployment and dynamic operation methods with two of the previously proposed techniques [15] [30] in the literature and a commercial optimization tool.

Although there are some studies in the literature related to the traffic-aware topology management, our method differs in the following aspects:

- Similar to the previous methods proposed for CCNs and PSCNs in Chapters 3 and 4, we utilize the dynamic power adjustment capability of the BSs in order to create more energy-aware network topologies.
- We justify our proposed methods by applying them to scenarios as close to real life conditions as possible. For this purpose, we created a detailed map of the Taksim area for a better estimation of the spatio-temporal user density. To the best of our knowledge, this kind of detailed user density estimation study of a particular area is one of its kind in the literature.
- We propose to deploy additional pico BSs on top of the existing network infrastructure to meet the increasing data exchange requirements of the subscribers. Therefore, our green networking strategy is not limited to dynamic operation only, but also encompasses the network design and deployment phases.
- We provide low complexity heuristics for both green pico BS deployment and green dynamic BS operation problems. These heuristics can be also considered as operating algorithms to achieve the provided power saving figures in Section 5.5.2.
- We derive both offline-centralized and online-distributed algorithms along with two centralized greedy algorithms to solve the green dynamic BS operation problem. Hence, cellular network operators have the freedom to apply the most suitable approach according to their specific requirements.

5.2. Spatio-temporal User Density Estimation of the Pilot Application Area

We select Taksim [85] as our pilot application area which is a highly crowded urban center composed of various places such as offices, schools, shopping malls, cafes, restaurants, bars and tourist attraction points. Firstly, a satellite image raster map

Figure 5.1. Blueprint of Taksim area shapes and labels.

of the Taksim area is created as a base for further operations. This base is obtained by merging 17 high resolution Google Earth [86] images into a single map. On top of the base map, each structure / building / street is drawn as rectangular shapes and a blueprint of the coverage area is created in Microsoft Visio [87] with a resolution of two meters. Subsequently, each rectangular shape is labeled with a unique id to facilitate the classification and prevent possible conflictions. Resulting blueprint of the Taksim area is given in Figure 5.1. This map, which includes 1365 lines and 1080 labels, is created with an effort of more than 80 working hours.

Before proceeding to collect the required data for traffic demand estimation, we created 17 class types for places in Taksim area and they are listed in Table 5.1. The reason behind this classification is to make a better spatio-temporal traffic estimation. By assigning a class type to each shape created in the blueprint, we will be able

Table 5.1. Shape types.

Type No	Type Name
1	Cafe/Restaurant Early Closing
2	Cafe/Restaurant Late Closing
3	Bar/Night Club
4	Shopping
5	Office/Work Place Early Closing
6	Office/Work Place Late Closing
7	Mosque/Church
8	School Weekday
9	School All Week
10	Pedestrian Road Heavily Crowded
11	Pedestrian Road Lightly Crowded
12	Residential
13	Movie Theater Art Gallery
14	Otel
15	Hostel
16	Hospital
17	Derelict Building

to simulate the overall traffic demand of the coverage area. Each class is carefully identified to create a model of the Taksim area as close to real life situation as possible. Since Taksim is a highly crowded urban area composed of a variety of places, further reduction in the number of classes may decrease the accuracy of the traffic demand estimation. On the other hand, the accuracy may be improved by increasing the number of classes with a cost of introducing additional overhead and complexity to the classification process. We try to keep the class count as low as possible while maintaining an acceptable level of traffic demand estimation accuracy.

In Table 5.2, an example of the collected data is depicted for traffic demand estimation. The first set of collected data is the X and Y coordinates of the shape corners. By collecting the coordinate data, we determine the boundaries of each shape and able

Table 5.2. Shape numeric values example.

Label	P1		P2		P3		P4		Floor		Type	Description
No	X	Y	X	Y	X	Y	X	Y	Start	End		
1	943	576	902	565	900	576	940	587	0	2	5	Institut Francais Office
2	978	587	943	576	928	633	941	636	0	2	9	Institut Francais Course
3	931	622	905	616	902	627	928	633	0	2	5	Institut Francais Office
4	914	580	900	576	888	624	902	627	0	2	9	Institut Francais Course
5	940	587	914	580	905	616	931	622	0	1	9	Institut Francais Course
6	885	560	869	555	863	580	885	588	0	2	1	Restaurant Early
									2	4	6	CHP Beyoglu District Presidency
7	885	588	863	580	851	622	876	628	0	2	7	Armenian Church
8	893	625	878	621	872	645	887	651	0	1	5	Dry Cleaning, Funeral and Undertaking
									1	3	5	Office Early
9	862	548	851	542	841	566	855	572	0	8	5	Office Early
10	851	542	844	539	834	562	841	566	0	1	2	Bereket Halk Doner
									1	8	6	Office Late
11	844	539	838	536	828	558	834	562	0	1	13	AFM Cinema
									1	5	2	Burger King
12	838	536	832	533	822	553	828	558	0	7	2	Borsa Restaurant
.	.	.	.	.	.	.	.	.	.	.	.	.
.	.	.	.	.	.	.	.	.	.	.	.	.
.	.	.	.	.	.	.	.	.	.	.	.	.
1079	333	469	327	468	324	522	329	523	0	1	11	Pedestrian Road Lightly Crowded
1080	318	398	314	396	268	443	271	448	0	1	11	Pedestrian Road Lightly Crowded

to associate each grid with their respective shape type. However, coordinates of the four corners only allow us to create a 2-Dimensional occupancy map of the area. Therefore, we also collected the ground and top floors of each place as an additional coordinate of Z to model the traffic demand in 3-Dimensions. Up to this point, collected data may be extracted by using satellite images and street view of Google [88], Yandex [89] and OpenStreet [90] Maps. However, it is not as easy as it seems to collect the ground and top floors of each place. Taksim area is required to be visited many times to collect this information properly. Last and the most time consuming part of the table is the type and brief description of the shape. Each place needs to be identified, which means tens of kilometers of hiking in the coverage area, and then classified as one of the types given in Table 5.1.

The reader may notice that there are some shapes consisting of more than one place type. This issue raises when there are multiple type of places located in the same

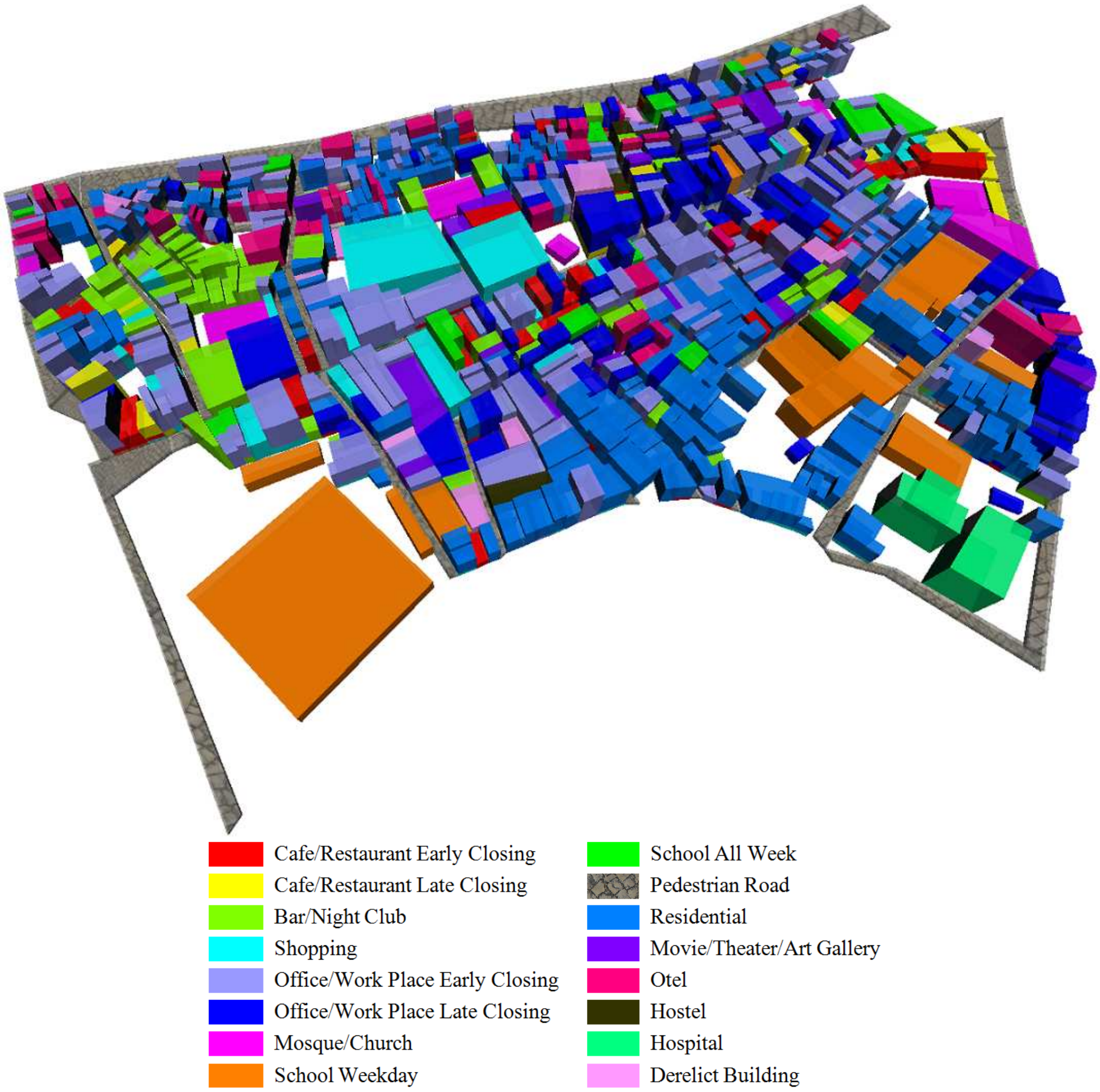

Figure 5.2. 3D model of the pilot coverage area.

building. Shape number 6 in Table 5.2, which is a four-story building, may be an example of this situation. There is a restaurant in the first two floors while the remaining two floors of the same building are occupied by the district presidency of a major political party in Turkey. Since the explained situation is very common in Taksim area, we identified 1534 different places although there are 1080 structure/building/street labeled in the blueprint given in Figure 5.1. Identification and classification of the places to fill Table 5.2 took approximately 200 working hours.

After completing the shape numeric values sheet given in Table 5.2, a 3D model of the coverage area is created by using X3D [91], an XML-based 3D graphics tool. The resulting 3D model along with its color code can be seen in Figure 5.2. An additional software is developed in Microsoft Visual Studio 2008 [92] to create the X3D code itself. Although the color-coded 3D model of the coverage area represents a useful visualization, it does not provide much by itself about the spatio-temporal user density of the area. Therefore, we are also required to estimate the average user densities of each place type throughout the day to create a complete traffic load view of Taksim area. For this purpose, we collected another set of data given in Table 5.3. In the table, estimated average user densities per $10m^2$ is provided both for weekday and weekend. Presented data is the result of countless observation expeditions being made to the coverage area during different times of the day. Besides its scientific side, the observer has also accumulated very precious social real life experience during these expeditions by having chance to visit various type of places located in one of the most crowded and cosmopolitan region around the world.

All the numbers provided in Table 5.3 are carefully assigned to each place type. As an example, the user density of Taksim Commercial Vocational High School, which needs to be classified as “School Weekday", increases dramatically just before the beginning of the class hours. User volume is maintained till the end of classes. However, the density in the evening does not drop as sharp as it increases in the morning due to many reasons such as club or sports activities, additional classes for the voluntary students. After a certain point, the school is quite vacant for the remainder of the day until the start of the class hour in the next day. As expected, the user density is observed to be very low for “School Weekday" type places during weekend. On the contrary, Cumhuriyet Meyhanesi, which needs to be classified as “Bar/Night Club", is very dense during nights. This density further increases at the weekends. As a result, complete 3-Dimensional view of the spatio-temporal user density estimation in Taksim area is obtained by applying the figures given in Table 5.3. To the best of our knowledge, this kind of detailed user density estimation study of a particular area is one of its kind in the literature.

Table 5.3. User density estimations of each type for $10m^2$ area.

Type	Timeslot																							
	#1	#2	#3	#4	#5	#6	#7	#8	#9	#10	#11	#12	#13	#14	#15	#16	#17	#18	#19	#20	#21	#22	#23	#24
WEEKDAY																								
1	0.1	0.1	0.1	0.1	0.1	0.5	0.5	1	1	1.5	1.5	2	3	3	2	1.5	1.5	2	2	2	1	0.5	0.5	0.1
2	3	3	2	2	1	0.5	0.5	0.1	0.1	0.1	0.1	0.1	0.1	0.5	0.5	0.5	0.5	0.5	0.5	1	1.5	1.5	2	3
3	5	4	3	2	1	0.1	0.1	0.1	0.1	0.1	0.1	0.1	0.1	0.1	0.1	0.1	0.1	0.1	0.5	1	2.5	4	5	5
4	0.1	0.1	0.1	0.1	0.1	0.1	0.5	0.5	1	1.5	1.5	1.5	2	2	2	2	2	2	2	2	1.5	1	0.5	0.1
5	0.1	0.1	0.1	0.1	0.1	0.5	0.5	1	2	3	3	3	2.5	3	3	3	3	2	1	0.5	0.1	0.1	0.1	0.1
6	0.1	0.1	0.1	0.1	0.1	0.5	0.5	1	2	3	3	3	2.5	3	3	3	3	3	3	3	2	1	0.5	0.1
7	0.1	0.1	0.1	0.1	0.1	1	0.5	0.5	0.5	1	1	1	2	1	1	2	1	1	2	1	1	0.5	0.1	0.1
8	0.1	0.1	0.1	0.1	0.5	2	3	5	5	5	5	5	5	5	5	5	5	3	1	1	0.5	0.1	0.1	0.1
9	0.1	0.1	0.1	0.1	0.5	0.5	1	2	2.5	2.5	2.5	2	2	2.5	2.5	2.5	2.5	2.5	2.5	2	2	1	0.1	0.1
10	4	3	2	1	1	2	3	3	3	3	3.5	4	4	3.5	3	3	3	4	5	5	4	4	4	4
11	1.2	0.9	0.6	0.3	0.3	0.6	0.9	0.9	0.9	0.9	1.05	1.2	1.2	1.05	0.9	0.9	0.9	1.2	1.5	1.5	1.2	1.2	1.2	1.2
12	1	1	1	1	1	1	1	0.5	0.5	0.5	0.5	0.5	0.5	0.5	0.5	0.5	0.5	0.5	1	1	1	1	1	1
13	0.1	0.1	0.1	0.1	0.1	0.1	0.5	0.5	1	2	2	3	3	4	4	4	4	5	5	5	5	5	4	2
14	2	2	2	2	2	2	2	1.5	1	1	1	1	1	1	1	1	1	1	1.5	1.5	1.5	2	2	2
15	5	5	5	5	5	5	5	4	2	2	2	2	2	2	2	2	2	2	3	4	4	5	5	5
16	1.2	1.2	1.2	1.2	1.2	1.2	2	2.5	2.5	2.5	2.5	2.5	2.5	2.5	2.5	2.5	2.5	2	1.2	1.2	1.2	1.2	1.2	1.2
17	0	0	0	0	0	0	0	0	0	0	0	0	0	0	0	0	0	0	0	0	0	0	0	0
WEEKEND																								
1	0.1	0.1	0.1	0.1	0.1	0.9	0.9	1.8	1.8	2.7	2.7	3.6	5.4	5.4	3.6	2.7	2.7	3.6	3.6	3.6	1.8	0.9	0.5	0.1
2	6	6	4	4	2	1	1	0.2	0.2	0.2	0.2	0.2	0.2	1	1	1	1	1	1	2	3	3	4	6
3	12	9.6	7.2	4.8	2.4	0.1	0.1	0.1	0.1	0.1	0.1	0.1	0.1	0.1	0.1	0.1	0.1	0.1	1.2	2.4	6	9.6	12	12
4	0.1	0.1	0.1	0.1	0.1	0.1	0.9	0.9	1.8	2.7	2.7	2.7	3.6	3.6	3.6	3.6	3.6	3.6	3.6	3.6	2.7	1.8	0.9	0.1
5	0.1	0.1	0.1	0.1	0.1	0.5	0.5	1	2	3	3	3	2.5	3	3	3	3	2	1	0.5	0.1	0.1	0.1	0.1
6	0.1	0.1	0.1	0.1	0.1	0.5	0.5	1	2	3	3	3	2.5	3	3	3	3	3	3	3	2	1	0.5	0.1
7	0.1	0.1	0.1	0.1	0.1	1	0.5	0.5	0.5	1	1	1	2	1	1	2	1	1	2	1	1	0.5	0.1	0.1
8	0.01	0.01	0.01	0.01	0.05	0.2	0.3	0.5	0.5	0.5	0.5	0.5	0.5	0.5	0.5	0.5	0.5	0.3	0.1	0.1	0.05	0.01	0.01	0.01
9	0.1	0.1	0.1	0.1	0.75	0.75	1.5	3	3.75	3.75	3.75	3	3	3.75	3.75	3.75	3.75	3.75	3.75	3	3	1.5	0.1	0.1
10	8	6	4	2	2	4	6	6	6	6	7	8	8	7	6	6	6	8	10	10	10	10	10	10
11	2.4	1.8	1.2	0.6	0.6	1.2	1.8	1.8	1.8	1.8	2.1	2.4	2.4	2.1	1.8	1.8	1.8	2.4	3	3	2.4	2.4	2.4	2.4
12	1.2	1.2	1.2	1.2	1.2	1.2	1.2	0.6	0.6	0.6	0.6	0.6	0.6	0.6	0.6	0.6	0.6	0.6	1.2	1.2	1.2	1.2	1.2	1.2
13	0.1	0.1	0.1	0.1	0.1	0.1	1	1	2	4	4	6	6	8	8	8	8	10	10	10	10	10	8	4
14	3	3	3	3	3	3	3	2.25	1.5	1.5	1.5	1.5	1.5	1.5	1.5	1.5	1.5	1.5	2.25	2.25	2.25	3	3	3
15	7.5	7.5	7.5	7.5	7.5	7.5	7.5	6	3	3	3	3	3	3	3	3	3	3	4.5	6	6	7.5	7.5	7.5
16	0.12	0.12	0.12	0.12	0.12	0.12	0.12	0.12	0.12	0.15	0.15	0.15	0.15	0.15	0.15	0.15	0.12	0.12	0.12	0.12	0.12	0.12	0.12	0.12
17	0	0	0	0	0	0	0	0	0	0	0	0	0	0	0	0	0	0	0	0	0	0	0	0

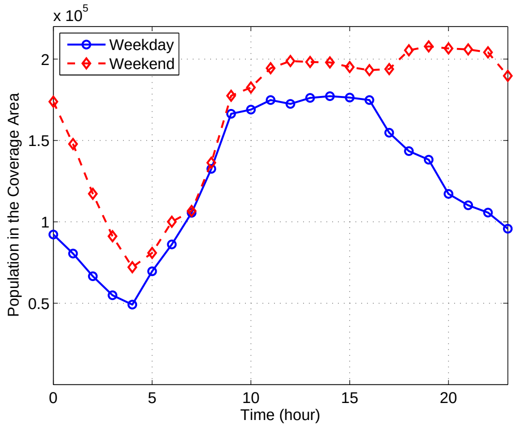

Figure 5.3. Average number of users in the coverage area.

The total number of individual subscribers throughout a day on weekday and weekend are depicted in Figure 5.3. Minimum of 49,166 and maximum of 177,260 population values are achieved during 04:00 and 14:00 on weekdays, while 72,165 and 207,809 population values are achieved during 04:00 and 19:00 on weekends respectively. In accordance with many previous studies in the literature which investigates the traffic load patterns of mobile access networks [1, 72, 73], weekday traffic of Taksim follows a sinusoidal pattern throughout the day. The traffic load in the coverage area drops significantly during night time whereas a high traffic demand is observed during day time, especially in working hours. On the contrary, weekend traffic profile in Taksim does not match with the general assumption of "low traffic load during weekend and holidays". Although this assumption may be quite reasonable for places comprising of business and trade centers, offices or schools; Taksim exhibits unique aspects in many ways with respect to other crowded urban areas. There are variety of different types of places including offices, residential areas, schools, weekend classes and tourist attraction points. Moreover, Taksim is the heart of night life in Istanbul, which is one of the most crowded cities in the world with an approximate population of 20 million. For the reasons mentioned, the weekend traffic load in Taksim is higher than the weekday traffic load. This behavior is observed both day and night time. Except from the spatial traffic change, Figure 5.3 also clearly shows that there are significant temporal traffic load changes throughout the day and we have enough margin to save energy with efficient green networking methods.

Table 5.4. Area ratio and traffic contribution of each place type.

Place Type	Total Area Ratio (%)	Traffic Contribution (%)	
		Weekday	Weekend
Cafe/Restaurant Early Closing	5.5	4.4	5.8
Cafe/Restaurant Late Closing	2.6	1.9	2.8
Bar/Night Club	7.7	7.6	13.3
Shopping	9.0	6.7	9.0
Office/Work Place Early Closing	19.0	17.3	13.0
Office/Work Place Late Closing	10.2	11.8	8.9
Mosque/Church	1.7	0.9	0.7
School Weekday	7.2	12.7	1.0
School All Week	2.0	2.0	2.3
Pedestrian Road Heavily Crowded	5.0	11.3	17.9
Pedestrian Road Lightly Crowded	3.1	2.1	3.1
Residential	15.1	8.0	7.2
Movie Theater Art Gallery	2.2	3.7	5.5
Otel	5.1	5.3	5.9
Hostel	0.8	2.0	2.3
Hospital	1.9	2.3	1.3
Derelict Building	2.0	0	0

Table 5.4 provides the ratio of the surface area for each place type over the whole coverage area along with their average contribution to the total created traffic load. Although the area ratio column is a vivid evidence of Taksim's cosmopolitan nature; offices, residential and shopping areas, bars, schools and cafeterias constitute the significant portion. It is also worth noting that the traffic load contribution of each type is not always proportional to their respective area ratio. More spacious types of places such as residential areas create lower traffic loads whereas more crowded places such as bars, night clubs and schools create higher traffic loads with respect to their actual total area. Another important observation is the traffic load contribution change between weekdays and weekends. Although there are significant variations between the weekday and weekend traffic load contributions, the change in bars, night clubs, weekday schools and pedestrian walkways can be counted as the most significant ones.

Installing a new BS to the location of an existing cell site is definitely cheaper than establishing a new site from the scratch. Contributing factors to this difference includes power and data cabling, mast installation, payment to the land owner, etc. Therefore, current cell sites are preferred to deploy the new BSs of another technology,

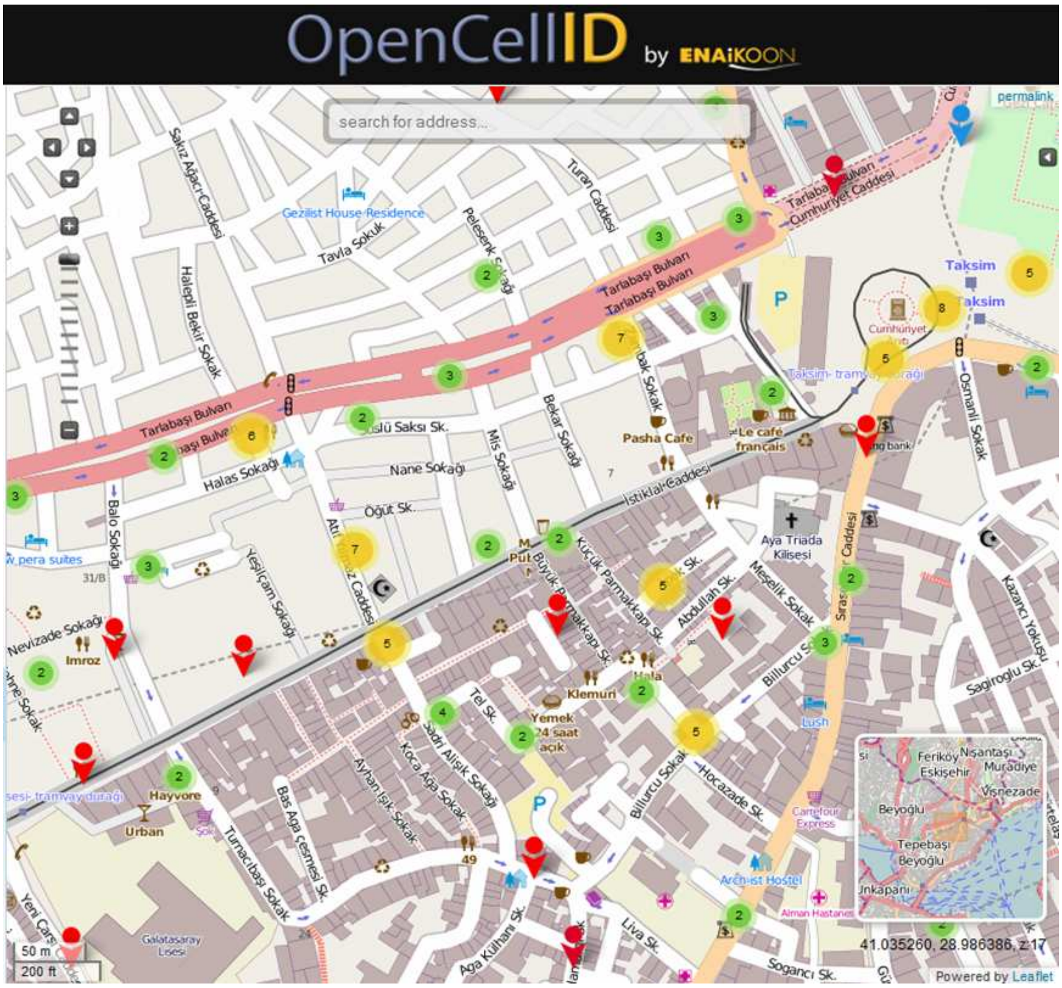

Figure 5.4. OpenCellID BS information repository loaded on OpenStreetMap.

which is assumed to be LTE in our case. However, obtaining the current BS location information is not an easy task. Although we attempted to get the BS locations and the traffic load information from two of Turkey's major mobile service providers, we could not manage to accomplish it. As a last resort, we decided to collect this data by ourselves with the help of a third party mobile application.

Although there are a bunch of available applications in the market, OpenCellID [93] was the most promising one for our case. OpenCellID is the world's largest collaborative community project that collects GPS positions of cell towers, for a multitude of commercial and private purposes. It has an Android OS based free mobile application used by the voluntary individuals. A simple log is maintained by the application which includes the discovered BS IDs, locations, discovery time stamp, operator name, etc. The OpenCellID project also keeps a huge database of the discovered BS

Figure 5.5. Current locations of micro BSs.

information. Each mobile application user can register himself/herself and obtain an API key. Then, the log file can be uploaded by using the obtained API key to the common database. According to their official statement, the OpenCellID database contains almost 7 million unique GSM Cell IDs and 1.2 billion measurements as of Jan 2015. The data can be downloaded from the database in a scalar format or can be applied as an additional layer on top of OpenStreetMap. In Figure 5.4, BS data of Taksim area obtained from the OpenCellID repository is plotted on top of OpenStreetMap.

Figure 5.5 depicts the BS locations of a major mobile service provider in Turkey. Although the coverage area is less than 1km^2, surprisingly there are 21 BSs belonging to a single operator. In order to discover the locations of the BSs, more than 20 km of walking was required while carrying an OpenCellID installed smart phone. The locations of the discovered cells are identified with an average accuracy of 5m.

5.3. Green Pico BS Deployment

In this section, our aim is to minimize the number of deployed pico BSs while guaranteeing a certain QoS level in terms of coverage and achievable data rate. For this purpose, we discretized the coverage area by dividing it into 1m^2 grids and each grid has a traffic occupancy according to its associated type as listed in Table 5.3. However, existing micro BSs along with to-be-deployed pico BSs are required to satisfy user requirements at all times. Therefore, we take the peak traffic loads of each place type into account. For example, the traffic demand in Istiklal Avenue peaks between 19:00-24:00 on weekends while the traffic demand in Pera Fine Arts High School is maximum during 08:00-17:00 on weekdays.

5.3.1. Problem Formulation

Given the peak traffic load of each place type and set of currently deployed micro BSs, we formulate a mathematical optimization problem for additional pico BS deployment.

Parameters:

N^{B^M} : Number of micro BSs

N^{B^P} : Number of pico BSs

N^{P^M} : Number of micro power levels

N^{G} : Number of coverage grids

$\mathbf{B}^M$: Set of micro BSs where $\mathbf{B}^M = \{1, \ldots, N^{B^M}\}$

$\mathbf{B}^P$: Set of pico BSs where $\mathbf{B}^P = \{1, \ldots, N^{B^P}\}$

$\mathbf{B}$: Set of BSs where $\mathbf{B} = \mathbf{B}^M \cup \mathbf{B}^P$

$\mathbf{G}$: Set of coverage grids

N^{X^P} : Number of candidate pico BSs deployment locations

$\mathbf{X}^P$: Set of candidate pico BSs deployment locations where $\mathbf{X}^P = \{1, \ldots, N^{X^P}\}$

$N^{X^{neig}}$: Number of neighboring candidate pico BSs deployment locations for overloaded BSs

$\mathbf{X}_b^{neig}$: Set of neighboring candidate pico BSs deployment locations for BS b where $\mathbf{X}_b^{neig} \subset \mathbf{X}^P$

D_b : Data flow capacity of BS b

$\beta^{\min}$: Minimum acceptable user satisfaction ratio where $0 \leq \beta^{\min} \leq 1$

β : User satisfaction ratio during peak traffic conditions where $0 \leq \beta \leq 1$

$\Psi^{\min}$: Minimum acceptable SINR at the receiver

Ψ_{gb} : Received SINR by grid g from BS b

$\mathcal{L}(b, g)$: Path loss exponent from BS b to grid g

f_b : Traffic load of BS b

Model variables:

$$\mathcal{S}_{gb} = \begin{cases} 1, & \text{if Grid } g \text{ is associated with BS } b \\ 0, & \text{otherwise} \end{cases}$$

The objective function is given as

$$\min \quad |\mathbf{B}^P| \tag{5.1}$$

subject to

$$f_b \leq D_b \quad \forall b \in \mathbf{B} \tag{5.2}$$

$$\Psi_{gb} \geq \mathcal{S}_{gb}\Psi^{\min} \quad \forall (g \in \mathbf{G}, b \in \mathbf{B}) \tag{5.3}$$

$$\beta \geq \beta^{\min} \tag{5.4}$$

$$\sum_{b \in \mathbf{B}} \mathcal{S}_{gb} \leq 1 \quad \forall g \in \mathbf{G} \tag{5.5}$$

Goal of our objective function in Equation 5.1 is to minimize the total number of deployed pico BSs for both energy efficiency and CAPEX reduction. Constraint in Equation 5.2 ensures that all BSs (both pico and micro) do not exceed their maximum data flow capacity. Equation 5.3 provides that each grid associated with a BS receives sufficient signal strength. By not violating the BS capacity and SINR constraints given in Equation 5.2 and Equation 5.3; proposed optimization problem ensures the subscriber satisfaction at all times by maintaining an acceptable level of quality in terms of both delay and achievable data rate. Equation 5.4 is responsible for obtaining the required user satisfaction ratio over all users, i.e., it is guaranteed that a certain percentage of the users are covered and served properly. The constraint in Equation 5.5 makes sure that a particular grid is being served by a single BS at a particular time slot.

5.3.2. Interference

As elaborated in Section 4.2.2.2, there are two sources of interference in LTE networks which are intra-cell and inter-cell. The intra-cell interference is the total interference caused by the signals emitted from the serving BS and the inter-cell interference is caused by the signals transmitted from all other BSs. In perfect transmission conditions, there should be no intra-cell interference since all of the signals are orthogonal. However, the intra-cell interference cannot be totally avoided due to multipath propagation and SINR is given by

$$\Psi = \frac{P^r}{\alpha_o I^{\text{in}} + I^{\text{out}} + \eta} \tag{5.6}$$

where P^r is the received signal power, I^{in} is the intra-cell interference, I^{out} is the inter-cell interference, α_o is the orthogonality loss factor and η is the noise power.

Since the interference dominates the SINR value, we will neglect the effect of the noise factor in the performance evaluation section for the sake of simplicity. For our calculations, we use the COST-Hata metropolitan area propagation model [12] which is assumed to be the most suitable model for crowded urban areas. However, this model is valid for the frequencies up to 2000 Mhz. COST-231 Walfisch-Ikegami [94] model is an extension of COST Hata-Hodel and can be used for frequencies higher than 2000 MHz. In Turkey, it is announced by the Ministry of Transport, Maritime Affairs and Communications that 4G frequency band auctions will be done for three different portions of the spectrum, namely 800, 1800 and 2600 Mhz. Therefore, a suitable propagation model is required to be selected according to the frequency band being used by the service provider. The SINR from BS b to coverage grid g is given by

$$\Psi_{bg} = \frac{P_b^{tx}\mathcal{L}(b,g)}{\alpha_o P_b^{tx}\mathcal{L}(b,g) + \sum\limits_{b'\in\mathbf{B}\setminus\{b\}} P_{b'}^{tx}\mathcal{L}(b',g) + \eta} \tag{5.7}$$

where P_b^{tx} is the transmission power of BS b.

5.3.3. Coverage

A particular grid g is assumed to be covered if the received SINR from any BS is higher than the minimum acceptable level $\Psi^{\min}$. The binary coverage function in the Green Pico BS Deployment Problem is given by

$$\Gamma(g) = \begin{cases} 1, & \text{if } \Psi_{gb} > \Psi^{\min} \quad \exists b \in \mathbf{B} \\ 0, & \text{otherwise} \end{cases} \tag{5.8}$$

The total coverage ratio for the area of interest is required to be higher than a threshold $\beta^{\min}$ and given by

$$\beta = \frac{\sum\limits_{g\in\mathbf{G}} \Gamma(g)}{N^G} \tag{5.9}$$

5.3.4. User Association

In Green Pico BS Deployment Problem, a MT stationed within a coverage grid is not necessarily being serviced by the closest BSs. Each coverage grid is associated with the BS which provides the highest SINR. However, a particular grid is said to be covered if and only if the received SINR value is higher than the minimum SINR requirement to guarantee an acceptable subscriber data rate. The Grid-BS association rule is given by

$$\mathcal{S}_{gb} = \begin{cases} 1, & \text{if } \Psi_{gb} \geq \Psi^{\min} \text{ and } b = \underset{b' \in \mathbf{B}}{\operatorname{argmax}}(\Psi_{gb'}) \\ 0, & \text{otherwise} \end{cases} \tag{5.10}$$

Although satisfying the SINR requirement is a big step for the coverage, it is not enough by itself for proper coverage. Since BSs have limited resources (i.e. bandwidth, backhaul link capacity), their traffic load is also important. Therefore, we need to be certain that the minimum received SINR requirement at the MT is satisfied and the respective traffic load of the serving BS is below its maximum capacity. Since we deploy pico BSs according to accommodate the peak time traffic conditions, we take the maximum traffic occupancy of the covered grids into account. Total traffic load of a BS b can be formulated as

$$f_b = \sum_{g \in \mathbf{G}} S_{gb} f_g^p \tag{5.11}$$

where f_g^p is the peak aggregate traffic occupancy of grid g.

5.3.5. Green Pico BS Deployment Algorithm

Although we formulate an optimization model for the Green Pico BS Deployment Problem, it is very challenging to solve large real-life instances of the problem with optimization tools due to prohibitive computational and space complexity. On the other hand, it may be possible to solve the problem by optimization tools for smaller number of candidate pico BS deployment locations N^{X^P} for our test case scenario. However, limiting the possible pico BS deployment locations reduces the feasible solution space significantly which in turn decreases the quality of the resulting topologies. Hence, in this section we focus on deriving an efficient heuristic to install the minimum number of pico BSs in order to support the peak traffic conditions without compromising the QoS requirements of the subscribers.

5.3.5.1. Area Spectral Efficiency. For the Green Pico BS Deployment Algorithm, we adopt the Area Spectral Efficiency (ASE) [95] as a performance indicator. ASE is defined as the summation of the spectral efficiency over the coverage area. According to Shannon-Hartley theorem, spectral efficiency (bits/sec/Hz) at coverage grid g is given by

$$\mathcal{C}(g) = log_2(1 + \max_{b \in \mathbf{B}}(\Psi_{gb})) \tag{5.12}$$

Area spectral efficiency(bits/sec/Hz/m^2) defines the sum of the maximum average data rates per unit bandwidth per unit area and given by

$$\mathcal{A} = \frac{\sum\limits_{g \in \mathbf{G}} \mathcal{C}(g)p(g)}{mN^G} \tag{5.13}$$

where $p(g)$ is the probability of a user being at a particular coverage grid g and m is the coverage grid size in square meters.

The ASE is a measure of the maximum average data rate per unit bandwidth per unit area supported by a BS and it is closely related with constraints in Equations 5.3 and 5.4. It is certain that deployment of an additional BS increases the ASE of the coverage area unless it is very close to an existing BS and interfering with each other. Moreover, ASE increment is expected to be higher in case a new BS is deployed to an area with low spectral efficiency. Therefore, iterative ASE increment steps provide better coverage of the area of interest along with high average SINR values. Let $\mathcal{A}_x$ is the ASE after deployment of a pico BS to candidate location x. Then, the ASE increase in the coverage area is identified by the difference between the ASE before and after deployment of the new pico BS and given by

$$\Delta\mathcal{A}_x = \mathcal{A}_x - \mathcal{A} \tag{5.14}$$

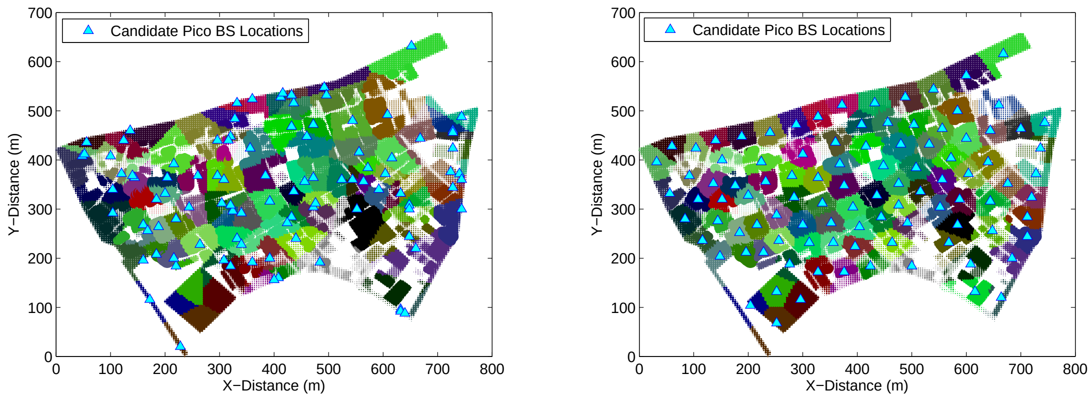

(a) Iteration #1 (b) Iteration #20

Figure 5.6. Possible pico BS locations with K-Means clustering.

Although Green Pico BS Deployment Algorithm can attempt to install BSs to any suitable location in the coverage area, this approach increases the complexity of the algorithm polynomially. Moreover, myriad of similar BS deployment results can be produced since the resolution of the coverage area is very high (1m^2 grid size). To overcome these challenges, we determine to limit the possible pico BS deployment locations and set to a sufficiently large number denoted by N^{X^P}. However, candidate pico BS deployment locations are required to be selected efficiently. Therefore, we used K-Means clustering [96], which is a widely-known machine learning method to identify the coordinates of the candidate locations. K-Means algorithm uses an iterative refinement technique and is composed of two steps, namely the Assignment and Update. In the Assignment step, each grid is assigned to its nearest mean where new mean locations are calculated according to the previous assignments in the Update step. Different from the original algorithm, we calculate the contribution of each coverage grid by multiplying the Euclidean distance to the mass center with its traffic occupancy. Hence, we keep the cluster centers, i.e. possible pico BS deployment locations, close to the grids where the traffic load concentration is higher. Although we take K=300 in our Green Pico BS Deployment Algorithm, an example set of candidate pico BS locations $\mathbf{X}^P$ with K=100 is depicted in Figure 5.6 for simplicity. Since the K-Means algorithm converges and improvements are negligible after the 20^{th} iteration, we set the iteration count as 20. In Figure 5.6(a), initial candidate pico BS deployment locations are plotted while final locations are given in Figure 5.6(b) after the last iteration.

We define a new decision parameter called Neighbor BS Deployment (NBD) metric to be used in the quality assurance phase of the Green Pico BS Deployment Algorithm and denoted by θ. The maximum NBD value is obtained when a to-be-deployed neighboring BS is able to alleviate as much traffic load as possible from the overloaded BS without exceeding its own maximum traffic load capacity. To simplify the NBD metric formulation, let $\Delta\ell_{bx}$ is the handed over traffic load from over-utilized BS b to the newly deployed neighboring pico BS at candidate location x and given by $\Delta\ell_{bx} = f_b - f'_{bx}$ where f'_{bx} is the traffic load of BS b after the neighboring BS is deployed at candidate location x. Let $\phi_x = D_x - f_x$ is the difference between the maximum traffic load capacity of the newly deployed BS at location x and its current load after the deployment. The NBD metric θ_{bx} between the overloaded BS b and the deployed neighbor pico BS at candidate location x is given by

$$\theta_{bx} = \Delta\ell_{bx} - \alpha_u|\phi_x| \tag{5.15}$$

where α_u is the utilization penalty. It is undesirable to create more overloaded BSs in the network while trying to minimize their total number. Therefore, a newly deployed BS should not be allowed to take too much load of its overloaded neighbor BS and become another overloaded BS itself. Deploying an under-utilized neighbor BS is also a waste of precious resources and will not alleviate the load of overloaded BS. Therefore, we introduce a penalty for both over-utilization and under-utilization cases of newly deployed BSs. Since exceeding the maximum load capacity does not improve the current situation anyhow, we set higher utilization penalty for over-utilized BSs where

$$a_u = \begin{cases} 1, & \text{if} \quad \phi_x \leq 0 \\ 20, & \text{otherwise} \end{cases} \tag{5.16}$$

By setting $a_u = 20$ for over-utilized BSs, we give our Green Pico BS Deployment Algorithm a chance to deploy a slightly overloaded pico BS in case of all other neighboring locations do not alleviate the load of the overloaded BS sufficiently.

————–*coverage assurance phase*————–

$\mathbf{B}^P = \{\emptyset\}$
while $\beta < \beta^{\min}$ **do**
  for all $x \in \mathbf{X}^P$ **do**
    Assume a pico BS b deployed at location x
    Calculate $\Delta\mathcal{A}_x$
  end for
  deploy pico BS b at location $x^* = \underset{x \in \mathbf{X}^P}{\operatorname{argmax}}(\Delta\mathcal{A}_x)$
  $\mathbf{B}^P = \mathbf{B}^P \cup \{b\}$, $\mathbf{X}^P = \mathbf{X}^P \backslash \{x\}$
end while

————–*quality assurance phase*————–

while $\big(\mathbf{B}^{\text{high}} = \{b \mid f_b > D_b,\ \forall b \in \mathbf{B}\}\big) \neq \{\emptyset\}$ **do**
  for all $b \in \mathbf{B}^{\text{high}}$ **do**
    Discover $\mathbf{X}_b^{neig}$ where $\mathbf{X}_b^{neig} \subset \mathbf{X}^P$
    for all $x \in \mathbf{X}_b^{neig}$ **do**
      Calculate θ_{bx}
    end for
    Deploy pico BS at location $x^* = \underset{x \in \mathbf{X}_b^{neig}}{\operatorname{argmax}}(\theta_{bx})$
    $\mathbf{B}^P = \mathbf{B}^P \cup \{b\}$, $\mathbf{X}^P = \mathbf{X}^P \backslash \{x^*\}$
  end for
end while

Figure 5.7. Green Pico BS Deployment Algorithm.

We set the number of neighboring candidate pico BSs deployment locations $N^{X^{neig}}$ to 10 in our simulations. Although higher number of $N^{X^{neig}}$ value enhances the solution space and may yield to better results theoretically, distant locations from a particular overloaded BS are less likely to reduce its load. Moreover, calculating the effect of more candidate locations increases the complexity of the algorithm. Therefore, limiting the $N^{X^{neig}}$ to a sufficiently large number results in lower runtime without degrading the performance of the algorithm.

The pseudo code of the Green Pico BS Deployment Algorithm is given in Figure 5.7. The ultimate goal is to minimize the total number of deployed pico BSs as given in Equation 5.1 while satisfying coverage and achievable data rate requirements. Our algorithm consists of two phases which are the coverage assurance and the quality assurance phases. The aim of the coverage assurance phase is to provide the required coverage with minimum amount of additional pico BS. At the beginning of the coverage assurance phase, a new pico BS is assumed to be deployed at each candidate pico BS deployment location x and $\Delta\mathcal{A}_x$ is calculated for all $x \in \mathbf{X}^P$. Then, a new pico BS is deployed to the location x having the highest $\Delta\mathcal{A}_x$ value. As the last step of this phase, deployed BS is added to the set $\mathbf{B}^P$ and the respective candidate location is removed from the set $\mathbf{X}^P$. By increasing the $\mathcal{A}^e$ in the reference coverage area, not only the coverage ratio but also the achievable data rate requirements of the subscribers given in Equations 5.3 and 5.4 improve.

The second phase is the quality assurance phase. The purpose of this phase is to ensure that all BSs are operating below their maximum traffic load as given in Equation (5.2). If there are overloaded BSs in the current network configuration, neighboring candidate pico BS deployment locations of overloaded BSs are identified and their respective NBD metric is calculated. Subsequently, a new pico BS is deployed to the neighboring candidate deployment location having the maximum NBD metric value. This step is repeated until no overloaded BS remains in the network. Since NBD metric is a measure of how efficiently a neighboring pico BS alleviates the load of overloaded BS without violating its own capacity constraints, quality assurance phase quickly eliminates overloaded BSs and deploys the minimum number of pico BSs as a remedy.

5.3.6. Greedy Pico BS Deployment Algorithm

In this section, we introduce a greedy heuristic to solve the formulated Green Pico BS Deployment Problem. The results of this heuristic are also used during the comparative performance evaluation in Section 5.5.2. Greedy Pico BS Deployment Algorithm exhaustively visits each candidate pico BS deployment location and calculates their respective ASE increase $\Delta\mathcal{A}_x$. Subsequently, it deploys a pico BS at the candidate location which provides the maximum ASE increase in the coverage area if and only if this augmentation does not violate the BS capacity constraint for all active BSs including itself. The pseudocode of the Greedy Pico BS Deployment Algorithm is given in Figure 5.8 and its performance is further investigated in Section 5.5.2.

while $\beta < \beta^{\min}$ **do**
  for all $x \in \mathbf{X}^P$ **do**
    Assume a pico BS is deployed at candidate location x
    Calculate $\Delta\mathcal{A}_x$
    Find overloaded BSs $\mathbf{B}_x^{\text{high}}$ after deployment at candidate location x
  end for
  Deploy a pico BS at location $x^* = \underset{x \in \mathbf{X}^P}{\operatorname{argmax}}(\Delta\mathcal{A}_x)$ iff $\mathbf{B}_x^{\text{high}} = \{\emptyset\}$
  $\mathbf{X}^P = \mathbf{X}^P \backslash \{x^*\}$
end while

Figure 5.8. Greedy Pico BS Deployment Algorithm.

5.4. Green Dynamic BS Operation

In this section, we formulate a mathematical optimization problem to minimize the network power consumption during the operation phase. According to the formulated problem, we then propose an offline-centralized and an online-distributed novel green dynamic BS operation algorithms for power saving.

5.4.1. Problem Formulation

Parameters:

N^T	: Number of time slots within the day
$\mathbf{T}$	: Set of discrete time slots within the day
$\mathbf{P}^M$	: Set of micro BS power levels
$\mathbf{P}^P$	: Set of pico BS power levels
$\mathbf{P}$	: Set of power levels where $\mathbf{P} = \mathbf{P}^M \cup \mathbf{P}^P$
$W^M(p, f)$	: Total consumed power by a micro BS transmitting with power level p and traffic load f
$W^P(p, f)$	: Total consumed power by a pico BS transmitting with power level p and traffic load f
f_{gt}	: Aggregate traffic occupancy of coverage grid g at time t
f_{bt}	: Traffic load of BS b at time t

Model variables:

$$K_{bpt} = \begin{cases} 1, & \text{BS } b \text{ transmits with power } p \text{ at time } t \\ 0, & \text{otherwise} \end{cases}$$

$$S_{gbt} = \begin{cases} 1, & \text{Grid } g \text{ is associated with BS } b \text{ at time } t \\ 0, & \text{otherwise} \end{cases}$$

The objective function for the Green Dynamic BS Operation Problem is given as

$$\min \quad \sum_{t \in \mathbf{T}} \left(\sum_{b \in \mathbf{B}^M} \sum_{p \in \mathbf{P}^M} K_{bpt} W^M(p, f_{bt}) + \sum_{b \in \mathbf{B}^P} \sum_{p \in \mathbf{P}^P} K_{bpt} W^P(p, f_{bt}) \right) \tag{5.17}$$

Subject to

$$f_{bt} \leq D_b \quad \forall (b \in \mathbf{B}, t \in \mathbf{T}) \tag{5.18}$$

$$\Psi_{gbt} \geq S_{gbt} \Psi^{\min} \quad \forall (g \in \mathbf{G}, b \in \mathbf{B}, t \in \mathbf{T}) \tag{5.19}$$

$$\beta(t) \geq \beta^{\min} \quad \forall t \in \mathbf{T} \tag{5.20}$$

$$\sum_{p \in \mathbf{P}} K_{bpt} = 1 \quad \forall (b \in \mathbf{B}, t \in \mathbf{T}) \tag{5.21}$$

$$\sum_{b \in \mathbf{B}} S_{gbt} \leq 1 \quad \forall (g \in \mathbf{G}, t \in \mathbf{T}) \tag{5.22}$$

Our objective function in Equation 5.17 aims to minimize the total energy consumption of both pico and micro BSs throughout the network. Equation 5.18 is responsible for the operation of all active BSs below their data flow capacity at all times. Equation 5.19 provides that each grid associated with a BS is being served by at least a certain SINR value. Equation 5.20 ensures that the required user satisfaction ratio is achieved over all users. In other words, a certain percentage of the users are covered and served properly according to their QoS requirements. The constraint in Equation 5.21 makes sure that a BS operates at a single transmission power level during a particular time slot and Equation 5.22 is responsible for that a grid is being served by a single BS at a particular instant.

5.4.2. BS Power Consumption

Power consumption of a BS can be broken down into two parts: (i) core (static) power and (ii) dynamic power. The core power consumption is constant as long as the BS is active whereas the dynamic power consumption is subject to change proportional to the present traffic load conditions of the BSs. Total power consumption of BS b, with transmit power p and traffic load f is given by

$$W(b,p,f) = \begin{cases} 0, & p = 1 \\ W_b^c + W_{bpf}^d, & \text{otherwise} \end{cases} \tag{5.23}$$

where W_b^c is the core (static) power consumed by the BS b and the W_{bpf}^d is the dynamic power consumed by the BS b with transmit power level p and traffic load of f.

Core and dynamic power consumption of BS are given by

$$W_b^c = W_b^{DC} + W_b^{MS} + W_b^{cool} \tag{5.24}$$

$$W_{bpf}^d = \frac{f}{D_b}\left(\frac{p}{\mu_b^{PA}} + P_b^{RF} + P_b^{BB}\right) \tag{5.25}$$

where W_b^{DC}, W_b^{MS}, W_b^{cool}, P_b^{RF} and P_b^{BB} are DC-DC power supply, mains supply (AC-DC unit), active cooling, RF transceiver, baseband unit (digital signal processing) power consumption and μ_b^{PA} is the power amplifier efficiency of BS b respectively [79, 80]. Typical values for micro and pico BSs power consumption are given in Table 5.7 in accordance with [80]. Power amplifier efficiencies for micro and pico BSs are assumed to be 22.8% and 6.7% in order [80].

Table 5.7. Typical BS power consumption figures.

	W^{DC}	W^{MS}	W^{cool}	P^{RF}	P^{BB}
Micro	9.3	11.1	6.2	13	54.6
Pico	1	1.4	n/a	2	6

Although as many BS types as required can be accommodated in our mathematical model, we remove the b index from the power consumption equations and simply provide the micro and pico BS power consumptions by

$$W^M(p, f) = 26.6 + \frac{f}{D_M}\left(\frac{p}{0.228} + 67.6\right) \tag{5.26}$$

$$W^P(p, f) = 2.4 + \frac{f}{D_P}\left(\frac{p}{0.067} + 8\right) \tag{5.27}$$

where $W^M(p, f)$ and $W^P(p, f)$ are respective power consumptions of micro and pico BSs with transmission power p, traffic load f, data flow capacity D_M for micro and D_P for pico BSs.

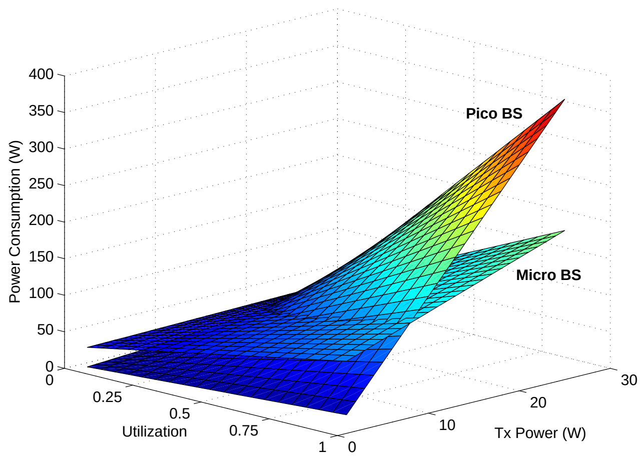

Figure 5.9. Change of micro and pico BS power consumption with utilization and tx power.

In Figure 5.9, change of micro and pico BS power consumption is given with respect to utilization and tx power. Pico BS power consumption figures are lower than the micro BS for smaller tx power values regardless of the utilization, since the core power consumption is the dominating factor. On the other hand, as the tx power and utilization increases and the dynamic power consumption becomes the dominating factor, the power consumption of the pico BS increases dramatically. The reason behind this increase is the low efficiency of the pico BS power amplifier. However, the pico BS equipment is not designed to transmit with high power levels and the majority of the pico BS manufacturers does not provide dynamic tx power adjustment ability. Therefore, we fixed the tx power of the pico BSs as 2 Watts in our performance evaluation simulations. For micro BSs, we defined 5 different tx power levels with corresponding power of 3, 8, 13, 18 and 24 Watts in order.

5.4.3. Interference

By using the same formula given in Equation 5.6, SINR from BS b in grid g at time slot t is given by

$$\Psi_{bgt} = \frac{\sum\limits_{p \in \mathbf{PA}} K_{bpt} \mathcal{L}(b,g) p}{\alpha_o \sum\limits_{p \in \mathbf{PA}} K_{bpt} \mathcal{L}(b,g) p + \sum\limits_{b' \in \mathbf{B} \setminus \{b\}} \sum\limits_{p \in \mathbf{PA}} K_{b'pt} \mathcal{L}(b',g) p + \eta} \tag{5.28}$$

where $\mathbf{PA} = \mathbf{P} \setminus \{p = 0\}$

5.4.4. Coverage

A particular grid g is covered at time t if the received SINR from any BS is higher than the minimum acceptable level and binary coverage function is given by

$$\Gamma(g,t) = \begin{cases} 1, & \text{if } \Psi_{gbt} > \Psi^{\min} \quad \exists b \in \mathbf{B} \\ 0, & \text{otherwise} \end{cases} \tag{5.29}$$

The total coverage ratio for the area of interest at time t is given by

$$\beta_t = \frac{\sum_{g \in \mathbf{G}} \Gamma(g,t)}{N^G} \tag{5.30}$$

5.4.5. User Association

A particular grid is associated with the BS providing the maximum SINR value unless the received SINR value is lower then the minimum acceptable threshold. Association rule of grid g with BS b at time t is given by

$$\mathcal{S}_{gbt} = \begin{cases} 1, & \text{if } \Psi_{gbt} \geq \Psi^{\min} \text{ and } b = \underset{b' \in \mathbf{B}}{\operatorname{argmax}}(\Psi_{gb't}) \\ 0, & \text{otherwise} \end{cases} \tag{5.31}$$

The total traffic load of a BS b at time t can be given as

$$f_{bt} = \sum_{g \in \mathbf{G}} S_{gbt} f_{gt} \tag{5.32}$$

5.4.6. Green Dynamic BS Operation Algorithms

It is possible to solve the Green Dynamic BS Operation Problem with optimization tools such as CPLEX [81] or GUROBI [82] since we put it in a mathematical form. However, finding optimum solutions is very challenging due to the computational and space complexity of our large-scale realistic test case scenario. Therefore, we propose fast and efficient heuristics to solve large realistic instances of the problem in this section.

5.4.6.1. Area Spectral Efficiency. Similar to the Green Pico BS Deployment, we also utilize the ASE metric for the Green Dynamic BS Operation. The Spectral efficiency (bits/sec/Hz) at coverage grid g at time t is given by

$$\mathcal{C}(g,t) = log_2(1 + \max_{b \in \mathbf{B}}(\Psi_{gbt})) \tag{5.33}$$

Area spectral efficiency (bits/sec/Hz/m^2) over the total coverage area at time t is given by

$$\mathcal{A}_t = \frac{\sum\limits_{g \in \mathbf{G}} \mathcal{C}(g,t) p(g,t)}{m N^G} \tag{5.34}$$

where $p(g,t)$ is the probability of a user being at a particular coverage grid g at time t.

However, this time we modify the ASE increment metric $\Delta\mathcal{A}$ defined in Section 5.3.5 to measure the increase on the provided average data rate per unit bandwidth per unit area per power. In other words, we use the ASE increment per watt as a performance metric. Hence, it is ensured that the maximum possible coverage and achievable data rate increase over the reference area is provided with the minimum amount of power consumption.

A natural question may arise why this metric is not used for the Green Pico BS Deployment. The reason lies with the homogeneity of the deployed BSs. Since the power consumption figures of the deployed pico BSs are identical, their respective ASE increase per power is also proportional with the ASE increase. Therefore, using the ASE increment per power metric does not change the results at all. Also, the effect of BS load on the power consumption is captured indirectly with θ_{bx} metric. On the other hand, ASE increase per watt metric ultimately makes sense for the Green Dynamic BS Operation since there are heterogenous BSs activated with different PLs.

The ASE increment per watt (bits/sec/Hz/m^2/watt) in the reference area when BS b is activated with PL p at time t is given by

$$\Delta\mathcal{A}_{bpt}^{w} = \frac{\mathcal{A}_t}{W(b,p,f_{bt})} \tag{5.35}$$

where the traffic load f_{bt} and power consumption $W(b, p, f)$ are given in Equations 5.32 and 5.23 respectively.

5.4.6.2. Offline-centralized Dynamic BS Operation Algorithm. The Green Pico BS Deployment and Green Dynamic BS Operation problems are very similar in nature. The similarity can be easily understood from the mathematical problem formulations given in Section 5.3.1 and 5.4.1. Therefore, it is convenient to use the Green Pico BS Deployment Algorithm as a template for the Offline-centralized Dynamic BS Operation Algorithm.

The main objective of the Offline-centralized Dynamic BS Operation Algorithm is to dynamically adjust the use of BS resources according to the temporal changes in the traffic load throughout the day and create a more energy-aware network as given in Equation 5.17. The Offline-centralized algorithm is executed by a central entity and determines the network topology beforehand. The traffic load estimations and existing BS topology are given to the algorithm as an input. The output is the energy-aware network topology. The decision parameters of the algorithm are the status of all BSs, i.e. on/off, and the tx power of active BSs.

Before proceeding to the algorithm itself, we need to redefine some of the parameters used in the Green Pico BS Deployment Algorithm. Let $\Delta\ell_{bb'p'}$ is the handed over traffic load from over-utilized BS b to the newly activated neighboring BS b' with PL p' and given by $\Delta\ell_{bb'p'} = f_b - f'_{bb'p'}$ where $f'_{bb'p'}$ is the traffic load of BS b after the neighboring BS b' is switched on with PL p'. Let $\phi_{b'p'} = D_{b'} - f_{b'p'}$ is the difference between the maximum traffic load capacity of the newly deployed BS b' and its current load after it has been switched on with PL p. The NBD metric $\theta_{bb'p'}$ between the overloaded BS b and the switched on b' with PL p' is given by

$$\theta_{bb'p'} = \Delta\ell_{bb'p'} - \alpha_u|\phi_{b'p'}| \tag{5.36}$$

where α_u is the same utilization penalty described in the Green Pico BS Deployment Algorithm. For the sake of mathematical simplicity, subscript t representing the time of day is omitted in the NBD formulation.

Similar to the Green Pico BS Deployment Algorithm, we change the status of neighboring BSs to alleviate the load of the overloaded BSs. We set the number of neighboring {BS,PL} pair $N^{B^{neig}}$ of an overloaded BS to 15 in our simulations for the same reasons explained in Section 5.3.5. We keep this number higher than the one used in the Green Pico BS Deployment Algorithm since a particular BS is represented by more than one field due to different PL configurations. We included the PL in the neighbor BS list because a PL increase of an already active neighboring BS may also reduce the load of an overloaded BS while a PL decrease most likely worsens the situation. Therefore, the set of neighboring {BS,PL} pairs of an overloaded BS b is composed of either (i) all possible PLs of the switched off neighboring BSs or (ii) higher PLs of an already active neighboring BSs and denoted by $\mathbf{B}_b^{\mathrm{neig}}$. In case there is an overloaded BS b is identified, each {b',p'} pair in the set of $\mathbf{B}_b^{\mathrm{neig}}$ visited and the one having the maximum $\theta_{bb'p'}$ is implemented.

The pseudocode of the Offline-centralized Dynamic BS Operation Algorithm is given in Figure 5.10. It tackles with each time slot independently. For each time slot, it starts with an empty set of active BSs. Then the algorithm activates {BS,PL} pairs which maximizes the ASE increase per watt ($\Delta\mathcal{A}^w_{bpt}$) metric in the coverage area. Iterative increment of this metric ensures not only increasing coverage ratio, but also higher average SINR values throughout the coverage area. This step is repeated until the minimum coverage ratio over all users are achieved for the current time slot. When the required coverage ratio is obtained, we utilize the redefined NBD metric to eliminate the overloaded BSs similar to the Green Pico BS Deployment Algorithm. Firstly, neighboring {BS,PL} pairs are discovered for each overloaded BS. In the next step, respective NBD metric of each discovered neighboring {BS,PL} pairs are calculated and the one having the maximum value is activated. By this way, activated neighboring BSs are able to alleviate the traffic load of the overloaded BSs as much as possible without exceeding their own traffic load limits.

for all $t \in \mathbf{T}$ **do**
  $\mathbf{B}_t = \{\emptyset\}$, $\mathbf{B}_t^{\text{off}} = \mathbf{B}$
  while $\beta_t < \beta^{\min}$ **do**
    for all feasible $\{b \in \mathbf{B}_t^{\text{off}}, p \in \mathbf{PA}\}$ pair **do**
      Assume BS b is switched on with PL p
      Calculate $\Delta\mathcal{A}_{bpt}^{w}$
    end for
    Switch on BS b with PL p having max $\Delta\mathcal{A}_{bpt}^{w}$
    $\mathbf{B}_t = \mathbf{B}_t \cup \{b, p\}$, $\mathbf{B}_t^{\text{off}} = \mathbf{B}_t^{\text{off}} \backslash \{b\}$
  end while
  while $\left(\mathbf{B}_t^{\text{high}} = \{b \mid f_{bt} > D_b,\ \forall b \in \mathbf{B}\}\right) \neq \{\emptyset\}$ **do**
    for all $b \in \mathbf{B}_t^{\text{high}}$ **do**
      Discover $\mathbf{B}_b^{\text{neig}}$
      for all $\{b', p'\}$ pair $\in \mathbf{B}_b^{\text{neig}}$ **do**
        Calculate $\theta_{bb'p'}$
      end for
      Switch on BS b' with PL p' having max $\theta_{bb'p'}$
      $\mathbf{B}_t = \mathbf{B}_t \cup \{b', p'\}$, $\mathbf{B}_t^{\text{off}} = \mathbf{B}_t^{\text{off}} \backslash \{b'\}$
    end for
  end while
end for

Figure 5.10. Offline-centralized Dynamic BS Operation Algorithm.

5.4.6.3. Online-distributed Dynamic BS Operation Algorithm. The online-distributed Dynamic BS Operation Algorithm aims to adapt the current network conditions and create an energy-aware topology in a distributed and online manner. Each BS takes its own decisions autonomously in coordination with the neighboring BSs. However, the topology adjustments are merely based on a limited set of network statistics collected by local observations. Another drawback of the online-distributed algorithms is the additional signaling overhead introduced by requirement of coordination with the neighboring BSs. Moreover, the overall impact of the local decisions on the whole network is not possible to comprehend from a BS point of view. Therefore, the quality of the BS switching and power adjustment decisions decreases in comparison with the centralized methods. On the other hand, online-distributed approaches are more responsive to unexpected traffic load variations and well adapt to the underestimated

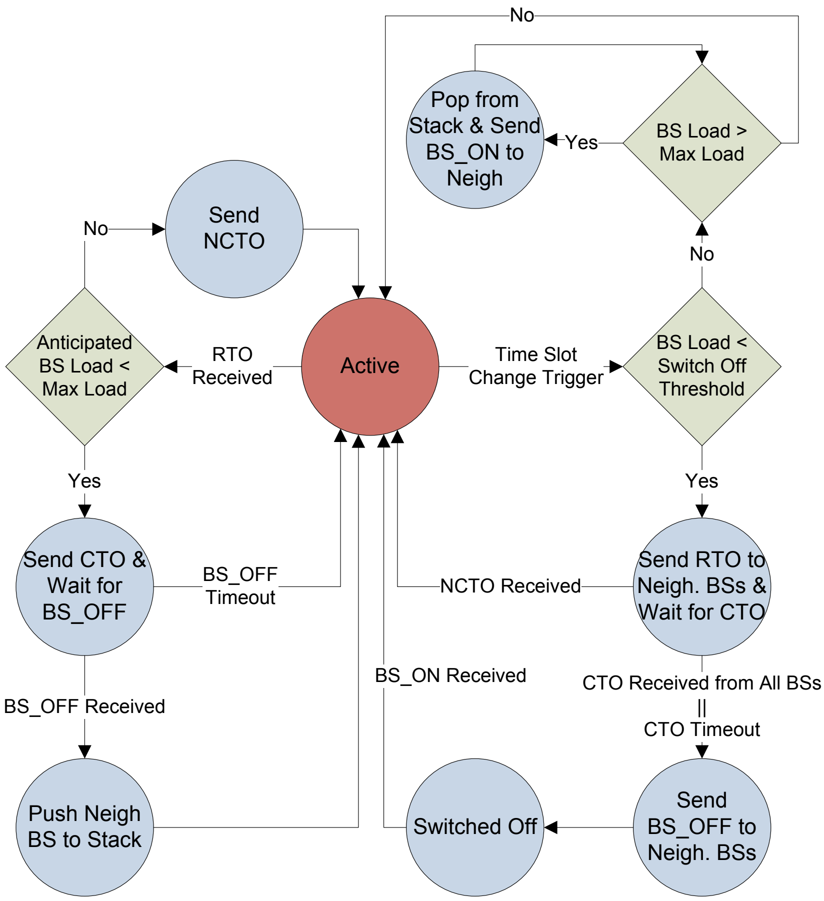

Figure 5.11. Simplified state transition diagram of the online-distributed dynamic BS operation algorithm.

or overestimated traffic load conditions with respect to offline-centralized methods.

Simplified state transition diagram of Online-distributed Dynamic BS Operation Algorithm is given in Figure 5.11. Before entering the green operation mode, each BS undertakes a neighbor discovery routine. During this routine, all BSs located in the area of interest should be switched on and the minimum acceptable coverage ratio must be satisfied. The latter requirement is crucial because after entering the distributed green operation mode, there is no central entity to check if the required coverage over the whole area is provided. Since each BS makes their local decisions, the distributed scheme relies on the amount of handovers to satisfy the coverage constraint through out the operation cycle.

Initially, each member of the energy saving scheme discovers its neighbors and enters the green operation mode starting from the *Active* state. Since defined time slices are our reference for network adjustments, each BS maintains a *Time Slot Change* timer. When the timer expires, a *Time Slot Change* event is triggered and every BS checks its respective traffic load. However, this timer can be easily replaced with a more frequent trigger to respond the traffic load changes instantly. On the other hand, frequent BS switch on/off transitions may result in unsatisfied users due to high amount of handover requests. Therefore, the time interval between each BS load check event needs to be carefully chosen.

If the current load of the BS is lower than the *Switch Off Threshold*, the BS sends Request to Switch Off (RTO) message to its neighbors and waits for Clear to Switch Off (CTO). Neighbor BSs receiving the RTO message check if they are able to accommodate the additional traffic load caused by switching the sender of the RTO off. Since all MTs keep track of BSs providing the best and the second best signal strength for better handover management, the required information is readily available. A simple exchange of this information between the BSs and serving MTs is sufficient to calculate the additional traffic load arising from a neighbor BS switch off. If the additional traffic load can be accommodated, the neighbor BS transmits a CTO message to the sender of the RTO. If the additional traffic load causes the neighbor BS to exceed its maximum capacity, a Negative CTO (NCTO) is sent. When the CTO messages are received from all neighbor BSs or *Wait For CTO Timer* expires, the BS sends BS_OFF signal to its neighbors announcing that it is going to be switched off and enters the *Switched Off* state. Neighbor BSs receiving the BS_OFF signal takes the necessary precautions to accept the to-be-handed-over users from the switching off BS and inserts the BS index of the to-be-switched-off BS into a stack called *Switched Off Neighbor BS Stack*. This stack is going to be used for load balancing of the overloaded BSs later. If a NCTO message is received, the BS goes back to the *Active* state and remains switched on.

If the load of a particular BS is higher than the maximum traffic load capacity when the *Time Slot Change* event is triggered, it pops a BS index from the *Switched Off Neighbor BS Stack* and transmits a BS_ON signal. After the neighbor BS is switched on, the overloaded BS hands over some of its load according to the current SINR measurements. This process is repeated until present load of the overloaded BS decreases below the maximum traffic load capacity. Since the *Switched Off Neighbor BS Stack* operates with a FIFO mechanism, each BS keeps track of temporal topology changes and able to restore back to the previous conditions if their respective traffic load exceeds the maximum capacity.

5.4.6.4. Greedy Dynamic BS Operation Algorithms. In this section, we propose two greedy heuristics to solve the formulated Green Dynamic BS Operation Problem. The results of these heuristics are going to be used during the comparative performance evaluation in Section 5.5.2. Greedy Dynamic BS Operation Algorithms (GDOA) initially activates all BSs with their maximum allowed transmission PL. Subsequently, they exhaustively attempt to decrease the transmission PL of each BS including the option of to be completely switched off in a centralized-offline manner. However, each iteration is performed unless the QoS requirements such as coverage, achievable data rate and BS traffic load capacity are not violated.

We noticed that the order in which BSs are evaluated for possible power consumption reduction has significant impact on the resulting network configuration. In order to obtain an energy efficient network topology, an optimum mixture of both pico and micro BSs are required where BSs with higher tx power act as umbrella cells and BSs with lower tx power act as hot spots to fill the coverage gaps. Therefore, greedily switching most of the micro BSs at the beginning eliminates the opportunity of switching under-loaded pico BSs afterwards due to coverage constraints. Hence, we proposed two different versions of the same greedy algorithm. The pseudocode of the GDOAs version 1 and 2 is given in Figures 5.12 and 5.13 in order. The first version starts with the micro BSs for possible power saving while the second version starts with the pico BSs. The impact of changing the BS evaluation order in performance evaluation is provided in Section 5.5.2.

Activate all BSs with max PL
for all $b \in \mathbf{B}^M$ and $p \in \mathbf{P}^M$ **do**
    Set PL of micro BS b to minimum possible[1] p without violating the QoS constraints
end for
for all $b \in \mathbf{B}^P$ and $p \in \mathbf{P}^P$ **do**
    Switch pico BS b off[2] unless QoS constraints are violated
end for

Figure 5.12. Greedy Dynamic BS Operation Algorithm v1.

Activate all BSs with max PL
for all $b \in \mathbf{B}^P$ and $p \in \mathbf{P}^P$ **do**
    Switch pico BS b off[2] unless QoS constraints are violated
end for
for all $b \in \mathbf{B}^M$ and $p \in \mathbf{P}^M$ **do**
    Set PL of micro BS b to minimum possible[1] p without violating the QoS constraints
end for

Figure 5.13. Greedy Dynamic BS Operation Algorithm v2.

5.5. Application Scenario and Performance Evaluation

5.5.1. Application Scenario and Parameters

In order to make proper performance evaluation of the proposed methods, we would like to create a test environment as close to the real life conditions as possible. Therefore, we selected Taksim, which is one of the Turkey's most famous and crowded places, as the pilot application area of the proposed green networking methods as mentioned in Section 5.2. In our system model, mobile service providers utilize the locations of the existing BSs for the NGMCNs motivated by a series of reasons led by the reduced installation cost. Therefore, we focus on deploying additional pico BSs as a remedy to a network where micro BSs are already deployed. The aim of the pico BS deployment is minimizing the number of deployed BSs while satisfying the QoS requirements. After the minimum number of required pico BSs and their respective

[1]Note that $p \in \mathbf{P}$ which includes switching a BS off with $p = 0$

[2]Recall from Section 5.4.2 that there is no dynamic tx power adjustment for pico BSs in our scenario where $\mathbf{P}^M = \{0, 1\}$ which represents on and off states of the pico BS

locations to support the peak traffic conditions are determined, green dynamic BS operation techniques are proposed to adapt the spatio-temporal traffic load variations and create an energy-aware network. We focus on the network topology adaptation and energy saving by both switching BSs on/off and adaptively adjusting their transmission powers according to the current traffic conditions.

We divided the coverage area into 17 different place types, and divided the places further $1m^2$ grids. Respective traffic loads of the grids are calculated according to their type by using Table 5.3 as a lookup. Although the total number of users located in a grid is proportional with the traffic occupancy of the grid, still we need to estimate the traffic load contribution of the users from the service provider's point of view. For this reason, we define a new parameter called *User Traffic Load Factor* to estimate the average traffic load contribution of the subscribers. In other words, *User Traffic Load Factor* represents the percentage of the users actively getting service from a particular operator at a particular instant. Considering numerous mobile consumer behavior reports [97–100] and subscriber numbers of each service provider in Turkey, we set the *User Traffic Load Factor* as 1%. However, this value is merely a parameter which can be easily changed as required.

Although we used pico and micro BSs in our test scenarios, our model can accommodate as many types of BSs as required. As QoS metrics, the resulting network topologies of the proposed green pico BS deployment and green dynamic BS operation techniques should satisfy the minimum aggregate data rate requirements of each grid and cover at least 99% of the area at all times. Important parameters used in the application scenario are summarized in Table 5.8. 10 different test cases were created randomly for the sake of variance control and the average of the results are presented.

5.5.2. Performance Evaluation

Performance of our proposed green pico BS deployment and dynamic operation methods are both evaluated by using real-life-scale test cases. For the green pico BS deployment, we compared our method with a greedy algorithm and a recently proposed

Table 5.8. Scenario parameters.

Parameter	Value
Coverage Area	$800 \times 680\, m^2$
Grid Area	$1 \times 1\, m^2$
# Place Types	17
Micro BS Tx PLs	3 - 8 - 13 - 18 - 24 Watt
Pico BS Tx Power	2 Watt
# Time Slots in a Day	24
Min. Coverage Ratio	99%
Min. SINR	6 dB
Orthogonality Loss Factor	0.5
Micro BS PA Efficiency	22.8%
Pico BS PA Efficiency	6.7%
# Candidate pico BS Deployment Locations	300
User Traffic Load Factor	1%

competitor energy-aware cellular network deployment technique [30]. In [30], authors propose a network energy consumption minimization framework which jointly optimizes the BS density and BS transmission power under coverage performance constraints. They utilize area power consumption (W/m^2) as the energy efficiency metric.

For the green dynamic BS operation, we compared the results of our methods with the conventional static operation, two centralized greedy heuristics, a competitor green BS operation algorithm called SWES [15] and an optimization tool IBM ILOG CPLEX [81]. However, finding the exact optimum solutions with CPLEX were not possible within reasonable amount of computation times. Therefore, we set a 3-hours run time limit and give the best results found until the limit along with their gap between the best integer objective and the objective of the best node remaining. On the other

Table 5.10. Comparison of computational complexity and average run times.

	Complexity	Average Run Time	Complexity Function
Green Pico BS Deployment Alg.	$O(N^4)$	2h 27m	$N^{B^M}.N^{X^P}.(N^G)^2$
Greedy Pico BS Deployment Alg.	$O(N^4)$	1h 22m	$N^{B^M}.N^{X^P}.(N^G)^2$
Peng *et al.* Alg. [30]	$O(N^4)$	2h 46m	$N^{B^M}.N^{X^P}.(N^G)^2$
Centralized Dynamic Operation Alg.	$O(N^6)$	7h 43m	$N^T.N^{B^M}.N^{B^P}.N^{P^M}.(N^G)^2$
Greedy Dynamic Operation Alg. v1	$O(N^6)$	4h 52m	$N^T.N^{B^M}.N^{B^P}.N^{P^M}.(N^G)^2$
Greedy Dynamic Operation Alg. v2		5h 10m	
Distributed Dynamic Operation Alg.	$O(N)$	N/A	N^T
SWES [15]	$O(N)$	N/A	N^T
CPLEX	N/A	144h (fixed)	N/A

hand, the other competitor SWES is an online and hybrid (distributed/centralized) algorithm which aims to reduce energy consumption of the network by switching BSs on/off. SWES switches off BSs one by one, taking the additional load increments brought to its neighboring BSs into account. Although the network impact of BS on/off transitions are calculated in a distributed manner, SWES still requires a central controller for the implementation of the topology adjustments.

The results presented in this section are collected from a computer with an AMD FX 8-core 4 Ghz processor and 16 GB of memory. Proposed methods are implemented in Microsoft Visual Studio 2008 [92] environment with more than ten thousand lines of C++ code. The total time spent to collect the results of 10 repetitions for each method is approximately ten days.

The computational complexity, average run times, and parameters effecting both computational and space complexity of the proposed and competitor methods are given in Table 5.10. The computational complexity of all investigated techniques are polynomial. For the dynamic operation algorithms, presented run times cover two separate execution of the same algorithm with different traffic load configurations for weekday and weekend. Therefore, it is convenient to say that a single execution takes approximately half of the given run times. For CPLEX, we set a 3-hours run time limit for each time slot which in turn results in total 144h runtime (for each time slot for weekday and weekend).

Pico BS deployment algorithms are the fastest methods since they are executed only once at the deployment phase and there is no time dimension in the effecting parameters as opposed to the dynamic BS operation algorithms. Among them, greedy pico BS deployment algorithm is the fastest. Our proposed Green Pico BS Deployment heuristic and Peng *et al.*'s Algorithm take approximately two and a half hours to finalize. On the other hand, dynamic BS operation algorithms take longer than pico BS deployment algorithms. Greedy algorithms obtain similar run times as expected since they are identical except their order of BS evaluation. Centralized Dynamic BS Operation Algorithm requires more than seven hours to find an energy efficient network topology for a cycle of one week. Lastly, we set a 3-hours run time limit for the optimization tool due to high complexity and give the best results found until the limit along with their gap value.

For the Green Pico BS Deployment Problem, our objective function given in Equation 5.1 is to minimize the number of deployed pico BSs to accommodate the peak traffic conditions without violating the user coverage and BS capacity constraints. According to our application scenario simulations based on the parameters given in Table 5.8; an average of 96, 100 and 138 pico BSs are deployed by the Green Pico BS Deployment Algorithm, Peng *et al.*'s Algorithm and Greedy Pico BS Deployment Algorithm respectively.

In Figure 5.14, comparative pico BS power consumption during peak traffic is given with respect to number of candidate pico BS deployment locations N^{X^P}. Our proposed Green Pico BS Deployment Algorithm and Peng *et al.*'s Algorithm achieve very similar power savings while greedy algorithm performs worse. For fewer N^{X^P}, the resulting topologies are infeasible since the user coverage and the BS capacity constraints are violated even though a pico BS is deployed in every candidate location. As the number of candidate pico BS deployment locations increases, pico BS deployment algorithms are able to achieve more power-efficient network configurations. How-

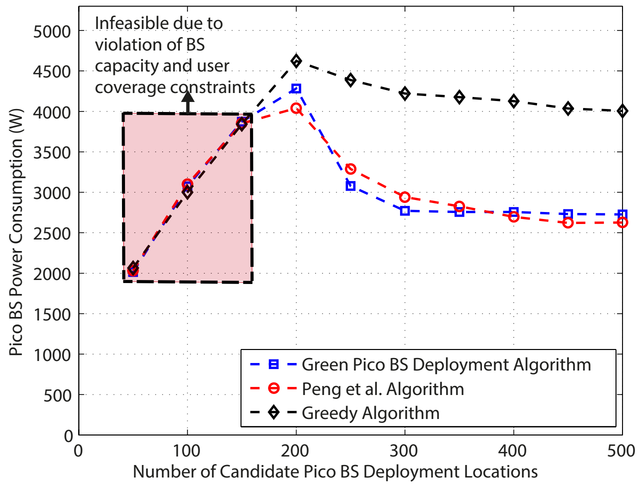

Figure 5.14. Comparative pico BS power consumption during peak traffic

ever, the additional power savings become negligible when compared to the introduced complexity for our proposed Green Pico BS Deployment Algorithm and Peng *et al.*'s Algorithm for $N^{X^P} > 300$. Although our Green Pico BS Deployment Algorithm and Peng *et al.*'s Algorithm obtain similar power savings without violating the user coverage and BS capacity constraints, it is convenient to say that our algorithm provides higher achievable data rates since it utilizes the ASE as performance metric.

In this section, we evaluate the comparative performance of our proposed green dynamic BS operation techniques. Figure 5.15(a) depicts the comparative power consumptions on weekdays. It is observed that the power expenditure trends of all methods follow a similar pattern with the traffic load given in Figure 5.3. Proposed algorithms dynamically respond to the traffic load changes and try to save energy without violating the QoS requirements of the subscribers. The reason behind the energy expenditure fluctuations in static operation or “no green method applied scenario" is the BS power consumption model introduced in Section 5.4.2. Since the consumed power in a BS is correlated with its respective traffic load, the total network power consumption is subject to change although no dynamic topology adjustment is being applied. The offline-centralized algorithm saves the largest amount of power whereas the online-distributed algorithm, SWES and GDOA v1 achieve nearly the same performance. On the other hand, although GDOA v2 saves significant amount of power with respect to

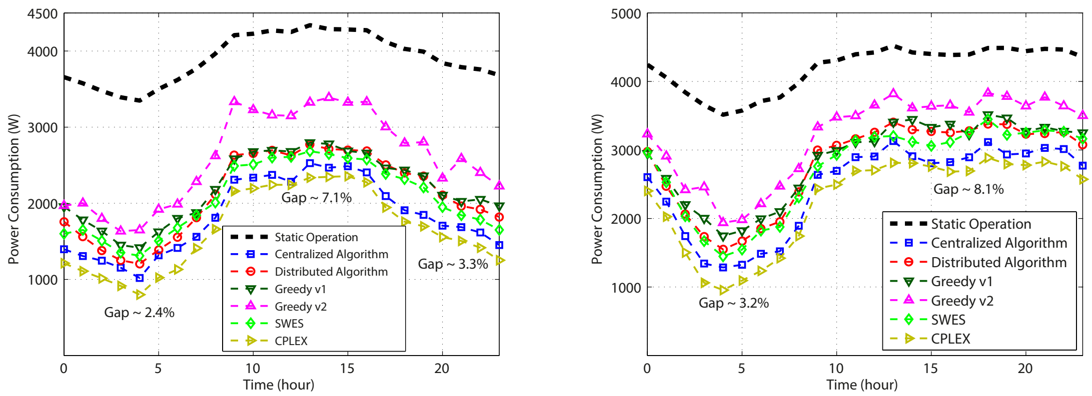

(a) Weekday. (b) Weekend.

Figure 5.15. Comparative power consumption throughout a day.

the static operation, this saving is less than the other proposed methods. By analyzing the results of the optimization tool and their average gap values, we can argue that the offline-centralized algorithm achieves energy-efficient topologies very close to the optimum.

Similar to the weekday results, weekend power consumption figures are proportional to the traffic load as observed in Figure 5.15(b). However, this time, the gap between the static operation and the green methods is narrower due to the high traffic load during weekends. The offline-centralized algorithm again achieves more power efficient results. SWES, Online-distributed algorithm, GDOA v1 and v2 follow the offline-centralized algorithm in order. The offline-centralized algorithm has both enough time and computational power to make complex resource management decisions. However, it requires a central entity for execution and does not respond well to unexpected traffic variations since the topology adjustment decisions are made beforehand. Although the online-distributed algorithm makes local decisions with limited number of observations, it obtains quite competitive results with respect to the other centralized algorithms which can take sophisticated network adjustment actions by utilizing plenty of network statistics. The online-distributed algorithm and SWES achieves similar results. However, SWES performs slightly better since it calculates the impact of BS transitions locally while makes the implementation decisions on a cental controller. On the other hand, the online-distributed algorithm does not require a central controller.

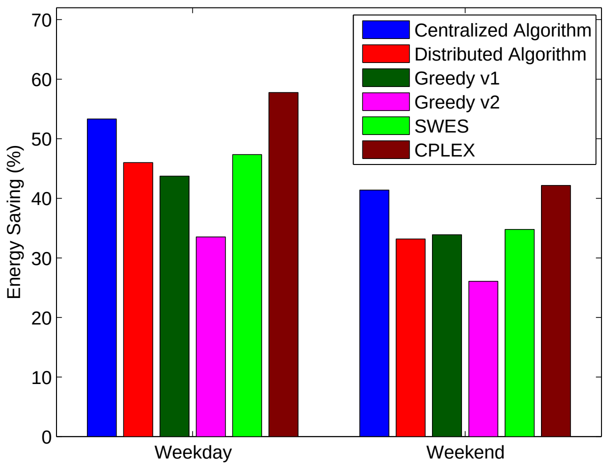

Figure 5.16. Comparative power saving ratio on weekday and weekend.

Another observation is that the average gap between the best integer objective and the objective of the best node remaining is smaller during low traffic conditions whereas the gap increases during high traffic conditions.

Comparative power saving ratio on a weekday and weekend is given in Figure 5.16. In fact, the results are obtained by extracting the integral of the static operation line from the integral of respective green method lines given in Figures 5.15(a) and 5.15(b) with an interval of [0,23]. Hence, this figure is also an overall visualization of how efficient each proposed method is in terms of power saving. Offline-centralized algorithm achieves more than 50% power saving on weekdays and 40% on weekends. On the other hand, SWES, Online-distributed algorithm and GDOA v1 achieves similar power saving ratios around 45% on weekday and 33% on weekend. As expected, the overall power saving ratios for weekend are considerably less than the weekday due to offered traffic loads depicted in Figure 5.3.

In Table 5.11; weekly, monthly and annual energy cost savings are given. The electricity prices for peak (5pm-10pm), morning (6am-5pm) and off-peak (10pm-6am) times are 41.61, 23.37 and 10.21 kurus/kWh (0,143, 0,081 and 0,035 \$/kWh) respectively including the 22% tax for the industrial consumers in compliance with the TEDAS [83], Turkey's governmental electricity retailer company. City-wide savings are calculated by

Table 5.11. Comparative energy cost saving.

	Weekly($)	Monthly($)	Annual($)			
			Test Case	City-wide	Country-wide	Country-wide with CE
Centralized Algorithm	25.6	110	1,321	3,726,694	13,788,769	39,160,104
Distributed Algorithm	21.3	92	1,100	3,101,602	11,475,927	32,591,634
Greedy v1	20.6	89	1,062	2,995,989	11,085,161	31,481,857
Greedy v2	15.1	65	783	2,208,119	8,170,040	23,202,914
SWES [15]	22.3	96	1,150	3,243,116	11,999,531	34,078,669
CPLEX	27.8	119	1,436	4,050, 512	14,986,895	42,562,783

comparing parameters of the test case (0.5 km^2 area and 136,346 average population) with the total urban surface area and population of Istanbul [101] (2761 km^2 urban area (out of total 5370 km^2) and 14.5 million inhabitants). Country-wide savings are also scaled similarly.

Proposed green dynamic BS operation techniques dramatically decrease the energy expenditures of the service providers as given in Table 5.11. According to our simulations, the centralized algorithm can achieve approximately 3.7 million $ cost savings for Istanbul and 13.7 million $ for Turkey annually. When the CE effect introduced in Section 4.5.2 is taken into account, the actual amount of cost savings become even more significant.

Due to its impact on the received signal strength and MT battery life, we also investigated the BS-User distance in our test cases. Figure 5.17 depicts the average BS-user distance throughout the day on weekdays and weekends. Since the deployed BS density in the Taksim area augmented with the pico BSs is very high, the average BS-User distance is slightly more than 20m when all of the BSs are active. However, when the green networking methods are applied and redundant BSs are started to be switched off, the average BS-user distance is also starting to increase. The average distance between BSs and users doubles when the offline-centralized algorithm is applied with respect to the static operation. The reason for observing high values during low-traffic conditions and low values during high-traffic conditions is related with the number of

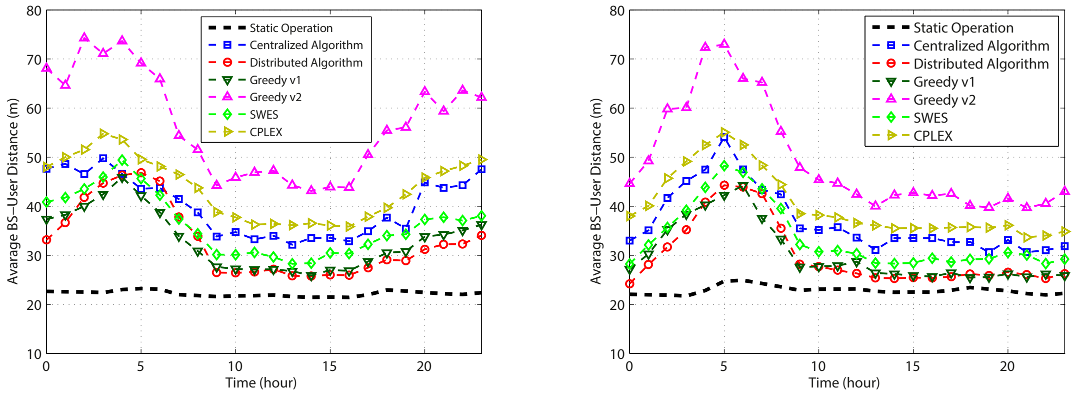

(a) Weekday. (b) Weekend.

Figure 5.17. Average BS-user distance.

active BSs. However, the fluctuations are not as much as the ones observed in Figure 5.3 because we carefully align the pico BS locations with the K-Means clustering algorithm according to the traffic hot spots prior to the deployment. Similar to the offline-centralized algorithm, we also observe higher average BS-user distances for CPLEX since it finds the minimum possible set of BSs with respect to the other methods. Another interesting observation is the relatively high BS-User distance for the GDOA v2. Since GDOA v2 first attempts to switch off the redundant pico BSs as long as the coverage and user QoS requirements are satisfied, most of the remaining active BSs are micro BSs. Fewer micro BSs are sufficient to provide those requirements since they have longer coverage ranges. Accordingly, the average BS-User distance increases when few micro BSs are active. Yet another importance of this metric is its effect on the MT power consumption. As the distance between the MTs and the serving BSs increases, MTs are obliged to increase their transmission power to communicate with the distant BSs. As investigated in Section 2.5, this results in faster depletion of the MT battery [61,62]. However, in a network with very high BS density such as our case, we assume that the effect of the BS-User distance on the MT power consumption is negligible.

The average BS utilization on weekdays and weekends are depicted in Figure 5.18. In perfect conditions, it is desired to observe a straight horizontal line in this figure regardless of the changing traffic conditions. This horizontal line means that the applied

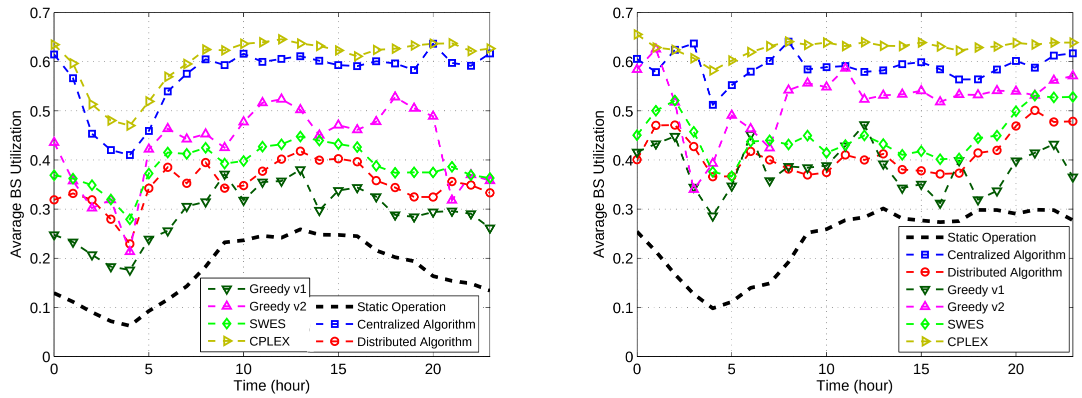

(a) Weekday.

(b) Weekend.

Figure 5.18. Average BS utilization.

green methods keep the traffic loads of active BSs in a desired level and hence, increase the overall utilization of the network resources. As observed in the figures, especially in Figure 5.18(a), there is a decrease in the average BS utilization during night time. This under-utilization is stemming from the minimum coverage ratio constraint where some BSs have to be switched on, although the traffic demand is low, in order to provide the required coverage ratio over the whole area. This yields to under-utilized active BSs for the sake of adequate coverage. In the previous figures, we observed that the offline-centralized algorithm adjusts to the changing traffic conditions better than the other methods except CPLEX and saves more power. As a result of this fact, the offline-centralized algorithm performs better with an average of 57% and 60% BS utilization on weekdays and weekends which are 3.35 and 2.6 times higher than the static operation. On the other hand, CPLEX achieves approximately 60% and 63% BS utilization on weekdays and weekends. For all methods, including the static operation, weekend BS utilizations are slightly higher than that of the weekdays. The cause of this observation is simply the higher traffic load in weekends as seen in Figure 5.3.

In Figures 5.19 and 5.20, occupancy of the coverage area on weekdays and weekends for time slots 10:00, 20:00 and 02:00 are given in order along with their active BS configurations obtained from the Offline-centralized Dynamic BS Operation Algorithm. The heat maps represent the user density per m^2 whereas their respective BS deployment configurations depict the location, type and tx power level of the switched on

BSs. It is clear in the color-coded user density maps that there are significant amount of both spatial and temporal user density variations. Schools and offices are crowded in the morning; pedestrian roads, shopping areas and restaurants are crowded in the evening; bars and night clubs are crowded at night. As expected, the offline-centralized Dynamic BS Operation Algorithm adjusts the network topology to the changing traffic demand conditions by switching BSs on/off and alternating BS tx power levels. The BS concentration on yellow-red coded areas is a clear demonstration of how green traffic-aware topology management framework operates.

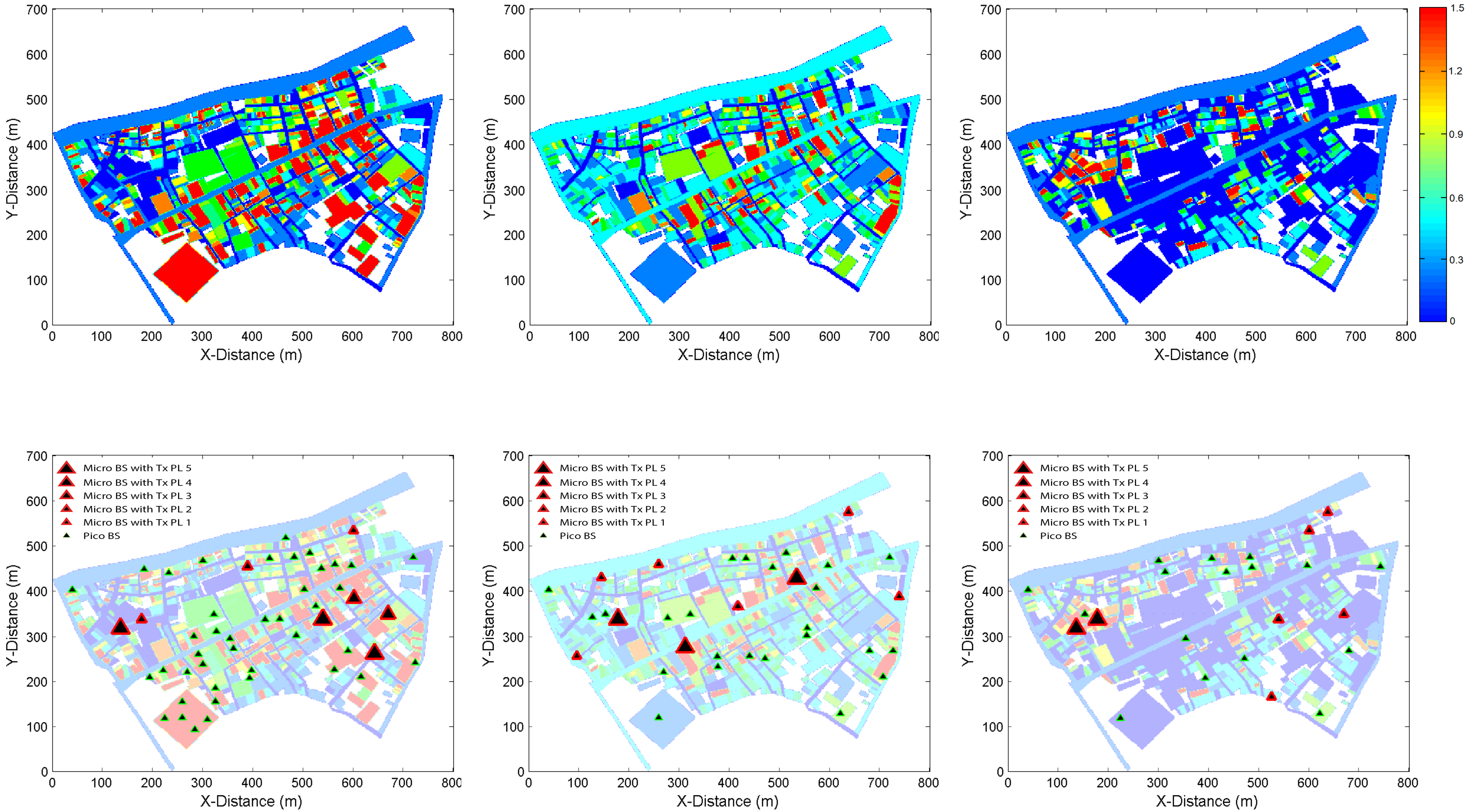

Figure 5.19. User density heat map and corresponding active BS status for time slot 10:00-20:00-02:00 on a weekday.

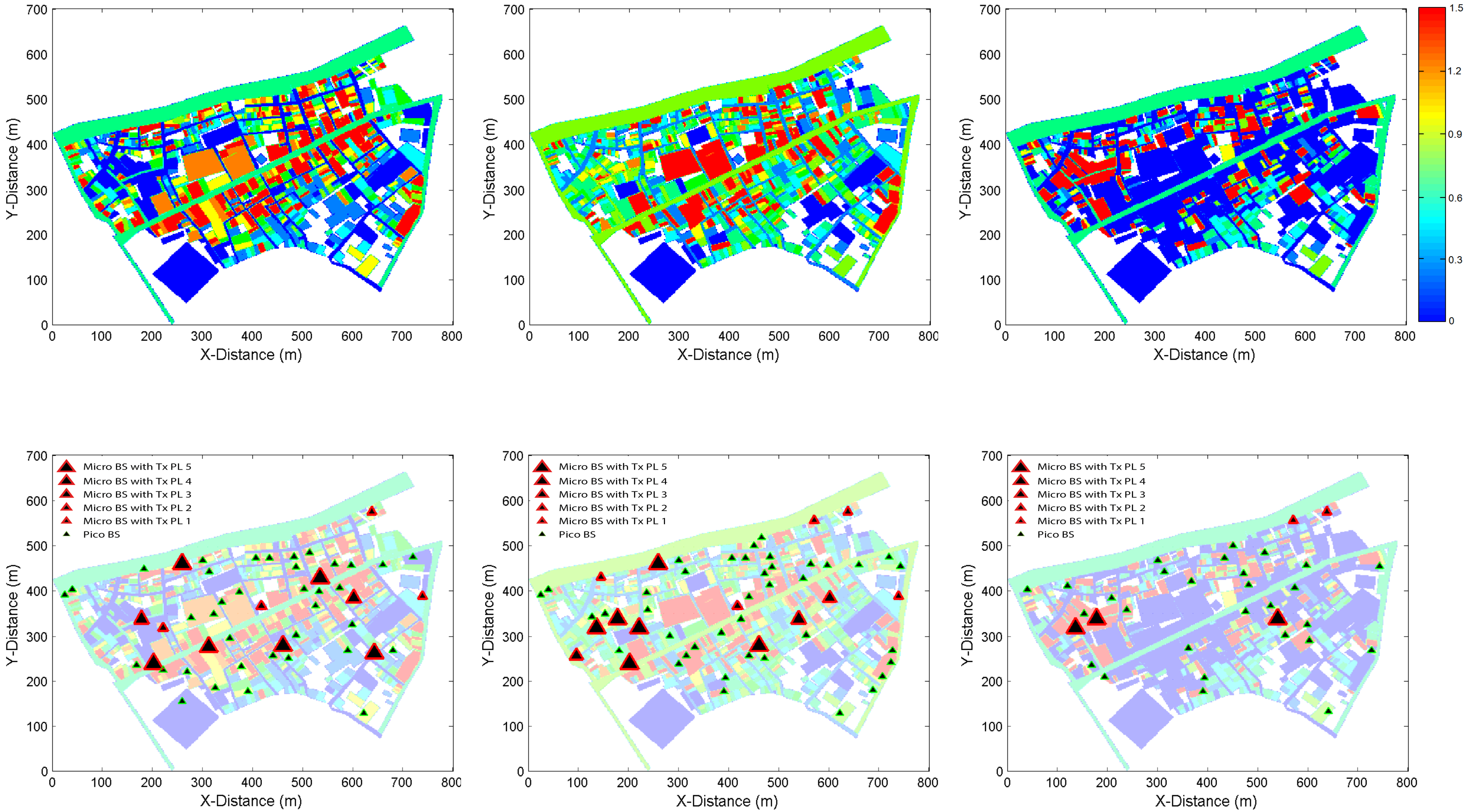

Figure 5.20. User density heat map and corresponding active BS status for time slot 10:00-20:00-02:00 at weekend.

5.6. Conclusion

In this chapter, we concentrated on green networking methodologies for NGMCNs. Unlike our previous proposals for the CCNs and PSCNs, we adopt a holistic approach and take all of the design, deployment and operation phases into account since NGMCNs are not fully deployed and operational yet. We started with mapping process of Taksim as our pilot application area in order to create a spatio-temporal user density. According to the extracted user density, we made an estimation of the traffic load and used this information to install additional pico BSs on top of the existing infrastructure to accommodate the peak traffic conditions. The proposed green pico BS deployment algorithm reduces both OPEX and CAPEX of the service providers by deploying minimum number of pico BSs while maintaining an acceptable level of QoS over the whole coverage area. Lastly, we propose an offline-centralized and an online-distributed green dynamic BS operation algorithms for power saving during the operation phase. The offline-centralized algorithm has both enough time and computational power to make complex resource management decisions. However, it requires a central entity for execution and does not respond well to unexpected traffic variations since topology adjustment decisions are made beforehand. On the other hand, the online-distributed algorithm makes topology adjustment decisions during operation and efficiently adapts to the unexpected traffic load changes. It also scales better than the offline-centralized algorithm since BSs determine their own status autonomously with their local observations in a distributed manner. The drawback of online-distributed algorithm is the additional signaling overhead introduced by requirement of coordination with the neighboring BSs. We also solve the Green Dynamic BS Operation problem with CPLEX, a commercial optimization tool, to give an insight about the efficiency of our algorithms with respect to the exact optimum solutions. Although we are able to use CPLEX for our test case scenario, low-complexity heuristics are still required for large realistic instances of the problem. Through a realistic test case scenario, we showed that both of our green BS deployment and dynamic operation methods achieve significant power savings with respect to the static operation, greedy heuristics and previously proposed two competitor algorithms [15] [30].

6. CONCLUSION

In this thesis, we focused on novel green networking methodologies for three different cellular network types; namely CCNs, PSCNs and NGMCNs. Unlike majority of the existing studies in the literature, we addressed the energy saving problem through (i) green BS design and deployment (ii) adaptive BS switching on/off and (iii) adaptive BS transmission power adjustment according to the present traffic conditions in the coverage area. However, the challenge is to decrease the energy expenditure while always guaranteeing an acceptable QoS level. Therefore, novel linear and nonlinear programming models are formulated to find the best possible BS topology which minimizes the energy consumption while satisfying the certain service quality requirements of the subscribers.

We started by surveying the previously proposed green networking studies in the literature. Our survey covers not only dynamic resource management schemes but also energy efficient BS deployment and cooperation, renewable energy resources and energy efficiency in MTs. We also present an extensive taxonomy of the surveyed strategies for better understanding.

For the CCNs, we concentrated on saving energy by adaptively switching the BSs of wireless cellular access networks on and off according to the current traffic conditions. Moreover, we also adopted dynamic transmission power adjustment with the help of high-efficiency power amplifiers. We formulate a novel NLP model for the GDBP problem to find the best possible BS topology which minimizes the energy consumption while satisfying the communication demands of the users. We then proposed a heuristic to solve that problem and compare our results with the results of a non-commercial optimization software and numerous MC experiments. It is shown that our green dynamic BS planning scheme saves significant amount of energy.

For the PSCNs, our focus was on creating an energy-aware network by adaptively switching the BSs of heterogeneous cellular networks on/off and by adjusting the BS transmission power levels. Different from the CCNs, we also take the effect of interference into account to come up with more realistic green networking methods. We formulate a novel LP model for the TAM problem to find the best possible energy-aware BS topology without violating the QoS requirements from the subscriber point of view. Although small instances of the TAM problem can be solved by the optimization tools, large realistic size problems are quite difficult to be handled due to their prohibitive space and computational complexity. Therefore, we propose a novel heuristic to solve the large-scale instances of the formulated problem and compare our results with the results of two previously proposed methods [13] [14], a greedy heuristic and a commercial optimization tool. It is shown that the proposed TAM scheme helps to maintain an energy-aware network and saves significant amount of energy by adjusting the network topology according to the present traffic conditions adaptively.

Finally for the NGMCNs, our goal was to derive efficient green network design, deployment and operation techniques for NGMCNs. We take the advantage of still ongoing standardization process and lack of fully deployed and operational infrastructure by adopting a holistic approach which encompasses not only the operation phase, but also design and deployment phases. We divided this portion of thesis into three packages. In the first package, we created a detailed map of the pilot application area and obtain a spatio-temporal user density estimation. According to this estimation, we designed and deployed additional pico BSs as a remedy on top of the existing infrastructure to accommodate the peak traffic conditions in the second package. Lastly, we proposed green dynamic BS operation techniques to minimize the overall energy consumption of the network consisting of heterogeneous elements. Unlike proposed methods for CCNs and PSCNs in the previous chapters, we proposed an offline-centralized and online-distributed version of the green dynamic BS operation algorithm. Extensive simulation runs based on collected data from the pilot application area demonstrated significant power savings compared to conventional static operation, greedy heuristics, CPLEX and previously proposed two competitor algorithms [15] [30].

In conclusion, making the mobile networks green could not only have a positive impact on saving the energy, but also help to achieve a long-term profitability of mobile service providers and sustainability of the environment. Increasing energy prices and environmental awareness has led the cellular network operators to reduce their OPEX and CO_2 footprints as well. Therefore, we need novel green networking techniques to minimize the overall network power consumption. In this thesis, we addressed the challenge of decreasing power consumption while maintaining an acceptable level of service quality. In summary, we proposed green BS design, deployment and dynamic operation techniques for CCNs, PSCNs and NGMCNs along with their mathematical optimization models. Through extensive comparative performance evaluations, it is shown that the proposed green networking methods help to maintain an energy-aware network and achieve significant amount of power savings.

As future work, we are planning to propose efficient techniques to alleviate the handoff overhead stemming from frequent topology changes. We believe that the integration of smart user-BS association rules to our dynamic BS operation techniques may reduce the number of handoff requests. Another promising research issue is utilizing multiple network access interfaces of MTs such as Bluetooth and Wi-Fi for transmitting their data packets to the BSs. This kind of inter-network cooperation may reduce the overall BS density and up time which in turn results in more energy efficient networks. Also, integrating the capability of using directional antennas into our green networking methods can improve the energy saving significantly. Lastly, we believe that non-technical factors such as pricing, marketing strategies, willingness to cooperate among service providers and law establishments are key factors in the success of the green mobile networking technology.

REFERENCES

1. Oh, E. and B. Krishnamachari, "Energy Savings through Dynamic Base Station Switching in Cellular Wireless Access Networks", *Global Telecommunications Conference (GLOBECOM), IEEE*, pp. 1–5, Dec 2010.

2. "Cisco white paper on Cisco Visual Networking Index: Forecast and Methodology, 2014-2019", 2015, http://www.cisco.com/c/en/us/solutions/collateral/service-provider/ip-ngn-ip-next-generation-network/white_paper_c11-481360.pdf, accessed at January 2016.

3. National Research Council, *Advancing the Science of Climate Change*, The National Academies Press, 2010.

4. "Smart 2020: Enabling the low carbon economy in the information age. The Climate Group, Global e-Sustainability Initiative (GeSI)", 2008, http://www.smart2020.org, accessed at December 2015.

5. "Understanding the Environmental Impact of Communication Systems", 2009, http://stakeholders.ofcom.org.uk/market-data-research/other/technology-research/research/sector-studies/environment, accessed at December 2015.

6. "Cisco white paper on Cisco Visual Networking Index: Global Mobile Data Traffic Forecast Update, 2014-2019", 2015, http://www.cisco.com/c/en/us/solutions/collateral/service-provider/visual-networking-index-vni/white_paper_c11-520862.pdf, accessed at January 2016.

7. Vadgama, S. and M. Hunukumbure, "Trends in Green Wireless Access Networks", *Communications Workshops (ICC), IEEE International Conference on*, pp. 1–5, June 2011.

8. Mancuso, V. and S. Alouf, "Reducing costs and pollution in cellular networks",

Communications Magazine, IEEE, Vol. 49, No. 8, pp. 63–71, August 2011.

9. Han, C., T. Harrold, S. Armour, I. Krikidis, S. Videv, P. M. Grant, H. Haas, J. Thompson, I. Ku, C.-X. Wang, T. A. Le, M. Nakhai, J. Zhang and L. Hanzo, "Green radio: radio techniques to enable energy-efficient wireless networks", *Communications Magazine, IEEE*, Vol. 49, No. 6, pp. 46–54, June 2011.

10. Spench.net, "Australian Geographical Radio Frequency Map", 2014, http://maps.spench.net, accessed at January 2016.

11. *IEEE 802.16m Evaluation Methodology Document*, Tech. Rep. IEEE 802.16m-08/004r5, Piscataway, NJ, September 2009.

12. COST 231, "Urban transmission loss models for mobile radio in the 900-1800 MHz bands (Revision 2)", *COST 231 TD(90)119 Rev. 2*, The Hague, The Netherlands, September 1991.

13. Hossain, M., K. Munasinghe and A. Jamalipour, "A protocooperation-based sleep-wake architecture for next generation green cellular access networks", *Signal Processing and Communication Systems (ICSPCS), 4th International Conference on*, pp. 1–8, Dec 2010.

14. Niu, Z., Y. Wu, J. Gong and Z. Yang, "Cell zooming for cost-efficient green cellular networks", *Communications Magazine, IEEE*, Vol. 48, No. 11, pp. 74–79, November 2010.

15. Oh, E., K. Son and B. Krishnamachari, "Dynamic Base Station Switching-On/Off Strategies for Green Cellular Networks", *Wireless Communications, IEEE Transactions on*, Vol. 12, No. 5, pp. 2126–2136, May 2013.

16. Bhaumik, S., G. Narlikar, S. Chattopadhyay and S. Kanugovi, "Breathe to stay cool: adjusting cell sizes to reduce energy consumption", *Proceedings of the first ACM SIGCOMM workshop on Green networking*, pp. 41–46, 2010.

17. Kokkinogenis, S. and G. Koutitas, "Dynamic and static base station management schemes for cellular networks", *Global Communications Conference (GLOBECOM), IEEE*, pp. 3443–3448, 2012.

18. Chiaraviglio, L., D. Ciullo, M. Meo and M. Marsan, "Energy-efficient management of UMTS access networks", *Teletraffic Congress (ITC), 21st International*, pp. 1–8, September 2009.

19. Miao, G., N. Himayat, Y. G. Li and A. Swami, "Cross-layer optimization for energy-efficient wireless communications: a survey", *Wireless Communications and Mobile Computing*, Vol. 9, No. 4, pp. 529–542, 2009.

20. Meshkati, F., H. Poor, S. Schwartz and N. B. Mandayam, "An energy-efficient approach to power control and receiver design in wireless data networks", *Communications, IEEE Transactions on*, Vol. 53, No. 11, pp. 1885–1894, Nov 2005.

21. Pedram, M., "Power optimization and management in embedded systems", *Asia and South Pacific Design Automation Conference (ASP-DAC), Proceedings of the*, pp. 239–244, 2001.

22. Benini, L., A. Bogliolo and G. De Micheli, "A survey of design techniques for system-level dynamic power management", *Very Large Scale Integration (VLSI) Systems, IEEE Transactions on*, Vol. 8, No. 3, pp. 299–316, June 2000.

23. Ambrosy, A., O. Blume, H. Klessig and W. Wajda, "Energy saving potential of integrated hardware and resource management solutions for wireless base stations", *Personal Indoor and Mobile Radio Communications (PIMRC), IEEE 22nd International Symposium on*, pp. 2418–2423, Sept 2011.

24. Sisk, L. and D. Allen, "Energy efficient cooling strategies for telecom", *Telecommunications Energy Conference (INTELEC), 2014 IEEE 36th International*, pp. 1–6, Sept 2014.

25. Zheng, M., P. Pawelczak, S. Stanczak and H. Yu, “Planning of Cellular Networks Enhanced by Energy Harvesting”, *Communications Letters, IEEE*, Vol. 17, No. 6, pp. 1092–1095, June 2013.

26. Weicker, N., G. Szabo, K. Weicker and P. Widmayer, “Evolutionary multiobjective optimization for base station transmitter placement with frequency assignment”, *Evolutionary Computation, IEEE Transactions on*, Vol. 7, No. 2, pp. 189–203, April 2003.

27. Tutschku, K. and P. Tran-Gia, “Spatial traffic estimation and characterization for mobile communication network design”, *Selected Areas in Communications, IEEE Journal on*, Vol. 16, No. 5, pp. 804–811, Jun 1998.

28. Amaldi, E., A. Capone and F. Malucelli, “Planning UMTS base station location: optimization models with power control and algorithms”, *Wireless Communications, IEEE Transactions on*, Vol. 2, No. 5, pp. 939–952, Sept 2003.

29. Boiardi, S., A. Capone and B. Sanso, “Radio planning of energy-aware cellular networks”, *Computer Networks*, Vol. 57, No. 13, pp. 2564 – 2577, 2013.

30. Peng, J., P. Hong and K. Xue, “Energy-Aware Cellular Deployment Strategy Under Coverage Performance Constraints”, *Wireless Communications, IEEE Transactions on*, Vol. 14, No. 1, pp. 69–80, Jan 2015.

31. Cao, D., S. Zhou and Z. Niu, “Optimal Combination of Base Station Densities for Energy-Efficient Two-Tier Heterogeneous Cellular Networks”, *Wireless Communications, IEEE Transactions on*, Vol. 12, No. 9, pp. 4350–4362, September 2013.

32. EARTH project, “Definition and parameterization of reference systems and scenarios”, 2010, https://www.ict-earth.eu/publications/deliverables/deliverables.html, accessed at December 2015.

33. EARTH project, "Energy efficiency analysis of the reference systems, areas of improvements and target breakdown", 2010, https://www.ict-earth.eu/publications/deliverables/deliverables.html, accessed at December 2015.

34. Soh, Y. S., T. Quek, M. Kountouris and H. Shin, "Energy Efficient Heterogeneous Cellular Networks", *Selected Areas in Communications, IEEE Journal on*, Vol. 31, No. 5, pp. 840–850, May 2013.

35. Suarez, L., L. Nuaymi and J.-M. Bonnin, "Energy-efficient {BS} switching-off and cell topology management for macro/femto environments", *Computer Networks, Special Issue: Green Communications*, Vol. 78, pp. 182 – 201, 2015.

36. Son, K., E. Oh and B. Krishnamachari, "Energy-efficient design of heterogeneous cellular networks from deployment to operation", *Computer Networks, Special Issue: Green Communications*, Vol. 78, pp. 95 – 106, 2015.

37. Wu, J., S. Zhou and Z. Niu, "Traffic-Aware Base Station Sleeping Control and Power Matching for Energy-Delay Tradeoffs in Green Cellular Networks", *Wireless Communications, IEEE Transactions on*, Vol. 12, No. 8, pp. 4196–4209, August 2013.

38. Niu, Z., X. Guo, S. Zhou and P. Kumar, "Characterizing Energy-Delay Tradeoff in Hyper-Cellular Networks With Base Station Sleeping Control", *Selected Areas in Communications, IEEE Journal on*, Vol. 33, No. 4, pp. 641–650, April 2015.

39. Zheng, J., Y. Cai, X. Chen, R. Li and H. Zhang, "A game-theoretic approach for optimal base station sleeping in green cellular networks", *Wireless Communications and Signal Processing (WCSP), Sixth International Conference on*, pp. 1–6, Oct 2014.

40. Bousia, A., A. Antonopoulos, L. Alonso and C. Verikoukis, "Green distance-aware base station sleeping algorithm in LTE-Advanced", *Communications (ICC), IEEE International Conference on*, pp. 1347–1351, June 2012.

41. Kim, J., W. S. Jeon and D. G. Jeong, "Effect of Base Station-Sleeping Ratio on Energy Efficiency in Densely Deployed Femtocell Networks", *Communications Letters, IEEE*, Vol. 19, No. 4, pp. 641–644, April 2015.

42. Rengarajan, B., G. Rizzo and M. A. Marsan, "Energy-optimal base station density in cellular access networks with sleep modes", *Computer Networks, Special Issue: Green Communications*, Vol. 78, pp. 152 – 163, 2015.

43. Combes, R., S. E. Elayoubi, A. Ali, L. Saker and T. Chahed, "Optimal online control for sleep mode in green base stations", *Computer Networks, Special Issue: Green Communications*, Vol. 78, pp. 140 – 151, 2015.

44. Sinha, D., V. Kavitha and A. Karandikar, "Load dependent optimal ON-OFF policies in cellular heterogeneous networks", *Modeling and Optimization in Mobile, Ad Hoc, and Wireless Networks (WiOpt), 2014 12th International Symposium on*, pp. 159–166, May 2014.

45. Budzisz, L., F. Ganji, G. Rizzo, M. Marsan, M. Meo, Y. Zhang, G. Koutitas, L. Tassiulas, S. Lambert, B. Lannoo, M. Pickavet, A. Conte, I. Haratcherev and A. Wolisz, "Dynamic Resource Provisioning for Energy Efficiency in Wireless Access Networks: A Survey and an Outlook", *Communications Surveys Tutorials, IEEE*, Vol. 16, No. 4, pp. 2259–2285, 2014.

46. Han, T. and N. Ansari, "On greening cellular networks via multicell cooperation", *Wireless Communications, IEEE*, Vol. 20, No. 1, pp. 82–89, February 2013.

47. Ismail, M. and W. Zhuang, "Network cooperation for energy saving in green radio communications", *Wireless Communications, IEEE*, Vol. 18, No. 5, pp. 76–81, October 2011.

48. Ghazzai, H., E. Yaacoub and M.-S. Alouini, "Multi-Operator Collaboration for Green Cellular Networks under Roaming Price Consideration", *Vehicular Technology Conference (VTC), IEEE 80th*, pp. 1–5, Sept 2014.

49. Bousia, A., E. Kartsakli, A. Antonopoulos, L. Alonso and C. Verikoukis, "Game theoretic approach for switching off base stations in multi-operator environments", *Communications (ICC), IEEE International Conference on*, pp. 4420–4424, June 2013.

50. Han, F., Z. Safar and K. Liu, "Energy-Efficient Base-Station Cooperative Operation with Guaranteed QoS", *Communications, IEEE Transactions on*, Vol. 61, No. 8, pp. 3505–3517, August 2013.

51. Zou, Y., J. Zhu and B. Zheng, "Energy efficiency of network cooperation for cellular uplink transmissions", *Communications (ICC), IEEE International Conference on*, pp. 4394–4398, June 2013.

52. Ericsson Inc. Press Release, "Ericsson unveils wind-powered concept for its award-winning Tower Tube", 2008, http://www.ericsson.com/news/1258047, accessed at December 2015.

53. Nokia Press Release, "E-Plus, Nokia Siemens Networks build Germany's first off-grid base station", 2011, http://networks.nokia.com/news-events/press-room/press-releases/e-plus-nokia-siemens-networks-build-germany-s-first-off-grid-base-station, accessed at December 2015.

54. Marsan, M., G. Bucalo, A. Di Caro, M. Meo and Y. Zhang, "Towards zero grid electricity networking: Powering BSs with renewable energy sources", *Communications Workshops (ICC), IEEE International Conference on*, pp. 596–601, June 2013.

55. Han, T. and N. Ansari, "On Optimizing Green Energy Utilization for Cellular Networks with Hybrid Energy Supplies", *Wireless Communications, IEEE Transactions on*, Vol. 12, No. 8, pp. 3872–3882, August 2013.

56. Wang, H., H. Li, C. Tang, L. Ye, X. Chen, H. Tang and S. Ci, "Modeling, metrics, and optimal design for solar energy-powered base station system", *EURASIP*

Journal on Wireless Communications and Networking, Vol. 2015, No. 1, 2015.

57. Mao, Y., J. Zhang and K. Letaief, “A Lyapunov Optimization Approach for Green Cellular Networks with Hybrid Energy Supplies”, *Selected Areas in Communications, IEEE Journal on*, Vol. PP, No. 99, pp. 1–1, 2015.

58. Ismail, M., M. Kashef, E. Serpedin and K. Qaraqe, “Dynamic planning with balanced energy efficiency for network operators and mobile users”, *Green Communications (OnlineGreencomm), 2014 IEEE Online Conference on*, pp. 1–6, Nov 2014.

59. Turck, K. D., S. D. Vuyst, D. Fiems, S. Wittevrongel and H. Bruneel, “Performance analysis of sleep mode mechanisms in the presence of bidirectional traffic”, *Computer Networks*, Vol. 56, No. 10, pp. 2494 – 2505, 2012.

60. Wang, R., J. Tsai, C. Maciocco, T. Tai and J. Wu, “Reducing Power Consumption for Mobile Platforms via Adaptive Traffic Coalescing”, *Selected Areas in Communications, IEEE Journal on*, Vol. 29, No. 8, pp. 1618–1629, September 2011.

61. Ismail, M., W. Zhuang, E. Serpedin and K. Qaraqe, “A Survey on Green Mobile Networking: From The Perspectives of Network Operators and Mobile Users”, *Communications Surveys Tutorials, IEEE*, Vol. 17, No. 3, pp. 1535–1556, 2015.

62. Hoque, M., M. Siekkinen and J. Nurminen, “Energy Efficient Multimedia Streaming to Mobile Devices - A Survey”, *Communications Surveys Tutorials, IEEE*, Vol. 16, No. 1, pp. 579–597, 2014.

63. Azad, A., S. Alouf, E. Altman, V. Borkar and G. Paschos, “Optimal Control of Sleep Periods for Wireless Terminals”, *Selected Areas in Communications, IEEE Journal on*, Vol. 29, No. 8, pp. 1605–1617, September 2011.

64. Yigitel, M. A., O. D. Incel and C. Ersoy, “Dynamic base station planning with power adaptation for green wireless cellular networks”, *EURASIP Journal on*

Wireless Communications and Networking, Vol. 2014, No. 1, 2014.

65. Marsan, M., L. Chiaraviglio, D. Ciullo and M. Meo, "Optimal Energy Savings in Cellular Access Networks", *Communications (ICC) Workshops, IEEE International Conference on*, pp. 1–5, June 2009.

66. Kelif, J.-M., M. Coupechoux and F. Marache, "Limiting Power Transmission of Green Cellular Networks: Impact on Coverage and Capacity", *Communications (ICC), IEEE International Conference on*, pp. 1–6, May 2010.

67. Yigitel, M. A., O. D. Incel and C. Ersoy, "QoS vs. energy: A traffic-aware topology management scheme for green heterogeneous networks", *Computer Networks, Special Issue: Green Communications*, Vol. 78, pp. 130 – 139, 2015.

68. Richter, F., A. Fehske, P. Marsch and G. Fettweis, "Traffic Demand and Energy Efficiency in Heterogeneous Cellular Mobile Radio Networks", *Vehicular Technology Conference (VTC), IEEE 71st*, pp. 1–6, 2010.

69. Marsan, M., L. Chiaraviglio, D. Ciullo and M. Meo, "Switch-Off Transients in Cellular Access Networks with Sleep Modes", *Communications Workshops (ICC), IEEE International Conference on*, pp. 1–6, June 2011.

70. Sun, L., H. Tian and P. Zhang, "Decision-making models for group vertical handover in vehicular communications", *Telecommunication Systems*, Vol. 50, No. 4, pp. 257–266, 2012.

71. Lu, Q. and M. Ma, "Group mobility support in mobile WiMAX networks", *Journal of Network and Computer Applications*, Vol. 34, No. 4, pp. 1272 – 1282, 2011.

72. Willkomm, D., S. Machiraju, J. Bolot and A. Wolisz, "Primary Users in Cellular Networks: A Large-Scale Measurement Study", *New Frontiers in Dynamic Spectrum Access Networks (DySPAN), 3rd IEEE Symposium on*, pp. 1–11, October 2008.

73. Tipper, D., A. Rezgui, P. Krishnamurthy and P. Pacharintanakul, "Dimming Cellular Networks", *Global Telecommunications Conference (GLOBECOM), IEEE*, pp. 1–6, December 2010.

74. Rappaport, T. S., *Wireless Communications: Principles and Practice*, Prentice Hall, 2nd edn., January 2002.

75. "Basic Open-source Nonlinear Mixed INteger programming(BONMIN)", 2015, http://www.coin-or.org/Bonmin, accessed at January 2016.

76. "A Modeling Language for Mathematical Programming(AMPL)", 2015, http://www.ampl.com, accessed at January 2016.

77. "EnergyAustralia", 2015, http://www.energyaustralia.com.au, accessed at January 2016.

78. Zhou, S., J. Gong, Z. Yang, Z. Niu and P. Yang, "Green Mobile Access Network with Dynamic Base Station Energy Saving", *ACM MobiCom'09*, pp. 10–12, 2009.

79. Arnold, O., F. Richter, G. Fettweis and O. Blume, "Power consumption modeling of different base station types in heterogeneous cellular networks", *Future Network and Mobile Summit*, pp. 1–8, 2010.

80. Auer, G., V. Giannini, C. Desset, I. Godor, P. Skillermark, M. Olsson, M. Imran, D. Sabella, M. Gonzalez, O. Blume and A. Fehske, "How much energy is needed to run a wireless network?", *Wireless Communications, IEEE*, Vol. 18, No. 5, pp. 40–49, 2011.

81. "IBM ILOG CPLEX Optimizer", 2015, www.ibm.com/software/commerce/optimization/ cplex-optimizer/, accessed at January 2016.

82. "GUROBI Optimizer", 2015, http://www.gurobi.com/, accessed at December 2015.

83. “Turkish Electricity Distribution Company”, 2015, http://www.tedas.gov.tr, accessed at January 2016.

84. Emerson Network Power, “Energy Logic: Reducing Data Center Energy Consumption by Creating Savings that Cascade Across Systems, A White Paper from the Experts in Business-Critical Continuity”, 2013, http://www.emersonnetworkpower.com, accessed at December 2015.

85. Wikipedia, “Istiklal Avenue”, 2015, https://en.wikipedia.org/wiki/Istiklal_Avenue, accessed at February 2016.

86. “Google Earth”, 2015, http://earth.google.com, accessed at January 2016.

87. “Microsoft Visio”, 2015, https://products.office.com/en-us/Visio/flowchart-software, accessed at December 2015.

88. “Google Maps”, 2015, http://maps.google.com, accessed at January 2016.

89. “Yandex Maps”, 2015, http://maps.yandex.com, accessed at January 2016.

90. “OpenStreetMap”, 2015, http://www.openstreetmap.org, accessed at January 2016.

91. “Extensible 3D”, 2015, http://www.web3d.org, accessed at December 2015.

92. “Microsoft Visual Studio”, 2015, http://www.visualstudio.com, accessed at December 2015.

93. “OpenCellID”, 2015, http://opencellid.org, accessed at January 2016.

94. “COST 231 Final Report, Digital Mobile Radio Towards Future Generation Systems”, 1999, www.lx.it.pt/cost231/final-report.htm, accessed at December 2015.

95. Alouini, M. and A. Goldsmith, “Area spectral efficiency of cellular mobile radio

systems", *Vehicular Technology, IEEE Transactions on*, Vol. 48, No. 4, pp. 1047–1066, Jul 1999.

96. MacQueen, J., "Some methods for classification and analysis of multivariate observations.", Proc. 5th Berkeley Symp. Math. Stat. Probab., Univ. Calif. 1965/66, 1, 281-297., 1967.

97. Goncalves, L. C., P. Sebastiao, N. Souto and A. Correia, "On the impact of user segmentation and behaviour analysis over traffic generation in beyond 4G networks", *Transactions on Emerging Telecommunications Technologies*, 2015.

98. Ofcom, "The Communications Market Report", 2015, http://stakeholders.ofcom.org.uk/market-data-research/market-data/communications-market-reports/cmr15/, accessed at December 2015.

99. Deloitte, "Mobile Consumer 2014: The UK Cut, Revolution and Evolution", 2014, http://www.deloitte.co.uk/mobileuk, accessed at January 2016.

100. Salesforge, "2014 Mobile Behavior Report", 2014, http://www.salesforce.com/marketing-cloud, accessed at January 2016.

101. Istanbul Metropolitan Municipality, "Istanbul Il ve Ilce Alan Bilgileri", 2015, http://www.ibb.gov.tr/tr-tr/kurumsal/pages/ilceveilkkademe.aspx, accessed at January 2016.